



UNIVERSITÀ DEGLI STUDI DI FIRENZE

Scuola di Ingegneria

DOTTORATO DI RICERCA IN
INGEGNERIA INDUSTRIALE E DELL'AFFIDABILITÀ
CICLO XXXII

COORDINATORE DEL DOTTORATO

Prof. Ing. Maurizio De Lucia

Co-Simulation and Energetic Optimisation of Complex Railway Systems

A dissertation submitted in partial fulfillment of the requirements for the degree of Doctor of Philosophy

Settore scientifico disciplinare ING-IND/13

CANDIDATO

Benedetta Romani

TUTOR

Prof. Ing. Andrea Rindi

Co-TUTOR

Prof. Ing. Benedetto Allotta

ANNI ACCADEMICI 2016/2019

Intellettuali d'oggi
Idioti di domani
Ridatemi il cervello
Che basta alle mie mani
Profeti molto acrobati
Della rivoluzione
Oggi farò da me
Senza lezione

*Al Pipa, la Mara, la Sis
e, in particolar modo, a Bubo.*

Contents

List of Figures	III
List of Tables	IX
1 Introduction	3
1.1 General architecture of the model	7
1.2 Objectives of the developed model	10
2 State of art	12
3 Materials and methods	28
3.1 Vehicle dynamical model	30
3.1.1 Vehicle longitudinal dynamics and motion resistance	30
3.1.2 Adherence	33
3.1.3 Power	34
3.1.4 Line voltage limit	36
3.2 Electrical models	38

3.2.1	Feeding line and electrical substation model	39
3.2.2	Energy storage device model	48
3.2.3	Multi-vehicle line	55
3.3	Signalling model	57
3.3.1	Emergency Braking Deceleration curve calculation	60
3.3.2	Braking space calculation	62
3.4	Softwares and Mathematical Tools	71
4	Results	73
4.1	Test cases	74
4.1.1	E464 commuter train on Rimini-Bologna line	74
4.1.2	ETR 1000 high-speed train on the <i>Direttissima</i> line	77
4.2	Experimental validation	80
4.3	High-speed and commuter train systems: feasibility analysis	82
4.4	Optimisation investigation on different operating scenarios	90
4.5	Signalling results	105
4.6	Preliminary cost analysis	114
5	Conclusions and Future Developments	117
	Bibliography	121

List of Figures

- 1.1 European evolution of greenhouse gas emissions from 1990 to 2017 [1], [2]. 4
- 1.2 Energy management in an operating scenario. 5
- 1.3 General architecture of the developed model, composed of a vehicle longitudinal dynamics model, an electrical one, which includes feeding line, substations and energy storage devices, and a signalling model. 8

- 2.1 Electric motors four quadrants operating range. 13
- 2.2 Regenerative braking energy flow, from a braking vehicle to an accelerating one. . 14
- 2.3 Comparison of typical regenerative braking parameters for different railway vehicles: yellow arrows show how commuter trains have intermediate characteristics with respect to high speed and light vehicles, e.g. an equivalent inertia which is higher with respect to light railways but lower with respect to high speed trains. 15
- 2.4 Different methods to achieve an energetic efficiency improvement [3]. 16
- 2.5 Relation between the energy savings potential and the investment costs for energetic optimisation applications. 17
- 2.6 Example of usage of energy storage device installed on-board the vehicle. 18

2.7	Energy storage devices characterisation with respect to energy and power density. . .	19
2.8	Environmental impact of different batteries typologies, including losses due to the batteries mass and efficiency during the use [4].	20
2.9	Scheme of a track circuit operation: Excited relay corresponds to a go-head condition, while a Not-Excited relay means that the first wheelset of a vehicle has crossed the section.	21
2.10	Mobile block system: a) hard wall mobile block; b) soft wall mobile block.	23
2.11	Italian current signalling network, map from RFI Piano di sviluppo ERTMS [5]. . .	27
3.1	Architecture of the developed model.	29
3.2	Architecture of the vehicle dynamical model.	31
3.3	Example of typical braking and traction behaviour of electric motors, characterised by an isotorque phase, an isopower one and a phase where the power is inversely proportional to speed.	32
3.4	Comparison between Muller approach and TSI limitations.	34
3.5	Power fluxes involved in electrical traction and braking: W_e is the recovered electrical power, W_{esd} the power stored on energy storage devices, W_{aux} the contribution due to the auxiliary systems and W_l the power redirected to the line. . .	36
3.6	Scheme of calculation of pantograph voltage and power, including the voltage limiter.	37
3.7	Main SIMSCAPE TM blocks implemented in the developed model: a) resistance, b) capacity, c) inductance and d) voltage source.	39
3.8	Architecture of the electrical model.	40
3.9	Scheme of feeding line electrical model.	42
3.10	Example of complex topology configuration.	43
3.11	Scheme of a 3kV electric substation.	44

3.12	SIMSCAPE™ model of the electrical substation.	46
3.13	Generic energy storage device model scheme.	47
3.14	Implemented battery model, including the evaluation of the S.O.C..	49
3.15	Voltage as a function of S.O.C. for the implemented battery model.	49
3.16	Charge and discharge behaviour of the implemented battery model.	50
3.17	SIMSCAPE™-Simulink battery model implementation.	51
3.18	SIMSCAPE™-Simulink scheme of battery switch.	52
3.19	SIMSCAPE™-Simulink scheme of a battery switch for the scenario with two vehicles moving in opposite directions.	52
3.20	Multi-vehicle configuration scheme: vehicles with the same travelling direction.	55
3.21	Multi-vehicle configuration scheme: vehicles with opposite travelling directions.	56
3.22	Supervision phases of a signalling speed profile: Ceiling Speed Monitoring (CSM), Pre-Indication Monitoring (PIM), Target Speed Monitoring (TSM) and Release Speed Monitoring (RSM).	58
3.23	Supervision points (Indication, Permitted speed, Warning and Service Brakes Intervention) and EBD curve.	59
3.24	EBD evaluation through the a_{brake_safe} and $a_{gradient}$ contributions.	61
3.25	Emergency braking performance dispersion due to dry conditions.	62
3.26	MATLAB® function for braking curves calculation.	69
3.27	Vehicle speed as a result of the comparison between mission and signalling velocity profile.	70
4.1	Rimini-Bologna rail line, focus on the section from Forlì Villanova to Rimini.	75
4.2	Traction and electrical braking performances of E464 locomotive.	75

4.3	Equivalent slope for the even rail from Forlì Villanova to Rimini.	77
4.4	Traction and electrical braking performances of ETR 1000 high-speed train.	78
4.5	Equivalent slope of about 50 km of the <i>Direttissima</i> line.	78
4.6	Comparison between numerical results and experimental data for the ETR 1000: speed profiles.	80
4.7	Comparison between numerical results and experimental data for the ETR 1000: current at the pantograph.	81
4.8	Comparison between numerical results and experimental data for the ETR 1000: voltage at the pantograph.	81
4.9	Comparison between numerical results and experimental data for the ETR 1000: power consumption.	82
4.10	Feasibility analysis: ETR 1000 mission profile and simulated velocity.	83
4.11	Feasibility analysis: ETR 1000 braking distance with respect to the braking request.	84
4.12	Feasibility analysis: ETR 1000 braking time with respect to the braking request.	84
4.13	Feasibility analysis: ETR 1000 voltage peaks as a function of braking request and braking position.	85
4.14	Feasibility analysis: ETR 1000 energy fluxes at 50% of braking position.	86
4.15	Feasibility analysis: ETR 1000 energy fluxes at 80% of braking position.	86
4.16	Feasibility analysis: ETR 1000 energy contributions at 50% of braking position with a 45% of braking request.	87
4.17	Feasibility analysis: ETR 1000 energy contributions at 80% of braking position with a 45% of braking request.	88
4.18	Feasibility analysis: E464 locomotive and 5 ViValto coaches voltage peaks as a function of braking request and braking position.	89

4.19	Feasibility analysis: E464 locomotive and 5 ViValto coaches energy fluxes.	90
4.20	Feasibility analysis: E464 locomotive and 5 ViValto coaches energy contributions at 80% of braking position with the maximum braking request.	91
4.21	Considered operating scenarios: two vehicles, moving in the same direction and two vehicles moving in opposite directions.	92
4.22	Scheme of line architecture for the optimisation analysis.	93
4.23	ETR 1000 optimisation analysis, first scenario: delayed departures of the two trains.	94
4.24	ETR 1000 optimisation analysis, first scenario, first simulation: batteries behaviour.	94
4.25	ETR 1000 optimisation analysis, first scenario, first simulation: energy fluxes. . . .	95
4.26	ETR 1000 optimisation analysis, first scenario, second simulation: energy fluxes. .	95
4.27	ETR 1000 optimisation analysis, second scenario, first simulation: batteries behaviour.	96
4.28	ETR 1000 optimisation analysis, second scenario, first simulation: energy fluxes. .	97
4.29	ETR 1000 optimisation analysis, second scenario, second simulation: batteries behaviour.	98
4.30	ETR 1000 optimisation analysis, second scenario, second simulation: energy fluxes.	98
4.31	ETR 1000 optimisation analysis, second scenario, third simulation: batteries behaviour.	99
4.32	ETR 1000 optimisation analysis, second scenario, third simulation: energy fluxes. .	99
4.33	E464 optimisation analysis, first scenario, first simulation: delayed departures of the two trains.	100
4.34	E464 optimisation analysis, first scenario, first simulation: batteries behaviour. . . .	101
4.35	E464 optimisation analysis, first scenario, first simulation: energy fluxes.	101

4.36 E464 optimisation analysis, first scenario, second simulation simulation: batteries behaviour.	102
4.37 E464 optimisation analysis, second scenario, second simulation: battery behaviour.	103
4.38 E464 optimisation analysis, second scenario, third simulation: battery behaviour. .	104
4.39 Example of braking curves calculated by the developed model.	105
4.40 Example of comparison between signalling, mission and vehicle speed profiles. . .	106
4.41 Signalling profile division to supervise vehicle velocity and position.	107
4.42 Recovered energy, for the E464 commuter train, in presence or absence of the signalling system.	108
4.43 Recovered energy, for the ETR 1000 high-speed train, in presence or absence of the signalling system.	109
4.44 Energy contributions with a slowdown during the vehicle route.	110
4.45 Energy contributions with a service brake deceleration due the ETCS intervention, during the vehicle route.	111
4.46 Energy contributions with an emergency brake deceleration due to the ETCS intervention, during the vehicle route.	112
4.47 Results on saved energy with respect to different EBD application number, for the commuter train, for short, medium and long routes.	113
4.48 Results on saved energy with respect to different EBD application number, for the high-speed vehicle, for short, medium and long routes.	114
5.1 Example of station with its signalling plan.	119
5.2 Interaction between on board vehicle system and the ground subsystems, from RFI Sistema controllo marcia treno [6].	120

List of Tables

- 2.1 Main characteristics of different battery types. 20

- 3.1 Braking space parameters values range. 64
- 3.2 Braking time characteristics values range. 66
- 3.3 Speed limits parameters values range, *A1* approach. 68
- 3.4 Speed limits parameters values range, *A2* approach. 68

- 4.1 E464 commuter train and Rimini-Bologna line characteristics. 76
- 4.2 ETR 1000 High-Speed train and *Direttissima* line characteristics. 79
- 4.3 Analysis cost of battery implementation within the considered lines. 115

Symbols

a	Acceleration	$[m/s^2]$
a	Vehicle motion resistance coefficient	$[1/(m \cdot s^2)]$
a_v	Signalling calculation coefficient	$[-]$
b	Vehicle motion resistance coefficient	$[1/s^2]$
b_v	Signalling calculation coefficient	$[-]$
c	Vehicle motion resistance coefficient	$[m/s^2]$
c_r	Signalling coefficient	$[-]$
c_v	Signalling calculation coefficient	$[-]$
d	Vehicle motion resistance coefficient	$[m/s^2]$
d	Deceleration	$[m/s^2]$
f	Frequency	$[Hz]$
f_0	Static friction factor	$[Hz]$
g	Gravity acceleration	$[m/s^2]$
h	Delay time	$[s]$
i	Line slope	$[-]$
i_c	Curves resistance coefficient	$[-]$
k_{muller}	Muller coefficient	$[-]$
l	Line span length	$[m]$
m	Mass	$[kg]$

n_C	Signalling coefficient	[–]
n_{cell}	Energy storage device number of cells	[–]
r	Line curves radius	[m]
t	Time	[s]
v	Velocity	[m/s]
x	Vehicle position	[m]
x	Signalling coefficient	[–]
y	Signalling coefficient	[–]
A	Signalling coefficient	[–]
B	Signalling coefficient	[–]
C	Capacitance	[F]
C	Signalling coefficient	[–]
D	Safety coefficient	[–]
E	Energy	[J]
EP	Electro-pneumatic braking conditio	[–]
I	Current	[A]
I	Indication	[–]
K	Protection coefficient	[–]
K_{i1}	Signalling calculation coefficient	[–]
K_{i2}	Signalling calculation coefficient	[–]
K_{i3}	Signalling calculation coefficient	[–]
L	Inductance	[H]
L	Train length	[m]
P	Permitted Speed	[–]
R	Resistance	[Ω]
R	Rotating mass contribution	[$\%$]
S	Braking space	[m]
T	Vehicle traction and braking force	[N]

V	Voltage	[V]
V	Speed	[m/s]
V_c	Signalling coefficient	[-]
W	Power	[W]
W	Warning	[-]

Greek letters

α	Line slope	[rad]
β	Braking command	
Δ	Difference	
η	Efficiency	[-]
μ	Adherence	[-]
ρ	Line distributed impedance	[Ω/m]
ϕ	Phase	[rad]

Subscripts and superscripts

//	Parallel connection
*	Reference or limit value
0	Nominal
0	Target speed
1	Before the vehicle
2	After the vehicle
<i>appl</i>	Applied
<i>avail</i>	Available
<i>aux</i>	Auxiliary
<i>b</i>	Braking
<i>batt</i>	Battery
<i>brake_{safe}</i>	Emergency safe

<i>c</i>	Collected
<i>c</i>	Curves
<i>C</i>	Correction
<i>cell</i>	Energy storage device cell
<i>e</i>	Electrical
<i>eq</i>	Equivalent
<i>esd</i>	Energy Storage Device
<i>ESS</i>	Electrical substation
<i>f</i>	Final
<i>gearbox</i>	Transmission system
<i>gradient</i>	Track slope
<i>i</i>	Inertial
<i>i</i>	Track Slope
<i>init</i>	Initial
<i>kmh</i>	km/h
<i>l</i>	line
<i>m</i>	Mechanical
<i>max</i>	Maximum
<i>motor</i>	Electric motor
<i>motordrive</i>	Motor drive
<i>nom</i>	Nominal
<i>P</i>	Permitted
<i>p</i>	Line profile
<i>p</i>	Braking system
<i>r</i>	Braked mass percentage
<i>rec</i>	Recovered
<i>r</i>	Protection
<i>requested</i>	Requested

<i>safe</i>	Safe
<i>sav</i>	Saving
<i>SBI</i>	Service Brake Intervention
<i>t</i>	Traction
<i>T</i>	Maximum due to traction system
<i>tot</i>	Total
<i>TT</i>	Maximum Time
<i>W</i>	Warning
<i>wheels</i>	Wheel/rail contact point

Acronyms

<i>CSM</i>	Ceiling Speed Monitoring
<i>EBD</i>	Emergency Braking Deceleration
<i>EBI</i>	Emergency Braking Intervention
<i>ERA</i>	European Union Agency for Railway
<i>ERTMS</i>	European Rail Traffic Management System
<i>ESD</i>	Energy Storage Device
<i>ESS</i>	Electrical Substation
<i>ETCS</i>	European Train Control System
<i>ETR</i>	Elettro Treno Rapido
<i>MRS P</i>	Most Restrictive Speed Profile
<i>PIM</i>	Pre-Indication Monitoring
<i>RFI</i>	Rete Ferroviaria Italiana
<i>RS M</i>	Release Speed Monitoring
<i>SBI</i>	Service Brake Intervention
<i>SOC</i>	State Of Charge
<i>SSB</i>	Sotto Sistema di Bordo (on-board subsystem)
<i>SST</i>	Sotto Sistema di Terra (ground subsystem)

TSI Technical Specification for Interoperability

TSM Target Speed Monitoring

Abstract

Within the current worldwide economies and political scenarios, the transport sector has been pushing its investigation and research towards innovative technologies which can produce a lower environmental impact. The use of regenerative braking represents one of the most promising solution to improve the environmental sustainability of transport and the possibility to implement it both on commuter and high-speed vehicles represents an interesting scenario to improve the energetic efficiency of the whole railway sector. This thesis arises from the research activities of the TESYS Rail project, an Italian research project dedicated to the energetic innovation of railway systems. The development of a model which can simulate a complex railway system, including vehicle dynamics, feeding line with its substations, energy storage devices and signalling, represents the central target of this research work. The proposed model has been accurately validated from the energetic point of view considering experimental data provided by one of the industrial partners of the TESYS Rail project. After the experimental validation of the energetic model, a detailed feasibility analysis concerning the use of regenerative braking has been carried out, considering a commuter train, E464 locomotive with 5 ViValto coaches, within the Rimini-Bologna line, and a high-speed vehicle, the ETR 1000, within the Firenze-Roma line. The feasibility analysis has made possible to identify the perspectives of regenerative braking within railway systems which typically do not foresee such technology, highlighting how the energy savings could easily be significant. The following step of this research work is represented by the investigation of different traffic scenarios and their respective energy savings

for both types of vehicles: it has been possible to highlight that the ideal solution is the direct use of the energy, generated by a braking vehicle, by a close vehicle which is travelling within the same line. The analysis has also shown that the installation of energy storage devices in a line span where more than one braking vehicle is expected could greatly help recovered energy management. In the last part of the research activity, the supervision and intervention of the ETCS signalling system, through the use of the braking curves, have been implemented: the signalling system has a significant impact on the amount of recovered energy, in particular if the emergency brake system is used, but the economic and energetic savings are still important even in such more realistic scenario. The final outcome of this research work is that the future perspectives for the improvement of railway sustainability are significant and only need to be pursued and exploited: even if the search for new technological solutions represents the core of a real transport revolution, the path for a more sustainable railway sector could just start with the optimisation of vehicles time-tables and the harmonisation of railway traffic, which already prove to be a great opportunity to reach an improved environmental efficiency for railways.

1

Introduction

The economies and policies of worldwide countries are nowadays strongly focused on environmental sustainability: uncontrolled production of plastics, indiscriminate consumption of petroleum and the enormous CO_2 emissions have caused environmental problems which will be hard to resolve. To decrease this trend, the common objective of different nations is to find and investigate innovative technologies to enhance the environmental impact and the energetic efficiency of the main industrial fields.

The transport sector represents one of the fields on which the attention has focused: the European Environment Agency (EEA) studies and supervises the progress of EU transport sector on the environmental and climatic impact [1], [2]: greenhouse gas (GHG) emissions are increased since 2014. In particular, in 2016, transport emissions proved to be higher than about 26% with respect to 1990. Figure 1.1 shows the European greenhouse gas emissions, from 1990 to 2017: it is possible to highlight that, especially in certain sectors, as international aviation, the emissions have increased in the last period. These results fail the European targets in terms of environmental performances of the transport sector.

To answer to the worldwide demands, the improvement of environmental sustainability should go through the development of innovative technologies. The automotive field has invested on the development of vehicles with special traction systems: Granovskii et al. [7] have conducted analyses to compare economic and environmental aspects of conventional, electric, hybrid and

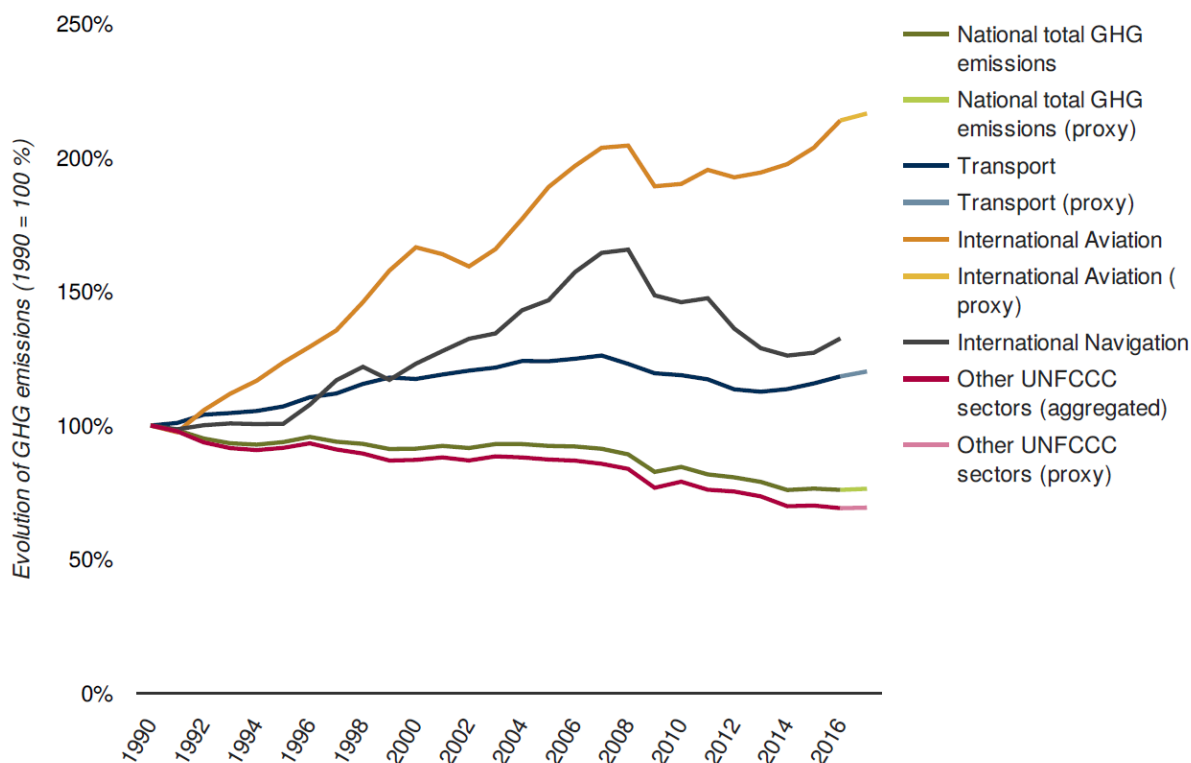


Figure 1.1: European evolution of greenhouse gas emissions from 1990 to 2017 [1], [2].

hydrogen fuelled vehicles. The analysis results show the advantages of the electric and hybrid cars with respect to the others, and the economics and environmental advantages, connected with these technology, depend on the source of the electric energy used by the vehicle.

While during the past years railways proved to be the most environmental-friendly transport system, especially due to the high number of passengers which can be transported, currently the gap with respect to the competitors is rapidly decreasing: the investigation of regenerative braking represents an important application to improve the energetic efficiency of the entire system. Furthermore, globalisation pushes towards the interoperability of vehicles among different nations: in Europe, Technical Specifications for Interoperability (TSIs) [8] have been developed to regulate the vehicles, which have to operate within different infrastructures and with different energy stakeholders. Figure 1.2 shows a scheme of the energy management according to TSI standards: a

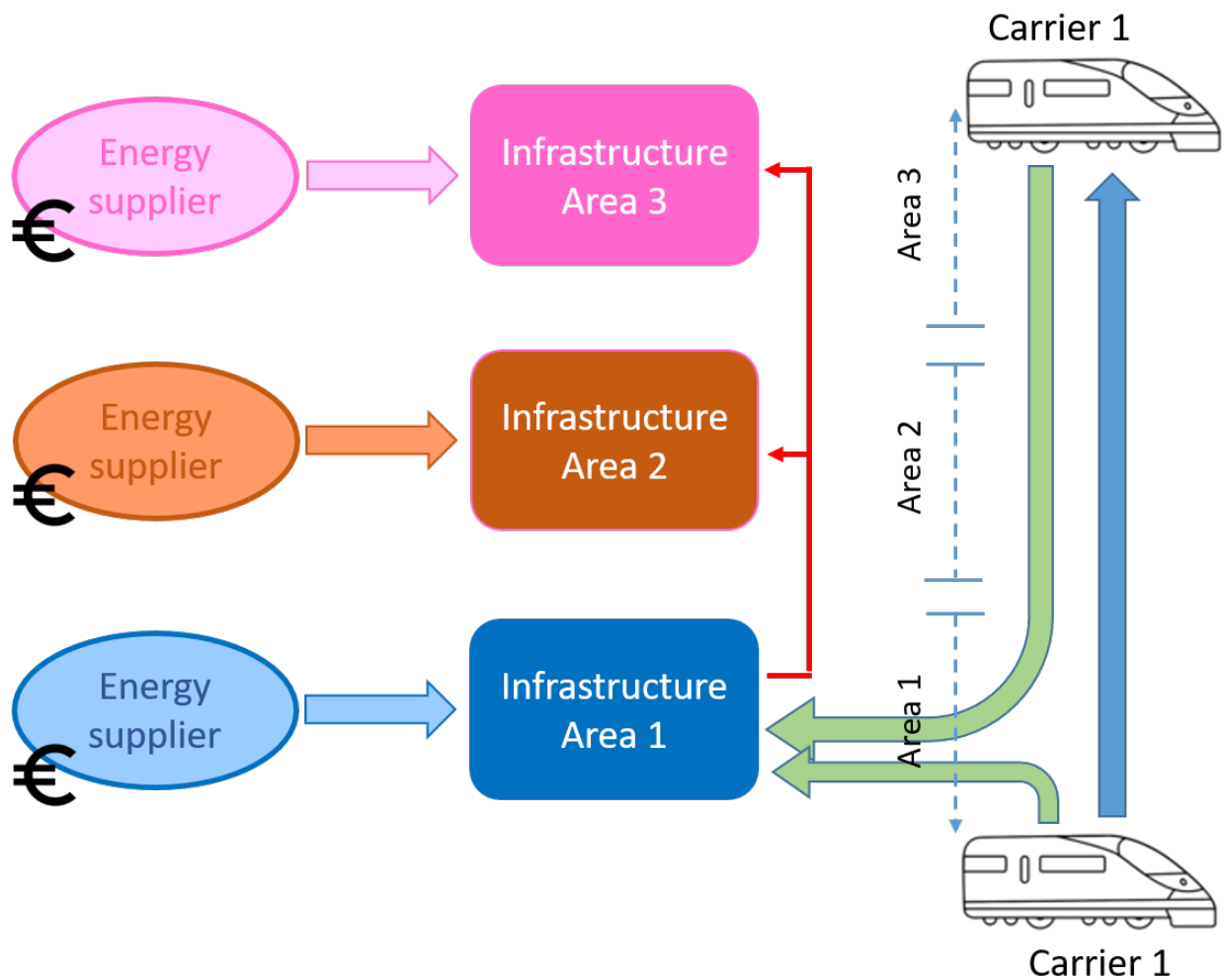


Figure 1.2: Energy management in an operating scenario.

vehicle, which is operated by a certain carrier, has to travel in different areas (e.g. different nations) equipped with different infrastructures. Furthermore, each infrastructure can be fed by a different energy supplier, with different costs and management strategies. The respect of TSI indications allows the coexistence of all different key players within a complex railway system.

To achieve the described target, regenerative braking represents one of the most promising sources to realise an energetic optimisation. This research work has started from the investigations on light railway applications, where the regenerative braking has a large diffusion [9], and then it has proceeded with the modelling of a more complex railway system. It has been developed within the

TESYS Rail project, acronym of *Methods and Instruments to improve environmental sustainability of railway systems*, which is an Italian research project, founded by the MIUR and involving a large number of different partners. Some operating conditions, included in the developed model and in the simulated scenarios, have been implemented to answer to the industrial partners requirements or availability.

1.1 General architecture of the model

The model, developed in this research work, has been realised through the use of MATLAB[®]-Simulink and MATLAB[®]-SIMSCAPE[™] environments, which allow the implementation of a parametric approach, currently used to simulate dynamical systems [10], [11].

The developed model is composed of three main sub-models, shown in Figure 1.3: the co-simulation of these three sub-models is based on the information interchanged between them at each time step, simulating the behaviour of a complex railway system.

The developed model includes the following elements:

- Vehicle longitudinal dynamics model: it analyses the mechanical behaviour of the vehicle, taking into account the interaction due to the braking and traction efforts and motion resistances, line and vehicle characteristics and adherence limits [12]. Moreover, a blending strategy, i.e. the handling of pneumatic and electric braking, has been implemented. The vehicle model provides, to the electrical and signalling ones, information concerning the vehicle position and velocity and the power requested or supplied, while, as inputs, it needs the power available along the line and the signalling speed profile.
- Electrical models: the feeding line, the energy storage devices and the substations have been modelled, taking advantage of the characteristics of the MATLAB[®]-SIMSCAPE[™] language. The line model is based on the variable impedance of the catenary due to the vehicle crossing, while the electrical substation has been modelled through a simplified approach, focusing on its energy supply function; the energy storage device has been modelled to represent a battery. These models provide information to the other sub-models concerning the available power within the line and they receive back vehicle position and speed.
- Signalling model: its goal is to supervise and control the vehicle mission and guarantee the respect of safety limits. The signalling model focuses on the implementation of the braking curves and on their intervention due to dynamical constraints, as red light signals

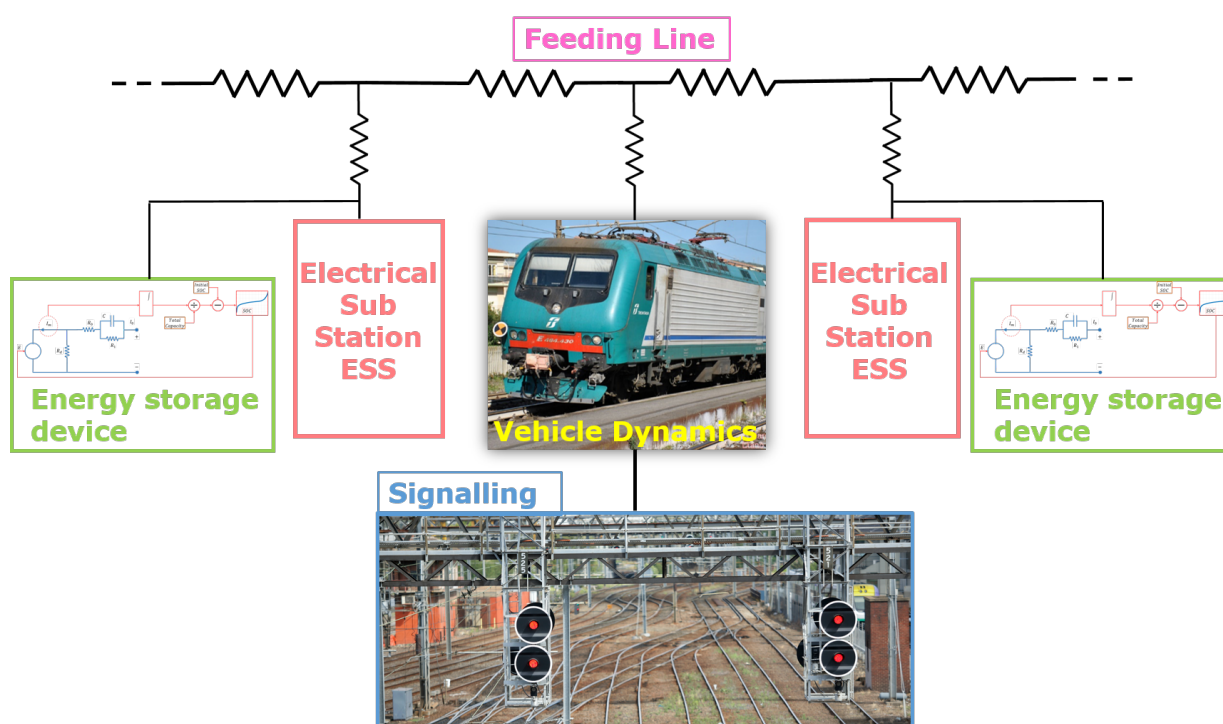


Figure 1.3: General architecture of the developed model, composed of a vehicle longitudinal dynamics model, an electrical one, which includes feeding line, substations and energy storage devices, and a signalling model.

or slowdowns. The signalling velocity is compared to the vehicle one, provided by the dynamical model, and the vehicle follows the lower between them.

The developed model proves to have the following characteristics:

- ✓ Modularity: the model can be adapted to reproduce different configurations.
- ✓ General and scalable approach: it is possible to simulate different operating scenarios with different railway vehicles, from light rail, as metros and trams, up to freight trains.
- ✓ High level language: an high level modelling environment has been used, allowing an easy maintenance and its use for industrial and research applications.
- ✓ Accuracy: the model represents a good compromise between accuracy and numerical

efficiency. Moreover, it can be adapted to produce code for real time applications, e.g for monitoring or diagnostic applications.

1.2 Objectives of the developed model

As mentioned, this research work has been developed within the TESYS Rail project, whose goal is to study how to improve the environmental sustainability of railway systems. The following list summarises the objectives of the proposed model:

- Development of a model able to co-simulate a complex railway system. In particular, it has to be able to simultaneously represent the behaviour of the main systems which intervenes in a railway operating scenario, i.e. the vehicle, the line and the connected electrical systems, and the signalling system.
- Focus on the system answer to the application of the regenerative braking. This represents one of the main source to achieve an energetic efficiency improvement and it can be performed by different vehicles, as commuter and high-speed trains.
- Investigation of different operating scenarios. Different lines travelled by different vehicles have to be studied, in particular investigating different traffic scenarios. These simulations provide important results in terms of energetic optimisation, detecting the ideal solution for different operating conditions.
- Analysis of a possible implementation of energy storage devices. The investigation of energy storage devices implementation along the lines can be carried out to evaluate the proper location for the devices, taking into account cost-benefit considerations.
- Investigation of the influence of the signalling system. To understand how the signalling can impact in an already optimised railway scenario, the effects of dynamical constraints and the application of the braking curves, which impedes the use of the regenerative braking, have to be considered.

The proposed model could be useful for the investigation of future designs of railway systems: the analysis of different lines and different vehicles, in different operating conditions, can be a fundamental tool for future investments concerning energy storage devices installation and for the

management of the railway traffic. The simulation of a realistic scenario can help to understand the possible applications of regenerative braking and the effective energy savings.

2

State of art

The main purpose of the TESYS Rail project, within which this research work has been developed, is the environmental sustainability of the railway system. One of the most promising possibility is represented by the use of regenerative braking: in light rail systems, the generation of usable energy through this technique represents a standard practice while, in the commuter and high-speed systems, it is usually neglected.

The application of regenerative braking is extensively used thanks to the standard implementation, in the modern vehicles, of distributed traction systems [13]: this braking procedure permits to achieve energy saving, avoiding the application of dissipative brake systems, both electrical and pneumatic, thus obtaining decrement concerning wear, due to the wheel/rail contact, and maintenance costs. Moreover, reducing the pollution, an improvement with respect to the environmental impact can be achieved [14], [15], [16]. The regenerative braking [17] is based on the capability to convert the kinetic energy of the vehicle, during the braked phase, in electrical energy: this is possible thanks to the electric motors, which can be used as generators, see Figure 2.1, which shows the four quadrant operating range, typical of these motors [13].

As shown in Chapter 3 and 4, those energy fluxes can be handled by energy storage devices [18], [19], connected in parallel to electrical substations or on-board the vehicle, or directly used by other vehicles, as shown in Figure 2.2: in fact, an accelerating vehicle can use the energy generated by a braking vehicle, which applies the regenerative braking, and sent back to the feeding line. If these

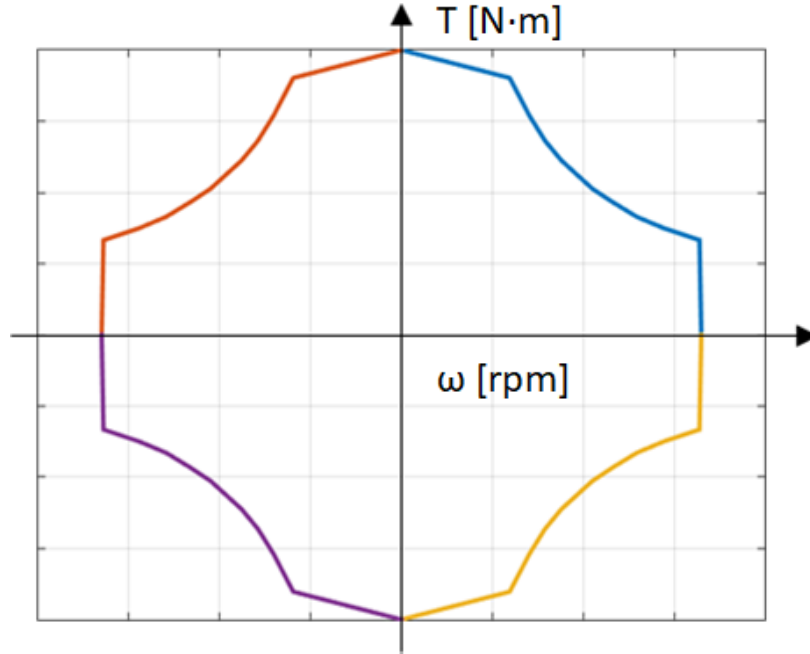


Figure 2.1: Electric motors four quadrants operating range.

solution are not available, the regenerated energy has to be dissipated, as well as it exceeds the safety limits, through resistors located on board the train, usually installed on the coach roof.

The mean and peak recovered power, during the braking phase, represent two important parameters to investigate the application of the regenerative braking. They can be investigated as follows:

$$W_{r,max} \propto m_i \dot{x}_{max} \ddot{x}_b, \quad (2.1)$$

$$W_{r,mean} \propto m_i \dot{x}_{max}^2 f_b, \quad (2.2)$$

where m_i represents the inertial mass, \dot{x}_{max} is the maximum train speed before the deceleration, \ddot{x}_b represents the imposed deceleration and f_b is the number of braking phases with respect to travelling time.

The main factors, which characterised Equations 2.1 and 2.2, assume different values with respect to the vehicle type: Figure 2.3 shows the comparison between these parameters. Due to the low

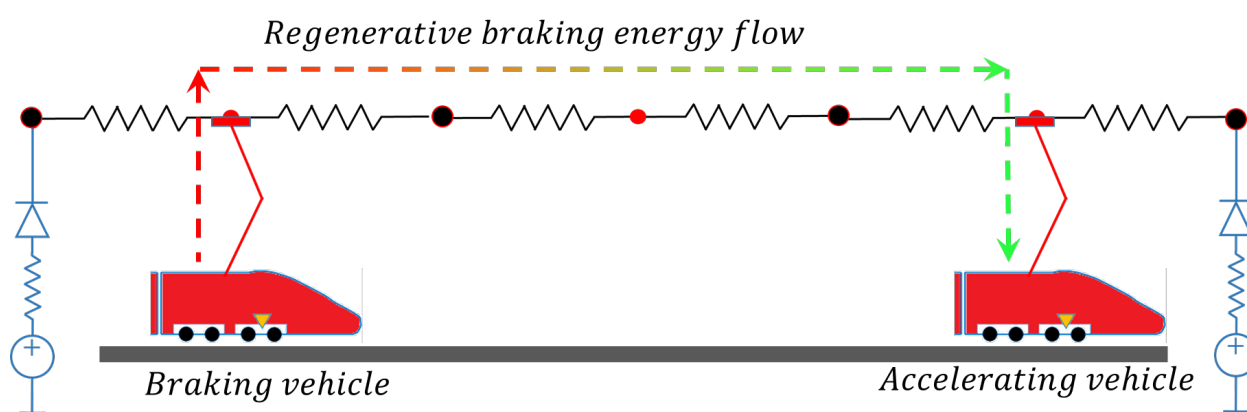


Figure 2.2: Regenerative braking energy flow, from a braking vehicle to an accelerating one.

masses and speeds, it proves to be extremely convenient and easy to perform regenerative braking within light railway systems [20],[21],[22], with different energy storage devices application and usage [23],[24] and different storage technologies [25]; concerning the high speed vehicles and commuter trains, the application of regenerative braking should be properly investigated. The high-speed vehicles, in fact, are characterised by high velocity and equivalent inertia, while the frequency of braking phases is lower than for light rail; the commuter trains parameters are located between the light and high-speed vehicles, thus proving to be another rail category which should be analysed.

The implementation of energy storage devices, on-board the vehicle [26] or along the feeding line [27], [28], does not represent the only method to obtain an improvement from an energetic optimisation point of view: Figure 2.4 [3] shows other methods to optimise the energetic efficiency of a railway systems. The investigation of these different possible applications is not the focus of this research work, but it is interesting to highlight how more than one solution can be adopted in a single system, each one with a different energetic impact, and the harmonization of these methods can lead to a really significant decrement of environmental and costs impact. Figure 2.5 highlights the relation between the energy savings and the investment costs of different optimisation approaches: the implementation of stationary storage devices or the use of reversible substations allows higher energy savings but the investment costs, including production and maintenance, are higher than the ones due to the application of the eco-driving and the optimisation













			
<i>Velocity</i>			
<i>Equivalent inertia</i>			
<i>Braking frequency</i>			

Figure 2.3: Comparison of typical regenerative braking parameters for different railway vehicles: yellow arrows show how commuter trains have intermediate characteristics with respect to high speed and light vehicles, e.g. an equivalent inertia which is higher with respect to light railways but lower with respect to high speed trains.

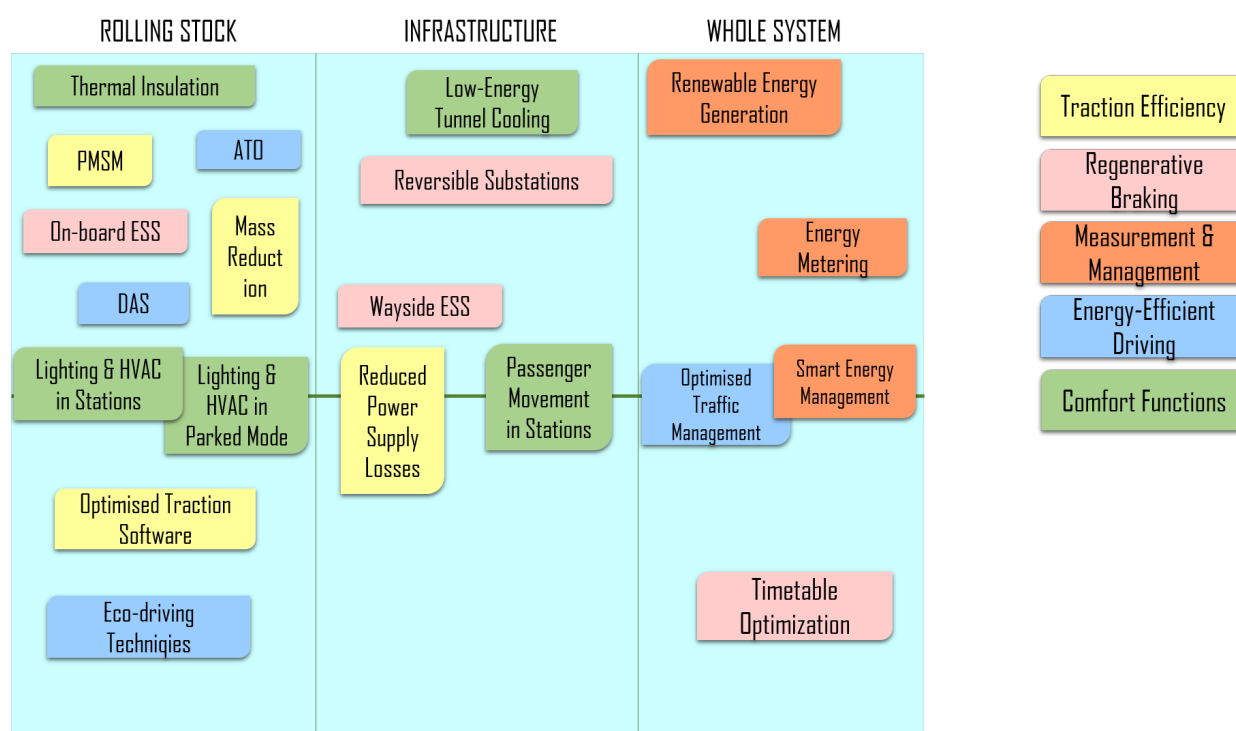


Figure 2.4: Different methods to achieve an energetic efficiency improvement [3].

of vehicles time-tables. The adopted solution hence will be the one which proves to be a better compromise between costs and benefits for the considered application.

A pneumatic brake system is installed on the vehicles, to cover the operating range where the use of the electric brake is limited. A compressed air system controls the movement of the brake pads on the discs, keyed on the wheelsets or on the wheels. The main problem connected with the use of pneumatic braking is represented by the wheel/rail wear, which increments the maintenance costs. The pneumatic braking system is also used for emergency braking, although this application is extraordinary and should be avoided. The blending strategy allows to control the use both electrical and pneumatic braking: safety and operational issues (such as the distinction between service and emergency braking) influence the complex interactions between different braking systems [29],[30],[31].

As above-mentioned, electrical motors are installed in modern rail vehicles and they can be used as generators, allowing the generation of energy flows, which can be saved and reused or, otherwise,

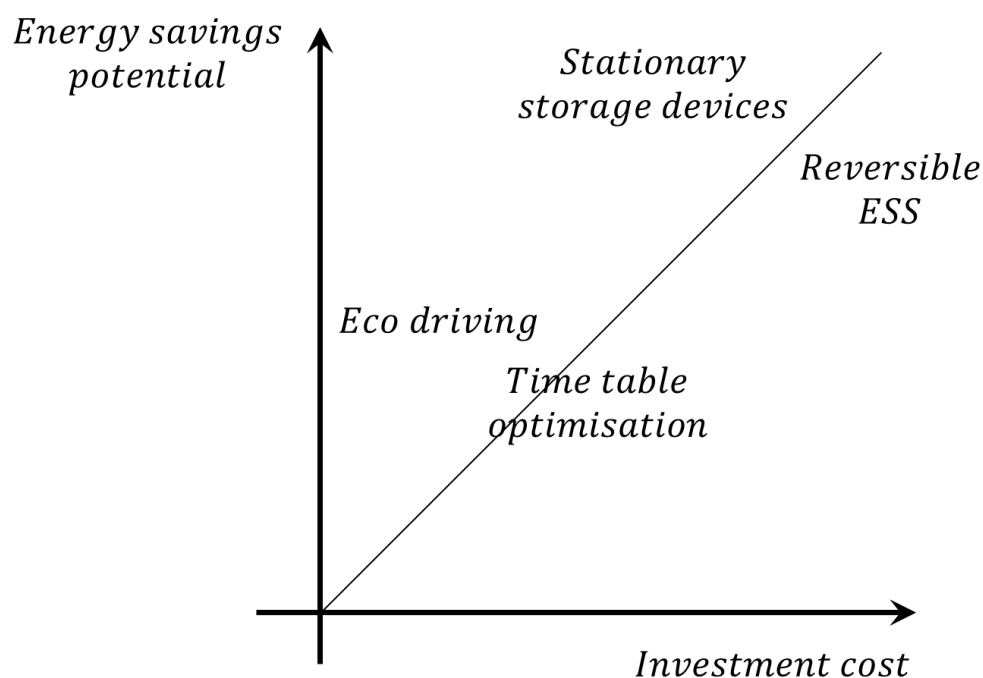


Figure 2.5: Relation between the energy savings potential and the investment costs for energetic optimisation applications.

dissipated [32]. Concerning the first case, the energy can be sent back to the line and it can be directly used by other close vehicles within the line, stored in energy storage devices [33] or received by electrical substations (to make it possible, they have to be reversible, i.e. they can receive back energy and not only provide it). The reintroduction of regenerated energy in the feeding line is related to problems of losses management (the European directive 440/91, which requires the accounting separation between carriers and infrastructure managers, is used in Italy). The energy storage devices can be installed along the line, able to receive energy from different vehicles, or on-board the vehicle: in this case, the recovered energy can be used only by the vehicle where the energy storage device is installed and it can be used, e.g., in catenary free operations, where the traction energy is not available from the feeding line, see Figure 2.6. They are composed by three main components: the energy storage device itself, a converter, which is able to manage the difference between the line and device voltage, and a controller, which can handle the charge and discharge process. The main parameters, which characterise energy storage

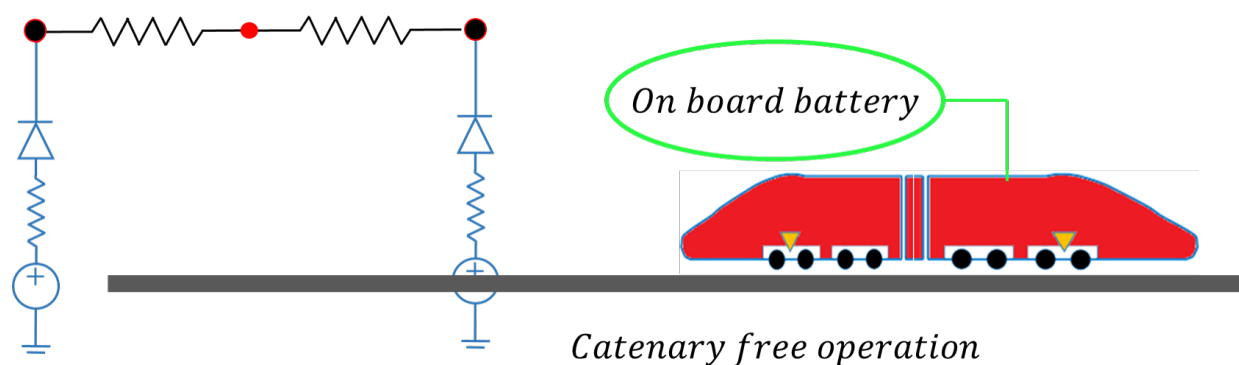


Figure 2.6: Example of usage of energy storage device installed on-board the vehicle.

devices, are represented by [34]:

- Specific energy: the unit is Wh/kg and it represents the energy which can be stored for unit mass.
- Specific power: the unit is W/kg and it represents the power, which can be provided for unit mass.

High specific energy and low specific power characterise the batteries, while the supercapacitors have opposite characteristics, as it is possible to see in Figure 2.7. Different types of batteries can be used, all of them based on electrochemical reactions; Table 2.1 reports the main typologies with their typical characteristics. Matheys et al. [4] have analysed the environmental impact of different electric vehicles batteries. Figure 2.8 shows the results concerning the environmental impact, in Eco-indicator points, of different batteries typologies, including the losses due to battery masses and to battery efficiencies during the usage.

Through the results provided by previous works, the energy storage devices which prove to be more suitable for high-speed and commuter train applications are represented by the batteries: despite the possibilities of supercapacitors, which typically have higher specific power, to handle the elevated peaks due to the high-speed vehicle braking, the batteries can store a larger quantity of energy and hence they have a higher autonomy. This represents an important aspect, due to the high cost of implementation and maintenance of the energy storage devices. Moreover, the

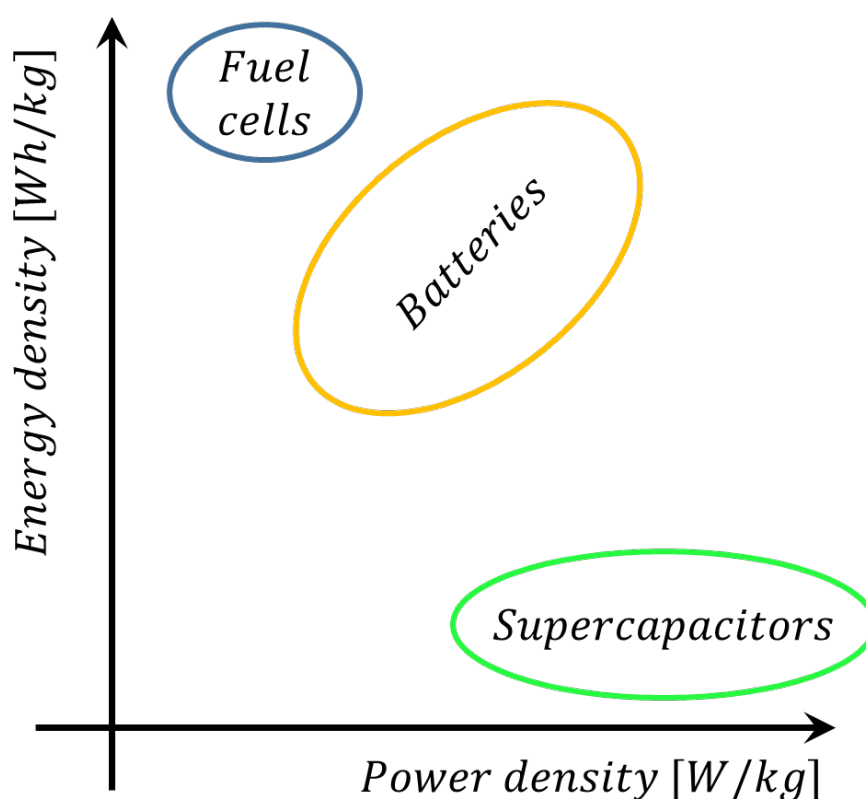


Figure 2.7: Energy storage devices characterisation with respect to energy and power density.

chosen battery for the model simulation is represented by the Li-ion battery [35], which has good characteristics (as reported in Table 2.1) and a low environmental impact (see Figure 2.8).

The vehicles have to interface, besides the feeding line [36], with another fundamental system, i.e. the signalling: it includes the supervision and control system, which allows to regulate the rail traffic and to respect safety standards, through a continuous information passage between the driver and the ground crew [37]. The signals denoted as *fixed* are permanently located along the line: they can be distinct in fixed or variable aspect, where the second typology includes the light signals.

The light signals can assume two different colours with respect to the following route occupation: a red light indicates that the rail section is occupied while a green light corresponds to a free section. When a vehicle travels along a rail section, the light signal changes from green to red, returning

Table 2.1: Main characteristics of different battery types.

Battery type	Specific energy [Wh/kg]	Specific power [W/kg]	Efficiency [%]
Pb-acid	20-50	25-300	70-90
Ni-Cd	30-75	50-300	60-80
Ni-MH	60-80	200-250	65-70
Li-ion	75-200	100-350	90-100
Li-Po	100-200	150-300	90-100
Na-S	120-240	120-230	75-90

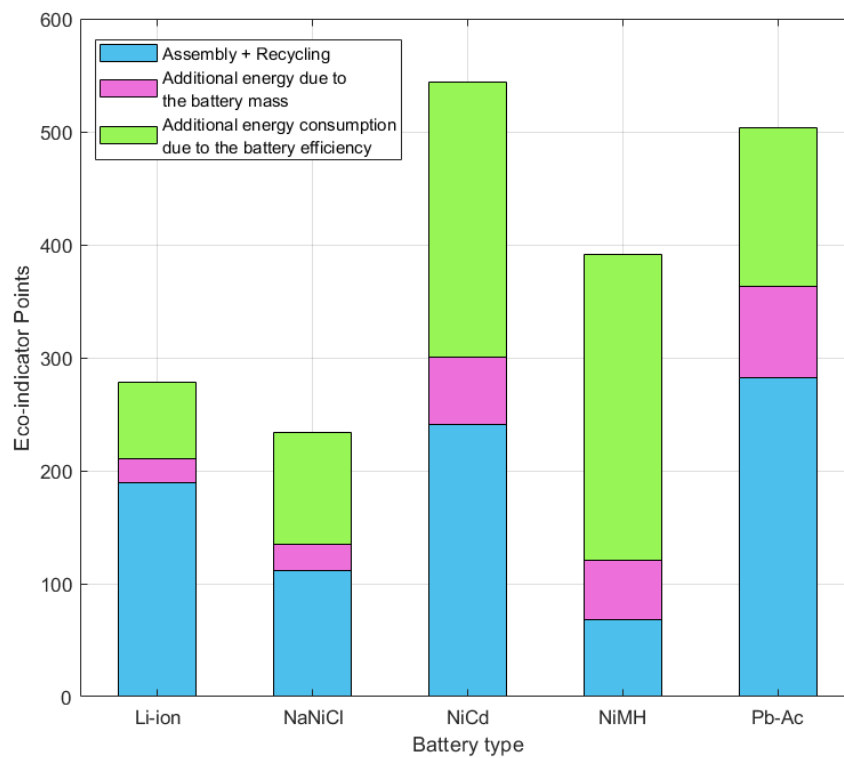


Figure 2.8: Environmental impact of different batteries typologies, including losses due to the batteries mass and efficiency during the use [4].

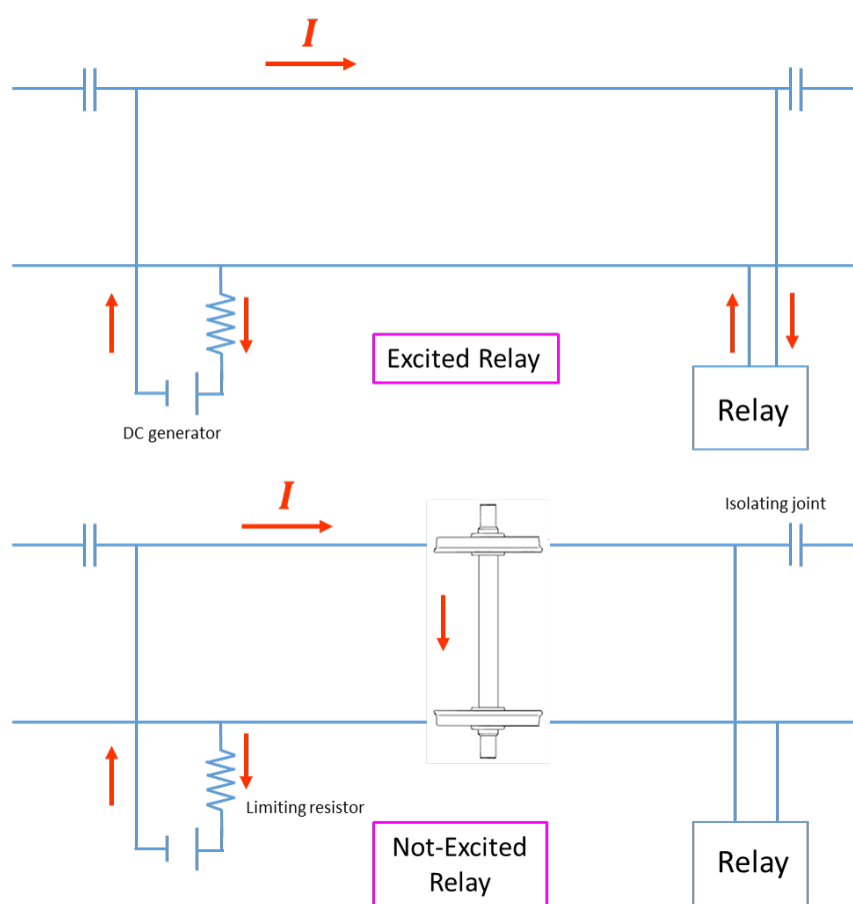


Figure 2.9: Scheme of a track circuit operation: Excited relay corresponds to a go-head condition, while a Not-Excited relay means that the first wheelset of a vehicle has crossed the section.

green when the train passes in another section. Moreover, an alert signal is located before the mentioned protection one to inform the train driver about the state of the following signal. The go-ahead permission can be granted by the ground crew or provided, automatically, through a system denoted as track circuit.

Figure 2.9 shows the functioning scheme of this electrical circuit: it is composed by the track rails, a generator and a track relay; the isolating joint, which disconnects just from an electrical point of view, delimits the track circuit. In a go-head condition, the current can cross the electrical circuit from the generator to the relay, which hence is in an excited condition; when the first wheelset of a vehicle crosses the section where the considered track circuit is installed, the wheelset itself causes a short circuit, which impedes the current circulation to the relay, making it not-excited. The track circuit is connected to a light signal, to inform the driver about the following section condition.

The described systems are the base of the vehicle distancing definition: the driver regulates the vehicle running through the information provided or received from the ground system, but the signalling system has to guarantee a proper vehicle distancing and the respect of safety limits, applying, in certain condition, proper braking curves (Chapter 3).

The modern railway signalling system realises a distancing based on the division of the line in section blocks and on the calculation of the space between two vehicles which travel along the same track in the same direction. The section blocks typology are divided in two categories:

- Fixed block: the line is split in fixed blocks section, where the vehicle is detected and occupies the track section. Through this approach, the vehicles are spaced considering the number of sections which allows the vehicle braking and the presence of a previous vehicle in a certain section. The fixed blocks distancing hence only permits the presence of one vehicle in each section. The transmission of information to the vehicle from the ground system can be discontinuous, when occurs only in defined points, where the light signals and/or commutative boas are located, or continuous, when the informations, e.g through the track circuit codified currents, are provided to the vehicle on an ongoing basis.
- Mobile blocks: the line is not divided in defined section blocks, because of the continuous

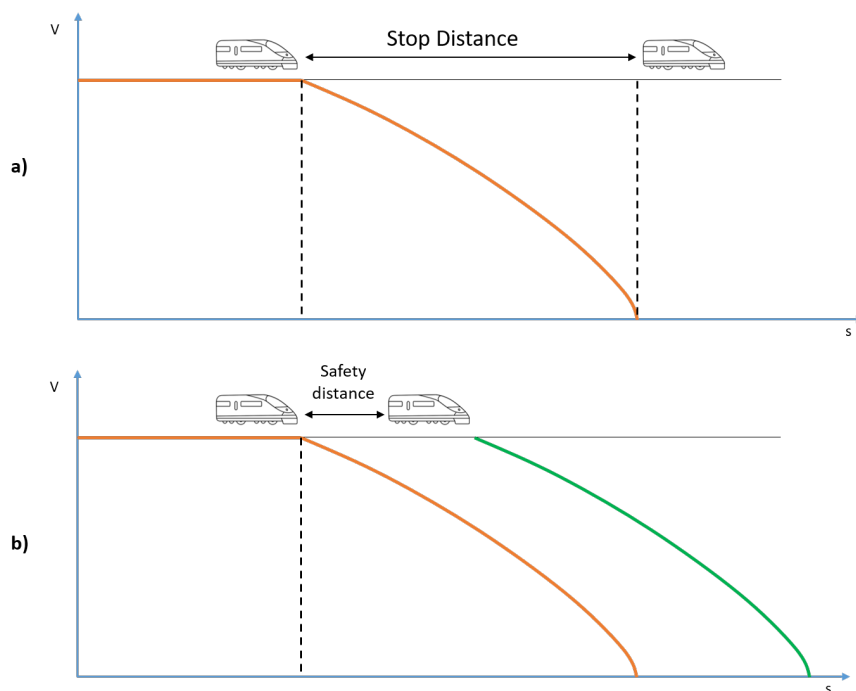


Figure 2.10: Mobile block system: a) hard wall mobile block; b) soft wall mobile block.

survey of the vehicles position; moreover, the vehicles can interchange these information with each others. The mobile blocks system can be divided in absolute and relative systems, see Figure 2.10. In the absolute ones, denotes as *hard wall moving block*, the minimum safety distance between the two vehicles, travelling along the same line in the same direction, is calculated assuming that, in a generic time step, the vehicle which is in an advanced position stops exactly in the position where it is, while the following vehicle has to be outdistanced of a safety distance, which has to be at least equal to the stopping distance. In the relative block system, denoted as *soft wall moving block*, the minimum distance between the two considered vehicle is calculated assuming that the following train reacts to the first train stop with a delay time and hence the safety distance has to be at least equal to the distance covered during the reaction delay time.

The available technologies allow the application of the hard wall mobile block, but the future research studies are projected to the realisation and implementation of the soft wall mobile block.

In the absolute mobile block approach, the minimum safety distance is calculated as follows:

$$S_d = R_d + S BMD, \quad (2.3)$$

where R_d represents the distance covered during the delay reaction time and $S BMD$ is the stop distance calculated through the application of the maximum service braking deceleration.

The relative mobile blocks approach evaluates the minimum safety distance through the following Equation:

$$S_d = R_d + BDM_{Firstvehicle} - BDM_{Secondvehicle}, \quad (2.4)$$

where $BDM_{Firstvehicle}$ and $BDM_{Secondvehicle}$ are respectively the stop distances of first and following vehicle.

The critical aspect which is imputed to the relative mobile block approach, is the possibility to run into a stop without almost covered space, as in the derailment case, or into an unexpected applied deceleration.

Rete Ferroviaria Italiana, part of Ferrovie dello Stato, since 2000, has elaborated an innovative control system which can be used with different circulation systems and denoted as *Sistema di Controllo Marcia Treno* (SCMT): it realises control and protection on the vehicle run, at every time step, applying a supervision function on the driver [6]. The SCMT intervention is activated by the exceeding of the following limits:

- Light signals defined conditions;
- Maximum allowed speed along the line;
- Maximum speed with respect to slowdowns;
- Maximum allowed speed for the rolling stock type.

The SCMT is composed of the ground subsystem (SST), which elaborates the information and transmits them to the vehicle, and the on-board subsystem (SSB), which receives the information and applies the proper protection, e.g., the intervention of the emergency brake in case of safety limits exceeding. The component of the SST are the station encoder systems, the line encoder

systems, the signal encoder and the infill system. The balises, or balises, of the line encoder systems, send information concerning the signalling operating conditions, line characteristics and possible slowdowns. To guarantee the respect of safety standards, two different balises are located close to each other (about 3m); they constitute an Information Point (PI). The SSB is composed of the on-board computer, which elaborates the information provided by the on-board sensors and the signalling system of the vehicle, the driver-machine interface, the collector antenna, which receives and elaborates the informations provided by the SST and then provides them to the on-board computer, and a collector system which can intercept the codified current.

The SSB compares, for each time step, the vehicle speed with respect to the signalling constraints and the vehicle and line characteristics: proper speedometers are installed on the vehicle and the measured space, velocity and acceleration are elaborated to generate a dynamic profile, which is compared with the allowed one. In case of excess, the driver is alerted through an acoustic signal and the on-board computer calculates the braking curves, compatible with the vehicle characteristics, to reach the safety limit velocity.

The signalling and control system are usually developed within every nation: thus the information and the components interfaces are different. Due to the modern interoperability goal in Europe states, the need of an integrated system, which can be used in more than one nation is arisen: the European Commission has thus developed the *European Rail Traffic Management System* (ERTMS), which allows advantages and upgrades in terms of performances, safety system and line potential. The ERTMS system is composed of two main components:

- √ European Train Control System (ETCS): it is a control and supervision system, which also provides to the vehicle driver information concerning the line and the imposed speed.
- √ GSM-R: it is a radio transmission system, which uses railway dedicated frequencies to interchange information between the SSB and the SST.

Moreover, the use of the ERTMS/ETCS can improve the train control approach, allowing:

- An increment of existing line potential: a continuous communication signalling system can reduce the vehicles distance up to 40 %;

- higher velocities (estimated up to 500 *km/h*);
- higher reliability;
- lower production costs;
- lower maintenance costs.

The greater advantage of the ERTMS/ETCS system is represented by what is at its base, i.e. the public access to technical specifications: this can guarantee the interoperability of the ETCS systems even through the components are provided by different supplier.

The ERTMS/ETCS system operates on 4 levels, differentiated on the base of vehicle and line equipments: the increment of level corresponds to an increment of potential and safety, even if the vehicle speed is continuously supervised and the exceeding of speed limits involves the emergency intervention for every ERTMS/ETCS level. Level 1 system allows the equipping of traditional signalling lines and the coexistence of two types of railway traffic, national and interoperable; it requires a fixed block distancing. Due to the large diffusion of the SCMT systems, the Italian railways has focused on the compatibility of this system with the 1st level ETCS; moreover, a development plan for the ERTMS/ETCS implementation and diffusion has been designed by RFI [5].

Figure 2.11 shows the current Italian railway signalling network.



Figure 2.11: Italian current signalling network, map from RFI Piano di sviluppo ERTMS [5].

3

Materials and methods

Chapter 3 aims to describe the different parts which compose the model behind this research project. In particular, the different sub-models components modelling and their interactions are described, in order to properly represent a complete railway system. Three main domains are investigated and modelled:

- √ Vehicle dynamics;
- √ Electrical line, including:
 - Feeding line;
 - Energy storage devices;
 - Substations;
- √ Signalling.

As shown in Figure 3.1, the whole model is designed for the co-simulation of different sub-models, which interchange information with each other. The dynamical vehicle model calculates, and provides to the electrical and signalling ones, position and velocity of the vehicle. The signalling model uses these data to calculate the braking curves, while the electrical one evaluates and gives back the available power. As a result of the signalling and mission profile comparison, the vehicle tries to follow, at each time step, the lower one, to respect the safety limits.

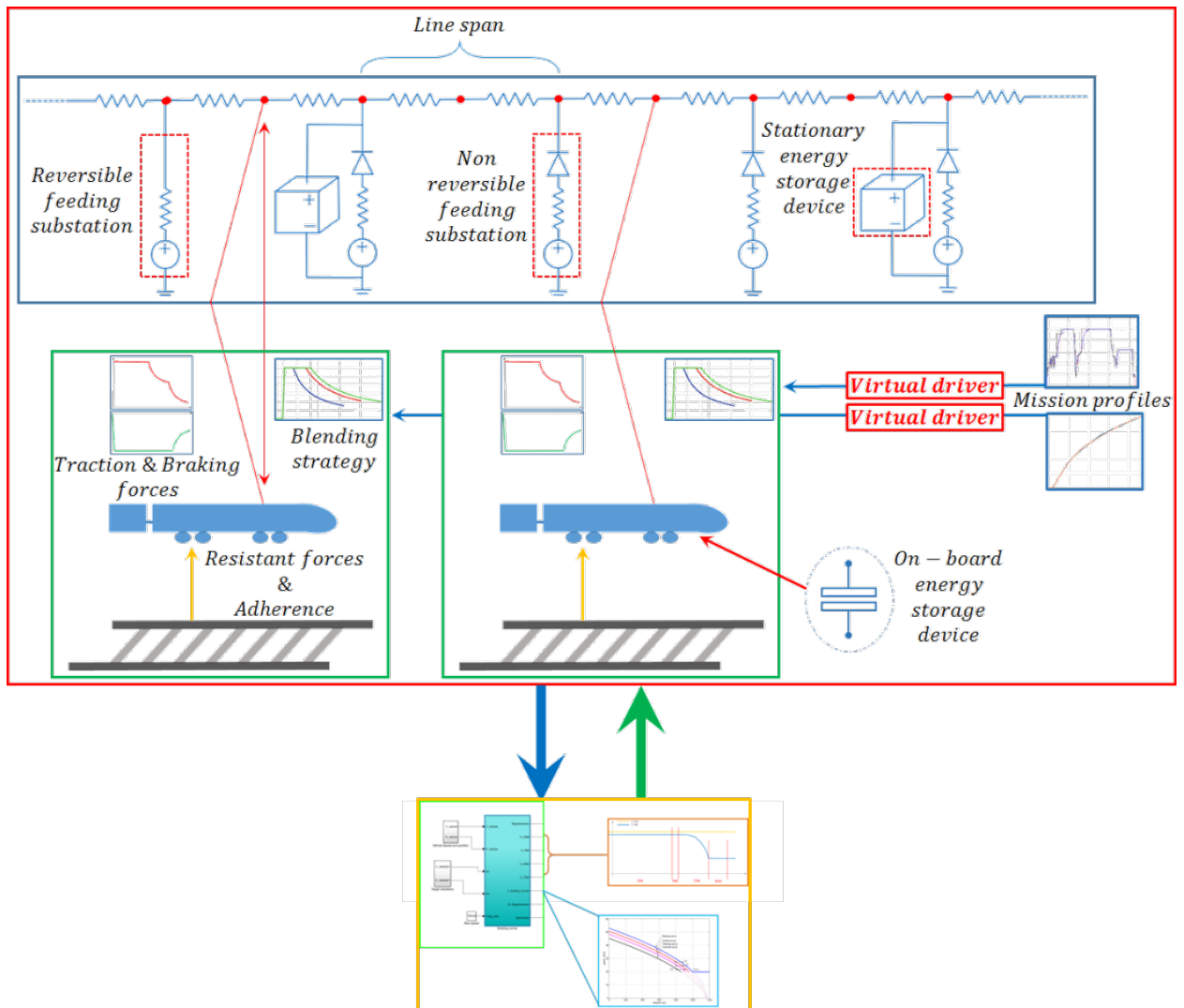


Figure 3.1: Architecture of the developed model.

3.1 Vehicle dynamical model

To investigate the behaviour of the vehicle and to represent his longitudinal dynamics, the lumped parameters approach has been used: through discrete elements, the system space is divided in a finite dimension and the continuous space and time partial differential equations, which describe the considered physical system, are simplified into ordinary differential ones, where the parameters number is finite. The proposed model is developed in MATLAB®-Simulink environment, where multi-domain dynamical systems can be modelled and simulated, in particular using MATLAB®-SIMSCAPE™ blocks. The dynamical model, shown in Figure 3.2, is composed of a set of subsystems, linked to each other. A mission profile can be chosen by the user: the braking and traction forces are applied dynamically and, when they reach the adherence limits, they are saturated; moreover, the model takes into account motion resistance. Through these forces and the train speed, the dynamical model can calculate the requested power (or the provided one, during the regenerative braking phase). As inputs for the feeding line and signalling models, the dynamical part provides the position, velocity and the power needed to follow the imposed mission profile.

3.1.1 Vehicle longitudinal dynamics and motion resistance

The equation of motion, on which the vehicle dynamics is based, is the following one:

$$m_i \ddot{x} = T - mg \sin \alpha - m(a\dot{x}^2 + b\dot{x} + c + d(r)) - mgi_c, \quad (3.1)$$

where m_i is the train inertial mass, T the longitudinal force, m the whole vehicle mass, g the gravitation acceleration, α the line slope, i_c the resistance due to the curves. Moreover, a , b , c and $d(r)$ are equivalent coefficients, which allow to represent the motion resistance as a function of velocity, internal frictions and additional resistance due to the curve with a radius equal to r .

The left side of the Equation 3.1 represents the inertial force and is calculated as follows:

$$F_i = -m_i a = -m_i \ddot{x}, \quad (3.2)$$

where m_i is the contribution of train inertial mass to the longitudinal motion, a is the acceleration (considered along the longitudinal coordinate). m_i is usually around 5–10% bigger than the vehicle

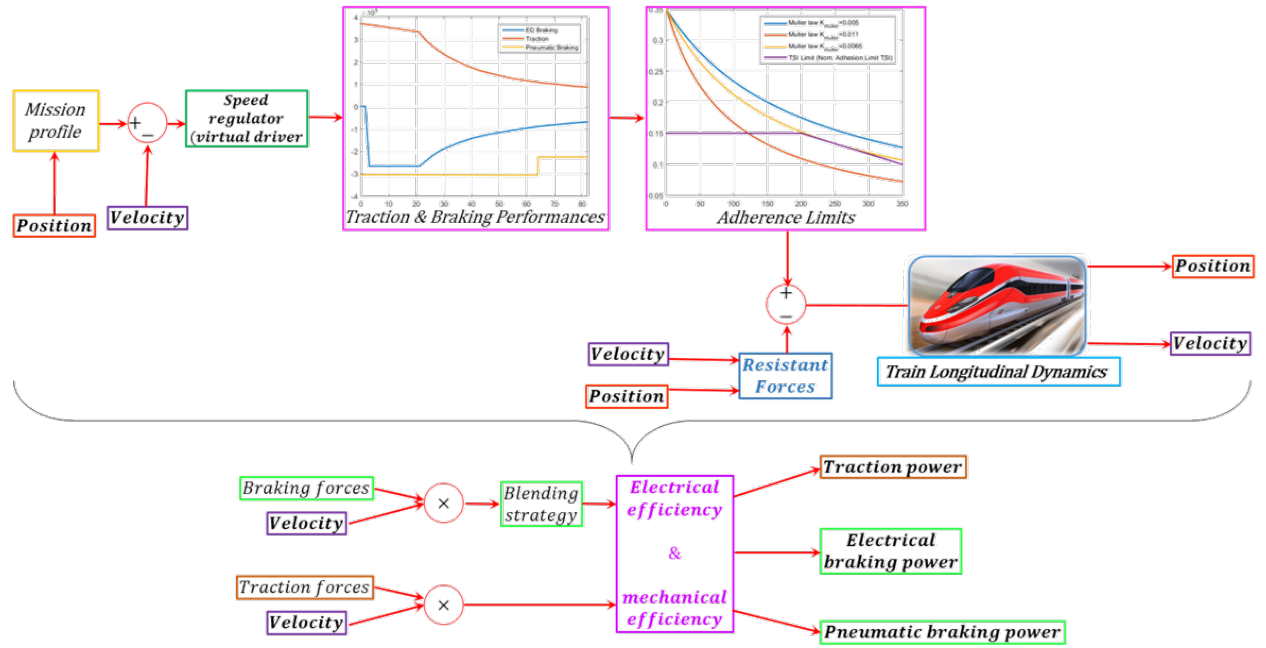


Figure 3.2: Architecture of the vehicle dynamical model.

mass: this is due to the contribution of the rotating masses, as transmission systems and motors. The third term of Equation 3.1 represents the force due to the line slope, i.e the altimetric profile of the track:

$$F_p = -mg \sin \alpha \approx -mgi. \quad (3.3)$$

The slope i is usually $< 20\%$: for this reason, $\sin \alpha$ can be approximated with the slope itself. Concerning the fourth term of the equation, it includes the aerodynamical resistance, the losses due to the contact between wheels and rail and the internal friction: the coefficients a , b , c and $d(r)$ depend on the vehicle type, especially on its mass and speed.

The last term, which can be denominated F_c , is the component which represents the resistance due to the curves of the track. To include these losses in the calculation of the equation of motion, the curves are implemented as an equivalent slope, estimated through the following formulation:

$$\begin{cases} i_c = \frac{650}{r-55} \%, & r > 400 \text{ m} \\ i_c = \frac{750}{r} \%, & 150 \text{ m} < r < 400 \text{ m} \\ i_c = 5\%, & r < 150 \text{ m} \end{cases} \quad (3.4)$$

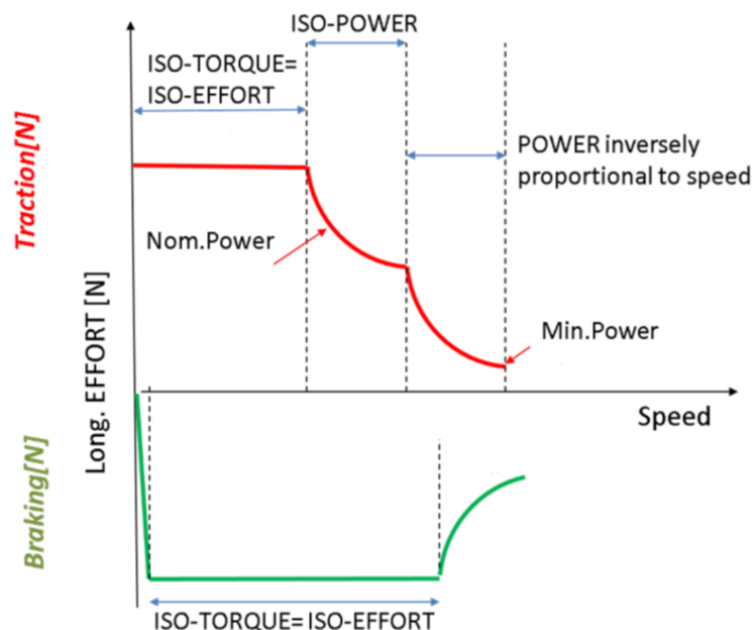


Figure 3.3: Example of typical braking and traction behaviour of electric motors, characterised by an isotorque phase, an isopower one and a phase where the power is inversely proportional to speed.

where this equivalent coefficient depends on the curves radius r .

The estimation of F_p and F_c is possible through MATLAB[®]-Simulink LookUp Tables: based on the train position, the software interpolates the technical data. The term which consider the aerodynamical and friction losses is calculated using the equivalent coefficient values, provided by the datasets of the vehicle. Through Equation 3.1, it is possible to calculate the vehicle acceleration and, integrating that variable, evaluate the train speed and position.

As mentioned, T represents the longitudinal force, which is applied by the traction and braking systems: it is exchanged between vehicle and rail, through the wheels, and it is saturated by the adherence limits (Section 3.1.2). Figure 3.3 shows the usual trend of the traction and braking curves of electric motors: concerning the traction effort, it is characterised by three different phases. The first one is an isotorque phase (i.e. a constant torque phase), described by the following Equation 3.5:

$$W = T v, \quad (3.5)$$

where W represent the requested power. This phase, once the vehicle has passed the nominal speed, is followed by an isopower one, where the power has a constant value (and the vehicle velocity is still under the maximum isopower speed); it is described as follows:

$$T = \frac{W}{v}. \quad (3.6)$$

In the last phase, which represents the final part of the operating condition, the power is inversely proportional to speed. The traction effort is properly saturated through the application of the adherence limit (Section 3.1.2).

The braking effort trend is shown in Figure 3.3. In the proposed model, the braking can be regulated by a variable, called *percen_fren*, which permits to decide the intensity of the braking effort: this approach permits to avoid to reach the line energy limit and, therefore, to avoid the dissipation of energy. The braking effort can be produced both by the mechanical and the electrical system and the handling of these two different braking systems is called *blending strategy*: it can be set by the user, depending on the application. Furthermore, through this strategy, it is possible to choose how to manage the electric braking energy: the extra energy, which cannot be accepted by the line (or all the braking energy if the line is not properly designed), can be dissipated and it is even possible to disable the regenerative braking. The pneumatic braking system takes into account TSI limitations.

3.1.2 Adherence

As mentioned in Section 3.1.1, concerning the traction and braking forces, in the developed model, the adherence, in wheel/rail contact, has been implemented to saturate the available efforts. The adherence μ is estimated both through the TSI limits and the Muller approach, which calculates the adherence coefficient as follow:

$$\mu = \frac{f_0}{1 + k_{Muller} \dot{x}_{kmh}}, \quad (3.7)$$

where the coefficient f_0 represents the static friction value (located in a values range between 0.35 and 0.4), k_{Muller} is a scaling parameter, valued between 0.005 and 0.011 and \dot{x}_{kmh} represents the

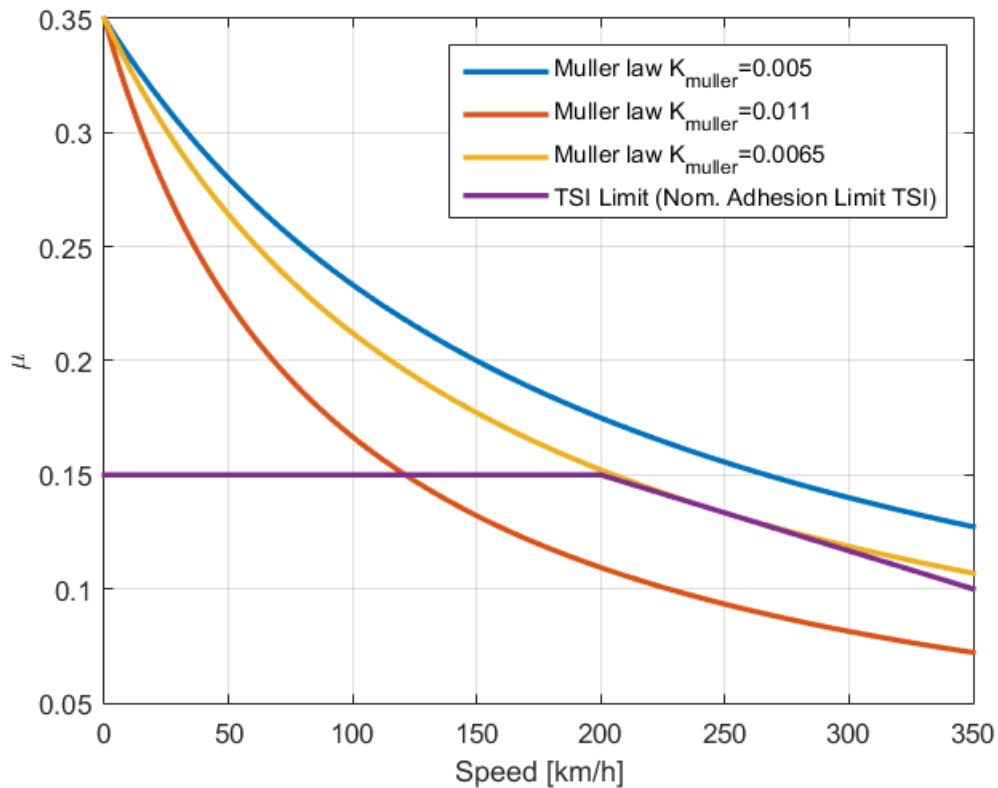


Figure 3.4: Comparison between Muller approach and TSI limitations.

vehicle velocity, expressed in km/h .

Figure 3.4 shows the comparison between the Muller approach and the TSI limitations.

3.1.3 Power

To optimise the vehicle energy consumption, the different contributions, which compose the energy balance, have to be calculated.

The power, requested to the electrical feeding line by the vehicle at the pantograph, is composed of the mechanical power provided by the traction system of the vehicle and the auxiliary power, due to the auxiliary systems contributions (e.g. air conditioning):

$$W_{requested} = W_{aux} + W_m. \quad (3.8)$$

W_m depends on the vehicle longitudinal velocity and on the T force, as it is possible to see in the following Equation:

$$W_m = T \dot{x}. \quad (3.9)$$

A part of W_m , during the braking phase, is dissipated by motion resistances and pneumatic brake, while the remaining part can be converted in electrical power, W_e , through the use of the motor as a generator.

The electrical power, generated during the braking phase, can be totally reused or partly dissipated: it depends on the blending strategy, used in the considered application, and on the safety limits of the line. To consider the correspondence between W_m and W_e , a coefficient of conversion η_{tot} , depending on longitudinal effort and velocity, has to be defined:

$$\eta_{tot}(T, \dot{x}) = \eta_e \eta_m \begin{cases} W_m \geq 0 \Rightarrow \eta_{tot} = \frac{W_m}{W_e} \\ W_m < 0 \Rightarrow \eta_{tot} = \frac{W_e}{W_m} \end{cases}. \quad (3.10)$$

The total conversion efficiency can be expressed as the product of the mechanical and electrical efficiencies, due to the different systems.

As mentioned before, the electrical power can be reused: it can be both redirected to the feeding line (and eventually used by another vehicle) and stored in energy storage devices. The application of one approach or another proves to be the result of an investigation on the vehicles traffic on the considered line and on the installation costs of on board or along the line devices.

Through Equation 3.11, the recovered electrical power W_e can be calculated as the sum of different contributions:

$$W_e = W_{esd} + W_l + W_{aux}, \quad (3.11)$$

where W_{esd} is the power stored on different energy storage devices, W_l is the power redirected to the line and W_{aux} represent the contribution due to the on board systems which request electrical power. The line impedance value is a function of the train position during the span crossing: in the W_l calculation, the power losses due to the line resistances has to be considered. Figure 3.5 shows the power fluxes, above described, involved in electrical traction and braking.

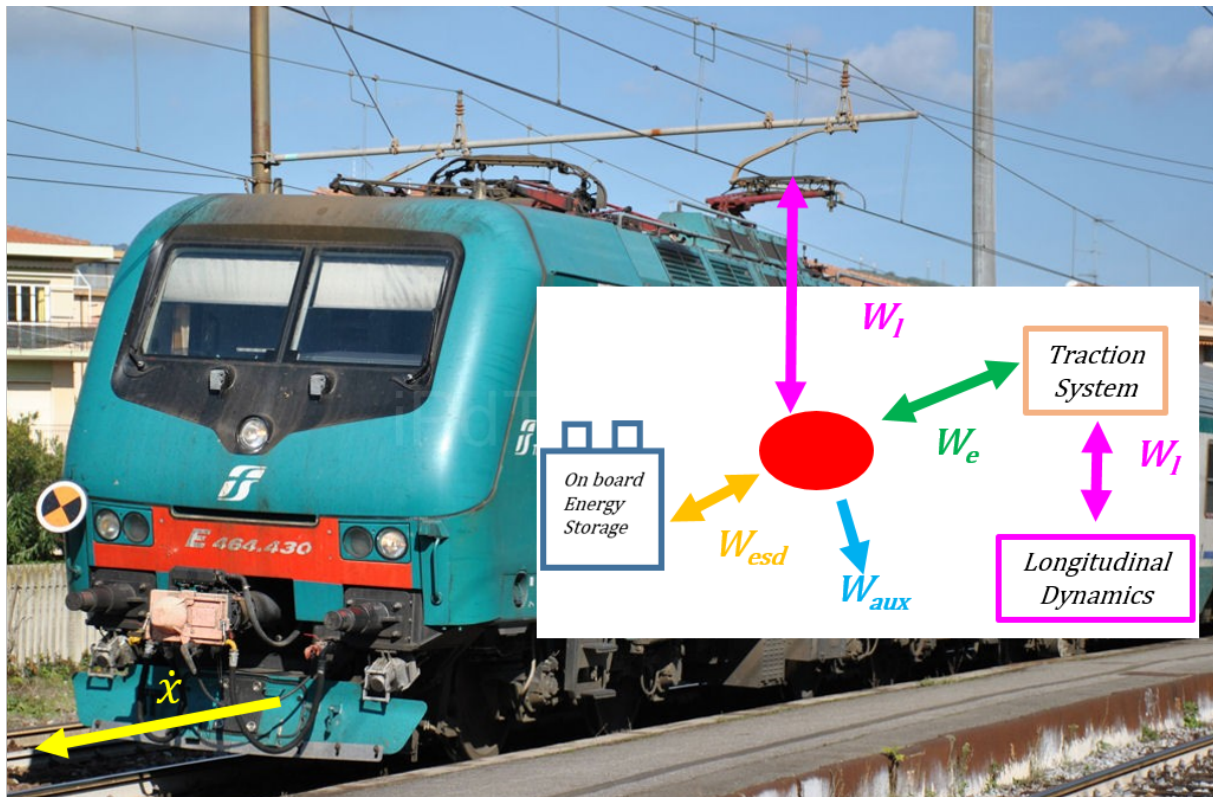


Figure 3.5: Power fluxes involved in electrical traction and braking: W_e is the recovered electrical power, W_{esd} the power stored on energy storage devices, W_{aux} the contribution due to the auxiliary systems and W_l the power redirected to the line.

3.1.4 Line voltage limit

Like in many others engineering fields, the users' and operators' safety represents one of the most important target of the whole design of a mechanical project. As a real operating condition, the line cannot receive an unlimited amount of energy provided by the regenerative braking of the vehicles: to consider the risks due to the excess of energy, a voltage limiter has been implemented in the proposed model.

Figure 3.6 shows the calculation of the effective pantograph power W_l . V_c represents the maximum voltage the line can bear respecting the safety limits: when the energy overcomes the aforesaid limitation, a first order filter regulates the power effectively sent back to the line. This first order

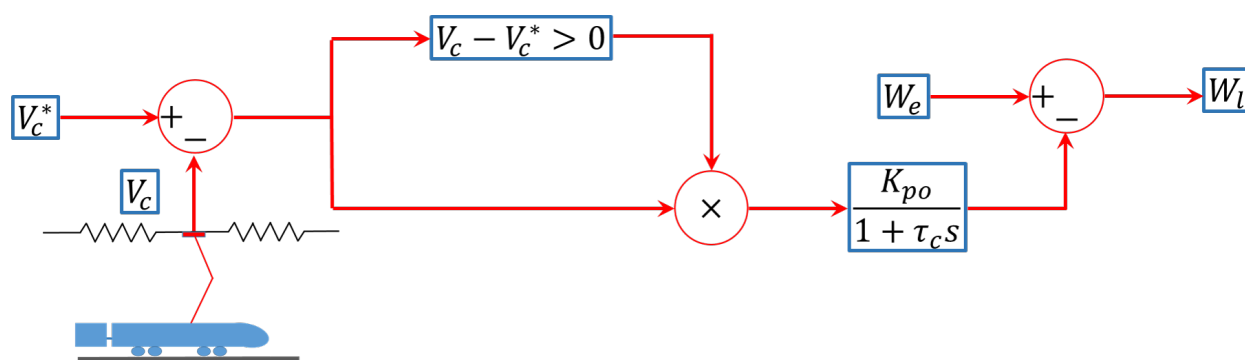


Figure 3.6: Scheme of calculation of pantograph voltage and power, including the voltage limiter.

filter is characterised as follows:

$$Filter = \frac{K_{po}}{1 + \tau_c s}, \quad (3.12)$$

where K_{po} represents a gain and τ_c is a time constant.

3.2 Electrical models

The electrical models of the feeding line, energy storage devices and substations have been developed in MATLAB®-Simulink environment, in particular using MATLAB®-SIMSCAPE™ blocks. The whole electrical system interchanges information with the dynamical one: the inputs are represented by the position of the vehicle and power requested or provided, while the outputs for the mechanical model are the main electrical quantities, as line safety voltage limit or available power. The main MATLAB®-SIMSCAPE™ blocks, used in the proposed model, are the resistance, the capacity, the inductance and the voltage source, shown in Figure 3.7. The SIMSCAPE™ blocks internally implement the characteristic constitutive equations: this modelling approach permits to relieve the computational cost and the needed information to describe a system is lower than with other approaches.

The resistor block is characterised by the constitutive Equation which evaluates the voltage drop:

$$V = RI, \quad (3.13)$$

where V represents the drop of the resistance voltage, while I and R respectively are the current and the constant resistance. The absorbed power, which is indeed dissipated, is always positive: it permits to represent the characteristic losses detected in a complex railway line.

The impedance of the feeding line depends on the train position: the use of a variable resistor block permits the dynamical calculation of the impedance value.

Another implemented block is the capacitive one, which is characterised by the constitutive Equation 3.14:

$$I = C \frac{dV}{dt}, \quad (3.14)$$

where C represents the capacitance of the element. This block has been used for the energy storage devices modelling, as the inductive block, characterised by the following constitutive Equation:

$$V = L \frac{dI}{dt}, \quad (3.15)$$

where L represents the element inductance.

Finally, the voltage source block has been used for the voltage generator modelling and its

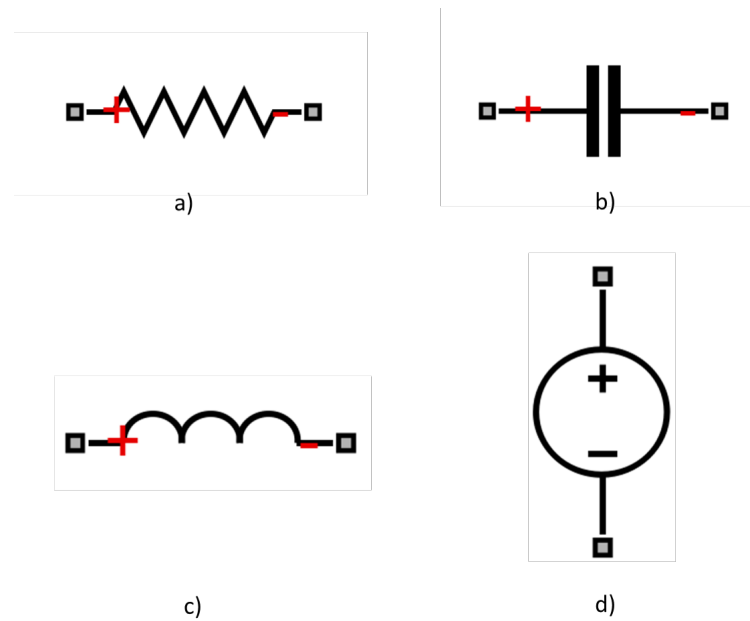


Figure 3.7: Main SIMSCAPE™ blocks implemented in the developed model: a) resistance, b) capacity, c) inductance and d) voltage source.

constitutive Equation is the following:

$$V = V_0 (2\pi ft + \phi), \quad (3.16)$$

where V_0 represents the voltage amplitude, f and ϕ are respectively the frequency and the phase. The substation modelling approach is based on the voltage source block implementation: in particular, for the considered test case, the constitutive equation is simplified to $V = V_0$, which represents the constitutive equation of a DC voltage source.

3.2.1 Feeding line and electrical substation model

The feeding line provides to the vehicle the necessary power to traction or it can receive back the energy generated by regenerative braking. It is fed by electrical substations. Three different operating conditions can be considered in a railway scenario:

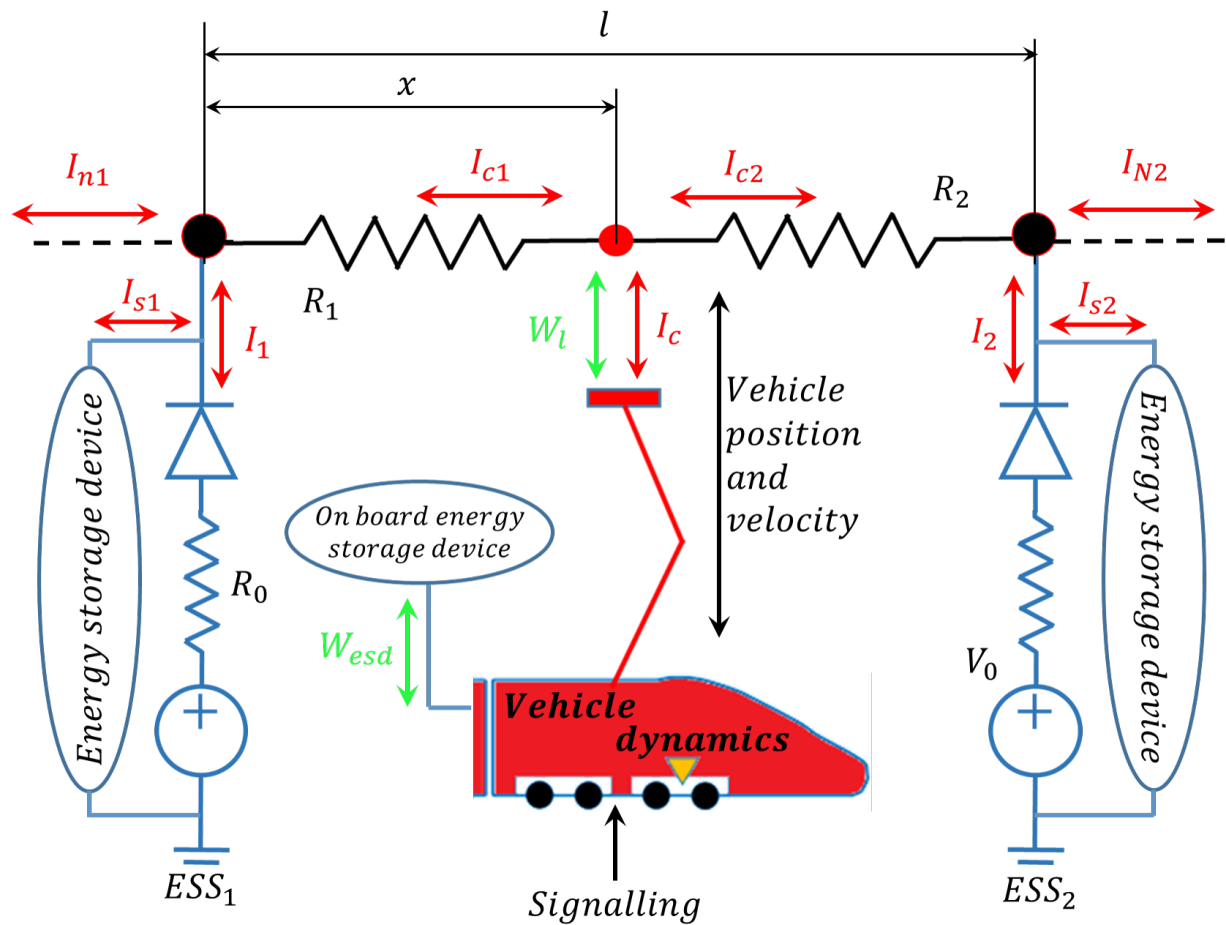


Figure 3.8: Architecture of the electrical model.

- Direct Current Substations: as in the considered test cases, in railway application, the voltage value, provided by the substation, is 3 kV and it is especially used on light railway application.
- Alternating Current Substations with industrial frequency: the operating voltage value is 25 kV at 50 Hz and it represents the most used operating condition for High Speed application.
- Alternating Current Substations with railway frequency: the operating voltage value is 15 kV at 16 and 2/3 Hz, standard solution for the central Europe.

In the considered test cases, DC substations have been implemented and the feeding line is bilateral: each span is fed by two substations.

The calculation of the requested or provided vehicle power is performed as shown in Equation 3.17 and Equation 3.2.1:

$$W_t = \frac{W_{wheels}}{(\eta_{gearbox}\eta_{motor}\eta_{motordrive})}, \quad (3.17)$$

$$W_b = W_{wheels}\eta_{gearbox}\eta_{motor}\eta_{motordrive}, \quad (3.18)$$

where W_t and W_B are the traction and braking power, W_{wheels} represents the wheel/rail contact power, $\eta_{gearbox}$, η_{motor} and $\eta_{motordrive}$ are respectively the transmission system, motor and motor drive efficiencies.

Figure 3.8 provides some hints on the general architecture of the electrical model of the feeding line, including the substations and the energy storage devices, described in Section 3.2.2. As above mentioned, each span is fed by two substations (bilateral power supply) and some energy storage devices can be installed in parallel to them. The vehicle divides the span in two sections, and hence, their impedance is position dependent. Equation 3.19 and 3.20 evaluate the resistance of the two aforementioned sections:

$$R_1 = \rho \cdot x, \quad (3.19)$$

$$R_2 = \rho \cdot (l - x), \quad (3.20)$$

where R_1 and R_2 represent the impedance evaluated before and after the vehicle within the span, ρ is the distributed impedance of the catenary, x is the train position and l represents the distance between the two substations, which feed the considered span.

The effective voltage of the substations is raised up to 30% higher than the nominal value: this expedient enables to provided the correct voltage to the vehicles, considering, as mentioned, the impedance dependency on position and, then, the voltage drops proportional to the substations distance.

As it is possible to see in Figure 3.8, ESS1 and ESS2 indicate the two substations which delimit the

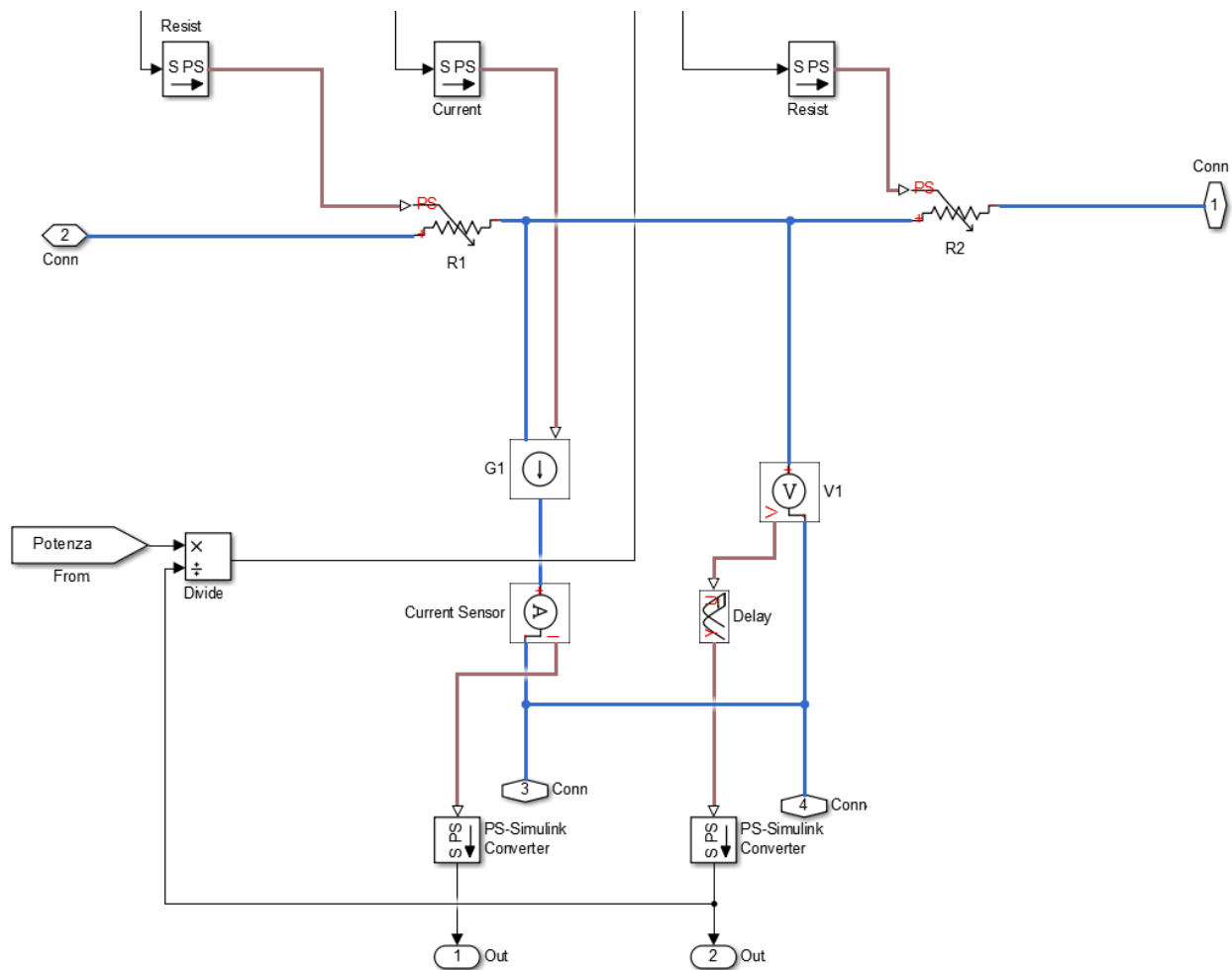


Figure 3.9: Scheme of feeding line electrical model.

considered line span. I_{c1} and I_{c2} represent the ESSs current contribution, respectively calculated in Equation 3.21 and Equation 3.22, and they compose the current, calculated at the line/pantograph contact, I_c :

$$I_{c1} = \frac{I_c \cdot (l - x)}{l}, \quad (3.21)$$

$$I_{c2} = \frac{I_c \cdot x}{l}, \quad (3.22)$$

where x is the train position, along the span, and l represents the ESSs distance. Current I_{n1} and I_{n2} are external current, due to adjacent spans (better explained in the paragraph at the end of this Subsection, where the complex topology configuration is described). It is possible to evaluate the

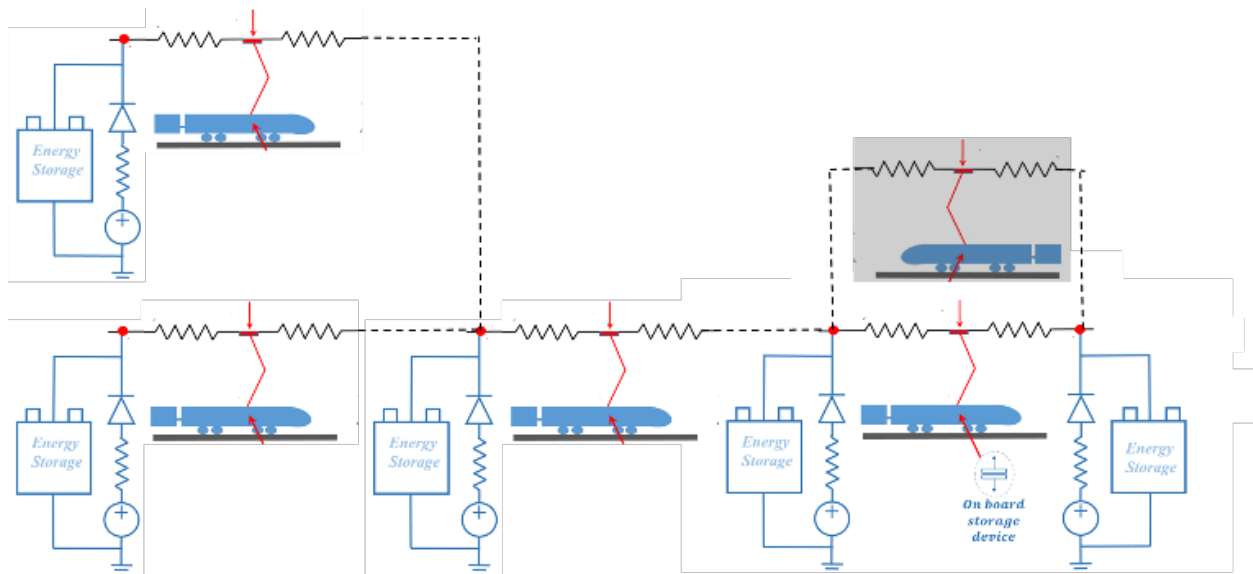


Figure 3.10: Example of complex topology configuration.

voltage drop within a line span, which has its maximum in the centre of the span itself, having a parabolic trend:

$$\Delta V = \frac{I_c \cdot x \cdot \rho \cdot (l - x)}{l}. \quad (3.23)$$

The considered test cases are DC lines and Figure 3.9 shows the implemented line model: special blocks (*SPS*), which permit to convert the MATLAB®-SIMSCAPE™ signal and convey physical information into MATLAB®-Simulink signal, so as to enable the use of different MATLAB® environments together, have been used. Furthermore, the MATLAB®-SIMSCAPE™ language permits an easy implementation of proper blocks, as inductive and capacitive elements, which better describe other line configuration, i.e. AC lines, where the induction or capacity effects are not negligible as in DC electrical lines.

The feeding line span is modelled to easily connect more than one section: it is possible, in fact, to assemble complex line topologies, as shown in Figure 3.10, adding loads to the line nodes (current I_{n1} and I_{n2} in Figure 3.8). The use of different topologies depends on many factors, first of all the user information and targets:

- Simplified topology: only one span has to be used to represent the entire line and it is, ideally

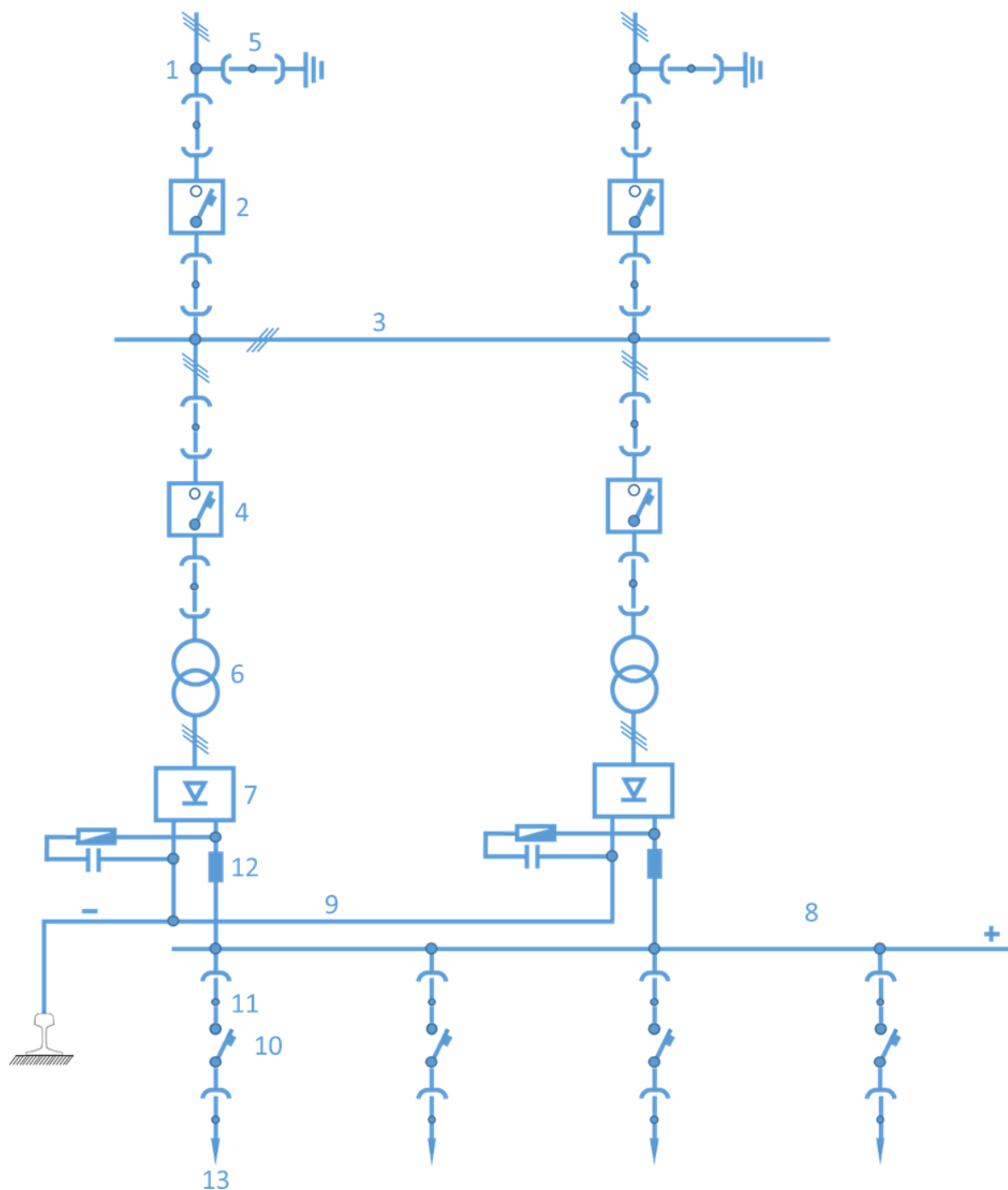


Figure 3.11: Scheme of a 3kV electric substation.

and periodically, crossed by the vehicle (changing dynamically the initial conditions). This approach needs a lower amount of information with respect to the complex one and it has a lower computational cost, but, at the same time, the results prove to be less accurate.

- Complex topology: the user details every span which composes the considered line. This approach requires higher computational times with respect to the simplified one and more details concerning the line characteristics, but it provides more accurate results.

To feed the line, electrical substations, denoted as *ESSs*, are located along the electrical line: these systems, through the catenary, provide traction energy to the vehicles. Furthermore, they are connected to the electrical grid through proper transformers. Figure 3.11 shows a detailed scheme of a DC substation (3 kV) circuit components:

1. primary HV three-phase line;
2. tripolar line switch;
3. HV three-phase bars;
4. tripolar group switch;
5. tripolar sectioner;
6. three-phase transformer;
7. silicon rectifier;
8. positive DC bar;
9. negative DC bar;
10. extra-fast switch;
11. DC sectioner;
12. filter;

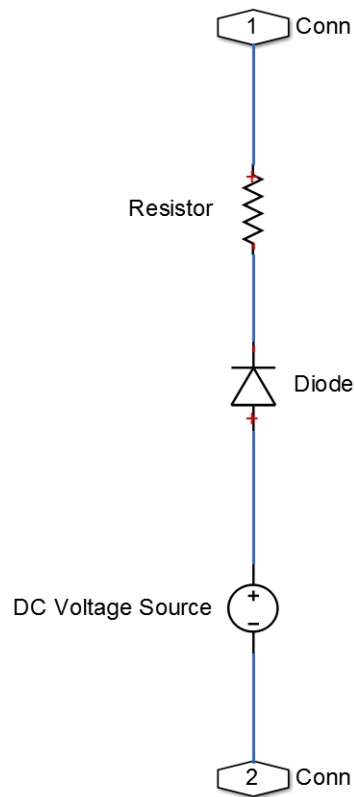


Figure 3.12: SIMSCAPE™ model of the electrical substation.

13. contact line supply.

One of the substation targets is the reduction of the grid voltage to the railway application value. In the first part of the substation circuit, the high voltage (HV) of the electrical grid is converted to a medium voltage (MV): this sector contains mainly the components from 1 to 6 of the above reported list. Within the second substation circuit part, the AC current is converted to DC current through the use of a rectifier. The rectifier group (which includes diodes and RC protection) is connected to a capacitors cell, used to filter the high frequency harmonics. In the third and final part, the feeding operations are performed and the ESS is connected to the line.

In the proposed model, the substation has been modelled in a simplified way, since the proposed work target is the modelling of a complex railway system, composed by vehicle, feeding line and signalling and not to detail a single component. Figure 3.12 reports the SIMSCAPE™ scheme of a DC substation, implemented in the model: it has been modelled as a real DC voltage generator.

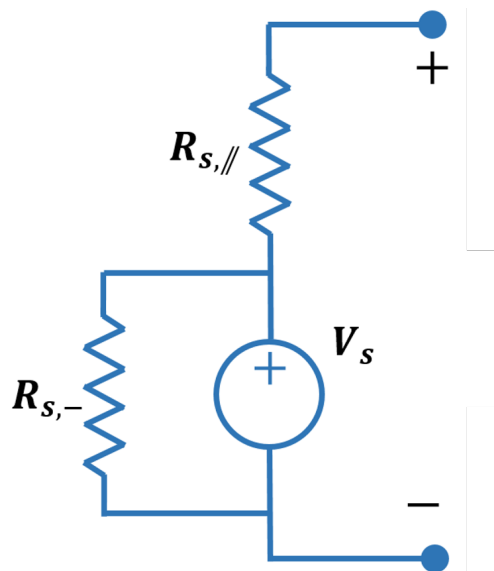


Figure 3.13: Generic energy storage device model scheme.

The diode is used to limit the operating condition of the substation, making it a non reversible system, i.e. not able to receive back regenerative energy from the vehicle braking; moreover, an equivalent impedance has been located in series to the diode, to simulate the internal losses of the substation. This modelling approach is often used in literature to represent the ESS, as in Zaninelli [38] and Perticaroli [39]. To collect the energy provided by the vehicle braking, an energy storage device can be connected in parallel to the substation or, as an alternative, the aforementioned energy can be instantaneously reused by another vehicle within the line. The reversible substations are not implemented in the proposed model, due to the considered test cases scenarios, where non reversible ESSs are installed; the reversible substations modelling has been investigated by other researchers, e.g. Cornic [40].

The line node, where the substation is linked, is characterised through the following Equations (see Figure 3.8):

$$\begin{cases} V_0 - (I_{c2} - I_{c1})R_0 = V_c \\ V_2 = V_c - R_2 I_{c2} \end{cases}, \quad (3.24)$$

where V_0 and R_0 are respectively voltage and resistance referred to the substation, V_c is the pantograph/line contact voltage, I_{c1} and I_{c2} are the ESSs current contribution and V_2 represents

the voltage at the line node, where the ESS2 is connected. When the condition $V_c > V_0$ occurs, the diode turns off: the substation is no more connected to the circuit and Equation 3.24 becomes Equation 3.25:

$$\begin{cases} I_{c2} = I_{c1} \\ V_2 = V_c - R_2 I_{c2} \end{cases} \quad (3.25)$$

The exposed substation model can be enabled to represent a reversible system by removing the diode. Furthermore, to represent a real substation, which is not able to provide infinite power, the constitutive equation of the ideal DC Voltage has been modified by adding a power limit (whose value depends on the considered ESS characteristics) and taking into account the traction power, needed by the vehicles, as follows:

if $W_t \leq 2 \cdot W_{ESS,max}$

$$V_{ESS} = V_0$$

else

$$V_{ESS} = W_{ESS,max} / I_{ESS}$$

end

where W_t is the traction power of the vehicle and $W_{ESS,max}$ represents the maximum power which can be provided by the substation. The previous cycle refers to one vehicle, crossing a bilateral line and it is a simplified version of the one which has been implemented in the proposed model.

3.2.2 Energy storage device model

The most used energy storage devices (*ESDs*) in the railway field are batteries and supercapacitors: they can be installed along the feeding line or located on-board on the vehicle. A generic energy storage device model, see Figure 3.13, is composed of an ideal DC Voltage generator, whose voltage is denoted as V_s , two resistances, $R_{s,||}$ and $R_{s,-}$, which simulate the transient discharge of the energy storage device and its internal losses (respectively in parallel and in series).

The proposed modelling approach, based on the use of SIMSCAPE™ language, permits to easily link the energy storage device model to the feeding line or to the vehicle and to analyse different

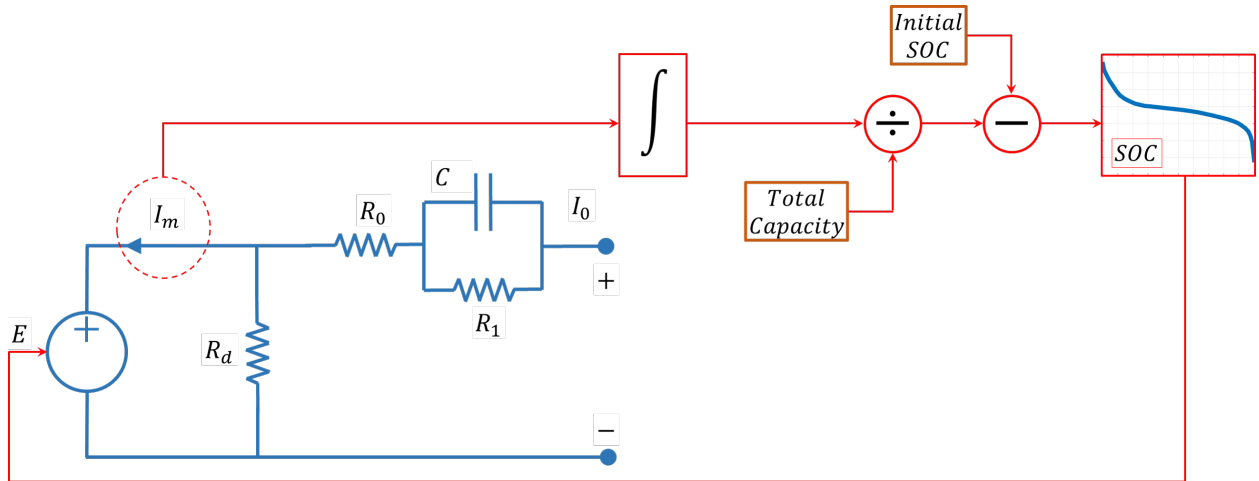


Figure 3.14: Implemented battery model, including the evaluation of the S.O.C..

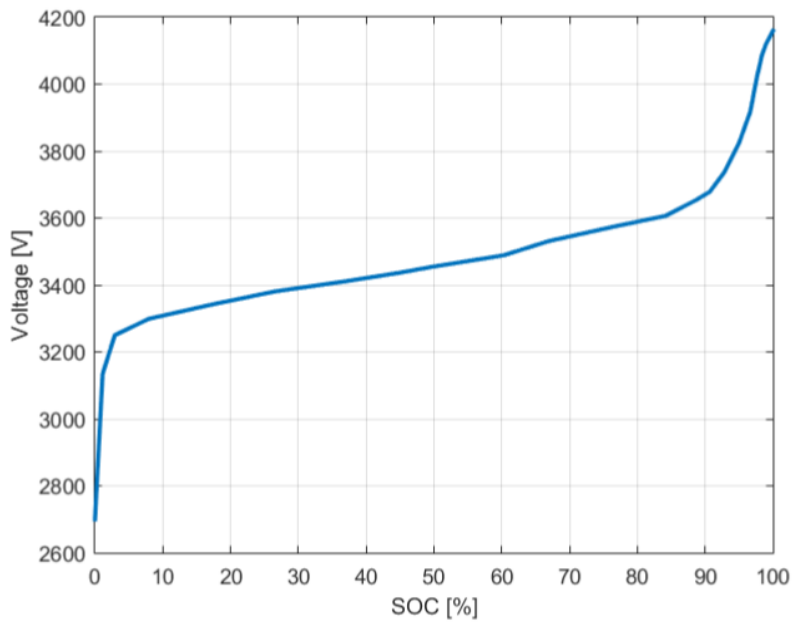


Figure 3.15: Voltage as a function of S.O.C. for the implemented battery model.

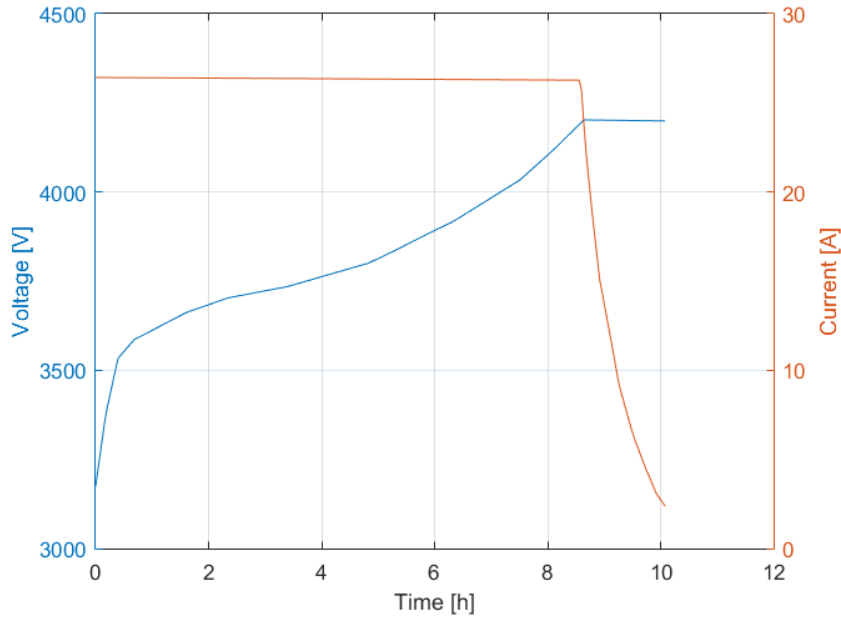


Figure 3.16: Charge and discharge behaviour of the implemented battery model.

operating scenarios. In particular, the proposed results are referred to the implementation of batteries, which, in previous research works, proved to have better performances in terms of energetic optimisation of a railway system analogous to those considered in this research work.

The energy storage devices are characterised by a voltage calculated as follows:

$$V_{0,ESD} = n_{cell} \cdot V_{cell}, \quad (3.26)$$

where $V_{0,ESD}$ represents the energy storage device voltage, n_{cell} is the number of cells of the considered ESD and V_{cell} is the nominal voltage of a cell.

The proposed modelling approach is based on the implementation of the batteries State of Charge, denoted as $S.O.C.$, which is defined as the ratio between the battery current energy and the maximum which can be stored. Figure 3.14 shows the $S.O.C.$ implementation, defined by the following Equation:

$$S.O.C. = \int \frac{\eta_{batt}(I_{batt}, S.O.C.) I_{batt}}{E_{max}} dt, \quad (3.27)$$

where η_{batt} represents the battery efficiency, I_{batt} is the battery current and E_{max} is the maximum energy which can be stored in the battery. As shown in Figure 3.14, the voltage, provided by

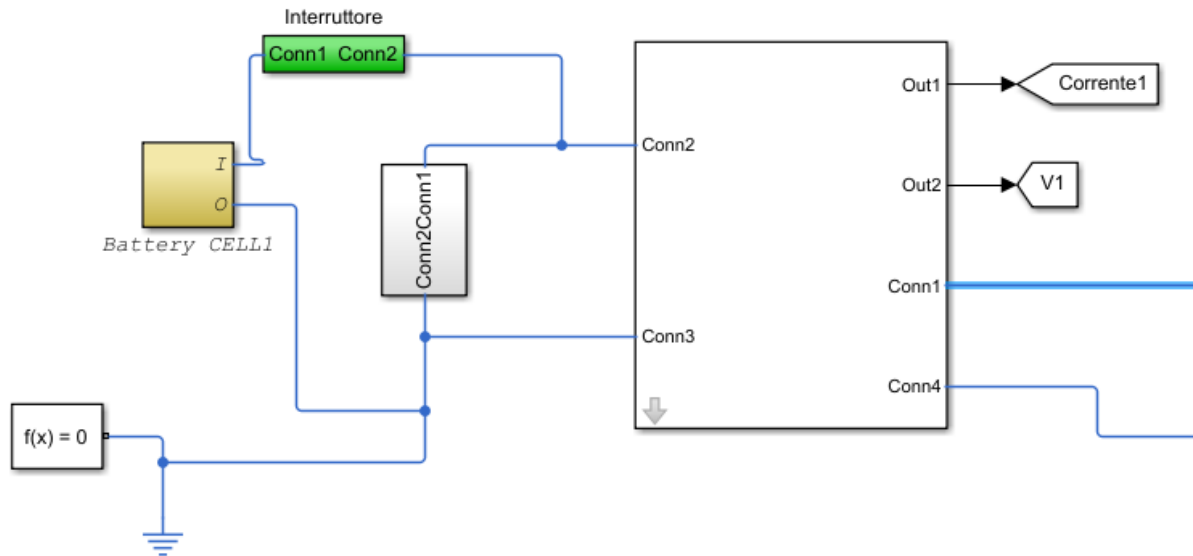


Figure 3.17: SIMSCAPE™-Simulink battery model implementation.

the ideal generator, is evaluated through the *S.O.C.* estimation, where V_{batt} is the no-load battery voltage, tabulated as a function of I_{batt} and *S.O.C.*, see Figure 3.15.

Different battery types have been analysed in previous works and the Li-ion ones proved to be the better energy storage devices for railway applications. To achieve the test cases line voltage, the modelled battery contains stacks of 1010 cells (in series, with an intermediate *S.O.C.* value), while, to reach the needed capacity, 4 stacks are connected in parallel. The mentioned capacity is determined basing on the maximum regenerative braking energy, which can be recovered (or the maximum provided one): it should be about 5 - 10 % of the total battery capacity. Such value permits to store enough braking energy avoiding the problems due to the charge/discharge cycles, which can impact on the batteries life.

As an example of the model behaviour, Figure 3.16 reports the charge and discharge behaviour of the previously exposed battery, obtained linking the energy storage device to a load: from these trends, it is possible to highlight how, since the braking involves a small energy percentage with respect to the entire battery capacity, the variation of the voltage with respect the nominal one can be considered acceptable. To understand the battery behaviour, within the vehicle/line model, an

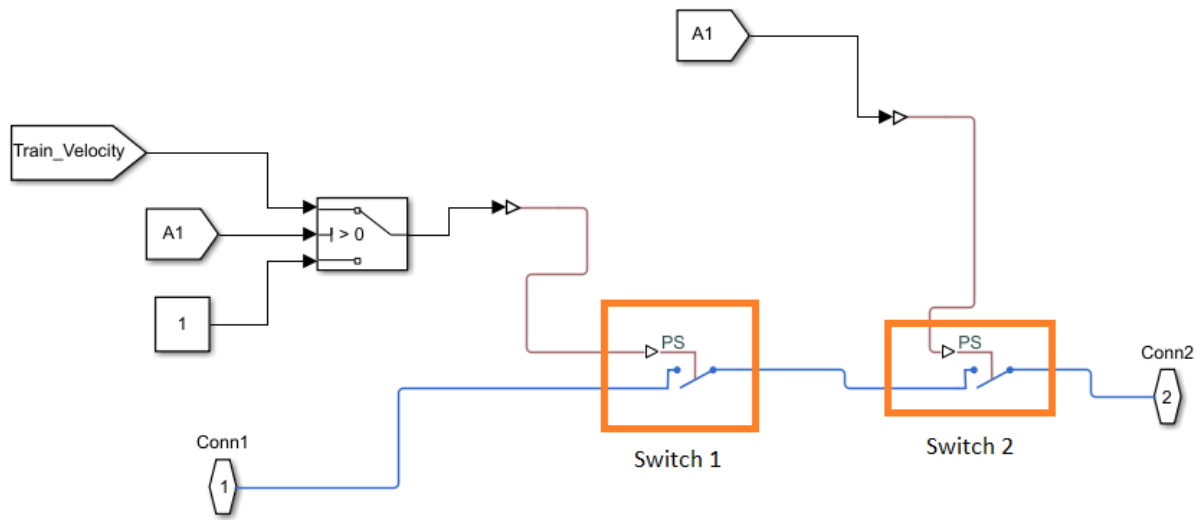


Figure 3.18: SIMSCAPE™-Simulink scheme of battery switch.

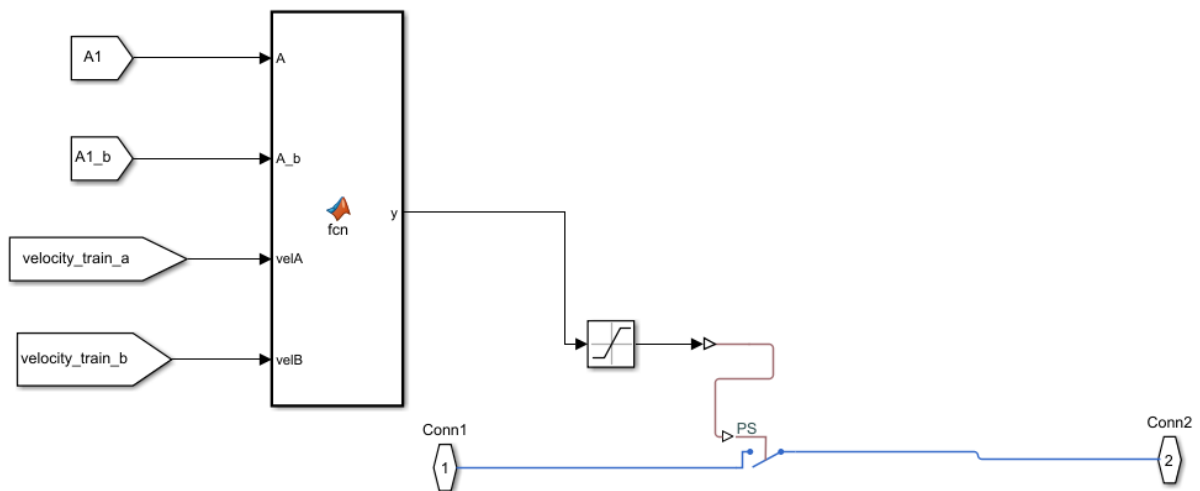


Figure 3.19: SIMSCAPE™-Simulink scheme of a battery switch for the scenario with two vehicles moving in opposite directions.

initial *S.O.C.* value equal to 50% has been used: this condition permits to operate near the nominal voltage, even if a vehicle traction manoeuvre requires the maximum discharge of the battery.

To store only the energy provided by the regenerative braking and not the one supplied by the substations, the battery voltage shall be higher with respect to the ESSs one, while during the traction manoeuvre, when the vehicle employs the battery energy, the line voltage cannot overcome the limit. To respect this condition, a DC/DC converter has been considered: this system, in addition to *S.O.C.* control, avoids continuous charge and discharge cycles and it decouples the battery voltage from those of substations and line. The DC/DC converter is modelled through equations which modify the output current with respect to the substation or line voltage. The mentioned current is evaluated through the power flux, considering the *S.O.C.* control and the equivalent losses.

Despite the possibility to connect the device model to the vehicle to simulate the batteries installed on-board, in the presented research work, the numerical results, reported in Section 4, are obtained considering the energy storage devices located only in parallel to the electrical substations. This strategy has been chosen mainly for economic reasons: batteries located on-board involve the use of small size systems, which usually entails great costs, and the railway operator, to install the energy storage devices, even with a small size, has to sacrifice passenger seats and spaces, reducing the payload.

Figure 3.17 shows the implementation of the battery model in the electrical feeding line one: the batteries are connected to the line through switches, to avoid charge and discharge cycles in unreal condition, e.g. a still vehicle or a train far from the span where the considered batteries are installed.

The above mentioned switch controls the current supply or absorption and it is represented in Figure 3.18: two SIMSCAPETM switch blocks have been implemented. The first one is controlled by the train velocity: if the speed assumes a value which is under a chosen limit (0.01 *m/s* in the developed model), the switch turns on the "open" phase, stopping the current circulation and avoiding the discharging of the battery. The second switch is controlled by a variable A_i , which is associated to the *i*-th span: the switch of the span upstream with respect to the train position and

the others downstream remain in the close condition and the corresponding batteries continue to supply or absorb energy.

This solution is suitable for the operating scenario with one train moving alone within a line, but different operating traffic conditions have been analysed in the presented research work (see Section 4.4). In the scenario where two vehicles move in the same direction within a feeding line, one in a backward position with respect to the other, the implementation is similar to the one explained in the previous paragraph: the switches are initially closed and the control is commanded by the vehicle in the backward position, which turns the switches in the *open* condition with its passage.

Another operating condition involves two vehicles which move in opposite directions within the same line, in two parallel rails. To implement the battery switch, a modification proved to be necessary: the two switches, above described, have been replaced with one switch commanded by the following MATLAB[®] function, see Figure 3.19.

```
function y = fcn(A, A_b, velA, velB)
if (A==1 && A_b==0)
    y=velA,
end
if (A==0 && A_b==1)
    y=velB;
end
if (A==0 && A_b==0)
    y=0
end
if (velA==0 && velB==0)
    y=0,
end
end
```

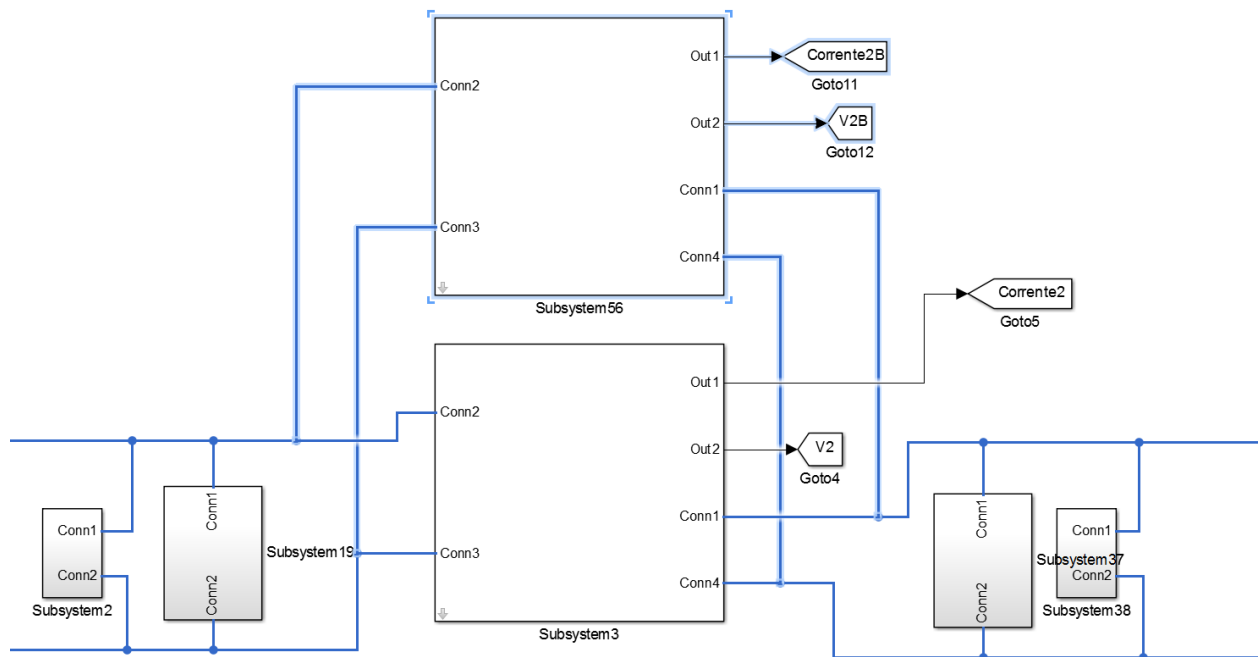



Figure 3.20: Multi-vehicle configuration scheme: vehicles with the same travelling direction.

Through the described function, the switches turn in the *open* condition after the vehicles meeting, in the already crossed spans.

3.2.3 Multi-vehicle line

To better investigate the behaviour of a complex railway system and the possibility to apply regenerative braking, more than one vehicle has been included within the line, in the same travelling direction or in opposite ones.

The first scenario, where more than one vehicle travels along the same line, is shown in Figure 3.20: the catenary is split in a great number of variable impedance sectors (considering up to 5 trains in the same line for safety limits), and, in the model, two different external MATLAB[®] functions have been included. In presence of more vehicles which travel in opposite ways, the modelling approach proves to be less complicated, due to the ease of connections through the SIMSCAPE[™] language: in fact, a second catenary has been implemented, see Figure 3.21. Every line span uses

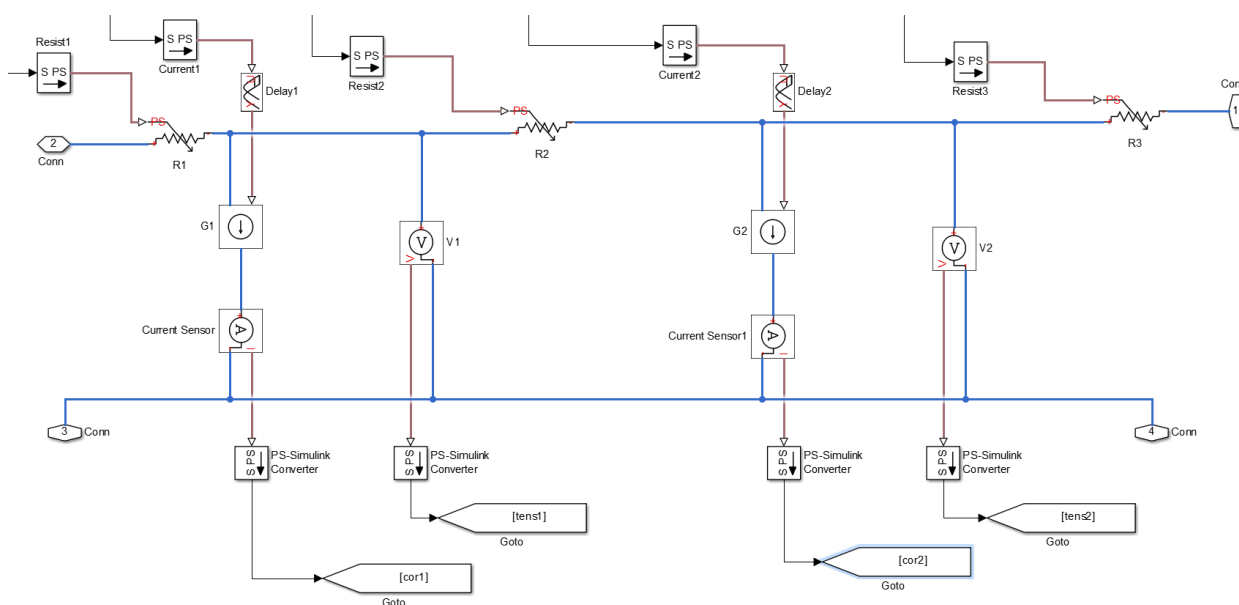


Figure 3.21: Multi-vehicle configuration scheme: vehicles with opposite travelling directions.

its own reference system and the vehicles positions are identified as the relative positions with respect to the line span initial substation.

3.3 Signalling model

To represent a complete railway system, a signalling model, based on the European Train Control System (*ETCS*), has been implemented: the *ETCS* system, in fact, supervises the vehicle position and velocity to guarantee the respect of the safety limits. Furthermore, it acts, independently from the driver reaction, if these limits are overcome.

To reach the research work goals, the developed model is focused on the implementation of the braking curves and their intervention, rather than on the modelling of the signalling system in terms of blocks sections and communications with the boas: in fact, the braking curves intervention has an important impact on the amount of regenerative energy and the feasibility of energetic optimisation application.

The system has to calculate proper braking curves to ensure the velocity decrease of the vehicle and, at the same time, achieve the stop at the correct position to respect the safety distance from another vehicle and from a possible obstacle. The implemented model is based on the ERA (*European Union Agency for Railway*) normative and on RFI (*Rete Ferroviaria Italiana*) indications; it receives as inputs the position and the vehicle speed, while as outputs it produces a speed profile which includes the maximum velocity allowed in the considered track section and some dynamical constraints, e.g. a red light or a failure along the line.

The speed control, performed by the *ETCS* system, is divided in four phases, depending on the distance between the vehicle and the *target location*, i.e. the point where a velocity decrease is present (Figure 3.22):

- Ceiling Speed Monitoring (*CSM*);
- Pre-Indication Monitoring (*PIM*);
- Target Speed Monitoring (*TSM*);
- Release Speed Monitoring (*RSM*).

The *CSM* phase acts when the supervision and action of the *ETCS* system occurs in the zone where

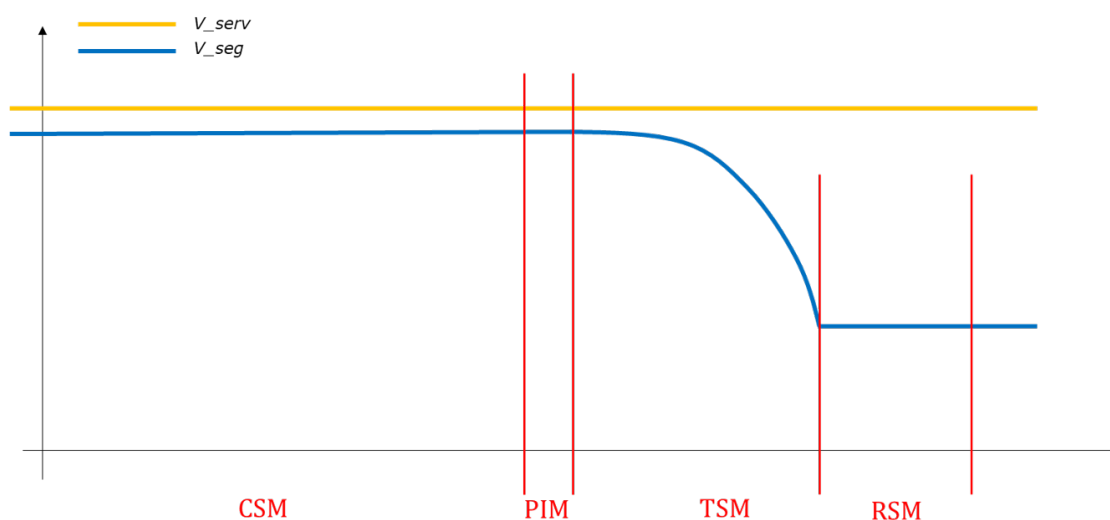


Figure 3.22: Supervision phases of a signalling speed profile: Ceiling Speed Monitoring (CSM), Pre-Indication Monitoring (PIM), Target Speed Monitoring (TSM) and Release Speed Monitoring (RSM).

the vehicle velocity can be the maximum allowed by the *Most Restrictive Speed Profile (MRSP)*, considering the static constraints (e.g. curves and bridges) and not the ones due to the signalling (i.e. the dynamic constraints). In the mentioned area, the speed does not have to decrease.

The PIM phase is the one just before the Pre-Indication point: in this zone, the driver is informed of the target location presence. The immediately following zone is supervised and controlled by the TSM phase: in this area, the speed decreases to the target one.

The last phase is the RSM: it is the supervision and intervention function in the area upcoming the point where, if the vehicle reaches the *release speed*, planned by the braking curves for that position, the ETCS system stops the intervention.

To supervise and control, this signalling system has to evaluate the vehicle deceleration a priori, taking into account the kinematic variables and the track characteristics: the *braking curves* predict the speed variation as a function of the stop distance. The use of the mentioned curves aids the driver for safety and passengers comfort reasons. Figure 3.23 shows the different braking curves of the ETCS signalling system.

The *EBD* represents the *Emergency Braking Deceleration* curve and it is related to the speed

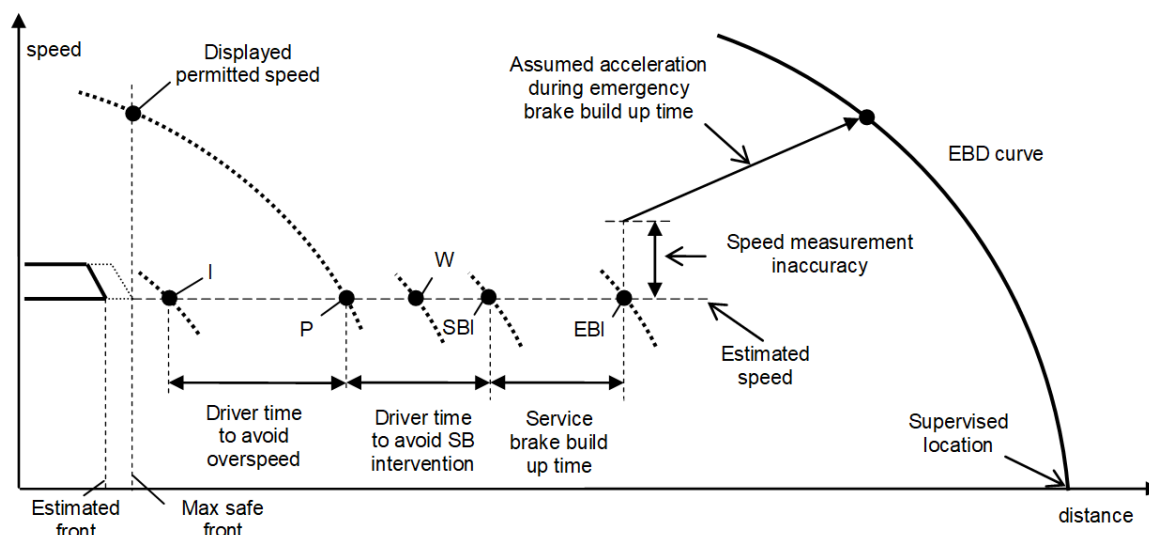


Figure 3.23: Supervision points (Indication, Permitted speed, Warning and Service Brakes Intervention) and EBD curve.

decreasing due to the emergency brake: the on-board system receives the track position where the velocity has to be lower than the allowed one (or a stop position) and, basing on the target position and speed, it elaborates a fully deterministic curve, which depends on the track and vehicle characteristics. Therefore, the ETCS system can calculate the braking distance point, through the use of the emergency braking apparatus: the distance is evaluated taking into account the worst operating conditions concerning both the dynamical characteristics, during the needed time to apply the maximum braking effort (*emergency brake build up time*), and the odometric errors on the measured velocity.

The distance necessary to achieve the target velocity or a planned stop, through the application of the maximum emergency deceleration, defines the *Emergency Braking Intervention (EBI)*, the supervision point from where the ETCS system disables the human driver and takes control of the vehicle: through the EBI point (and EBD curve), the respect of the signalling system and of the allowed speed, avoiding the so-called *override*, is guaranteed.

From the EBD curve, the ETCS system evaluates supervision points, to assist the train driver and ensure the respect of safety and comfort allowed limits:

- Indication (I);
- Permitted speed (P);
- Warning (W);
- Service Brakes Intervention (SBI).

The supervision point *I* informs the driver to start a deceleration phase through the use of service brakes: thus, it is possible to pass from the ceiling speed monitoring zone, where the vehicle assumes the maximum allowed speed, to the target speed monitoring zone, avoiding the permitted speed crossing.

P identify an additional supervision point to prevent the ETCS system intervention, providing an additional time for the vehicle driver to brake through the service apparatus: the permitted speed is still higher than the real vehicle velocity, to consider any possible errors and guarantee the safety limit. Once passed the *P* indication, the next control point is denoted as *W* limit and the crossing of this information point involves an acoustic emission to the driver to announce the Permitted speed overcoming.

Finally, the *SBI* supervision point identifies where the control system commands the service deceleration, avoiding the overcoming of the EBI point during the application of the maximum service braking effort. This control point is not mandatory for the ETCS standards, but it proves to be useful: the implementation of this limit permits to prevent the emergency braking, which causes additional wear of wheels and rails.

3.3.1 Emergency Braking Deceleration curve calculation

The ETCS standard [41] defines the EBD curve as a parabolic curve and it is evaluated basing on the target position and target speed. The final deceleration is the result of two contributions:

$$a_{safe}(v, d) = a_{brake_safe}(v) + a_{gradient}(d), \quad (3.28)$$

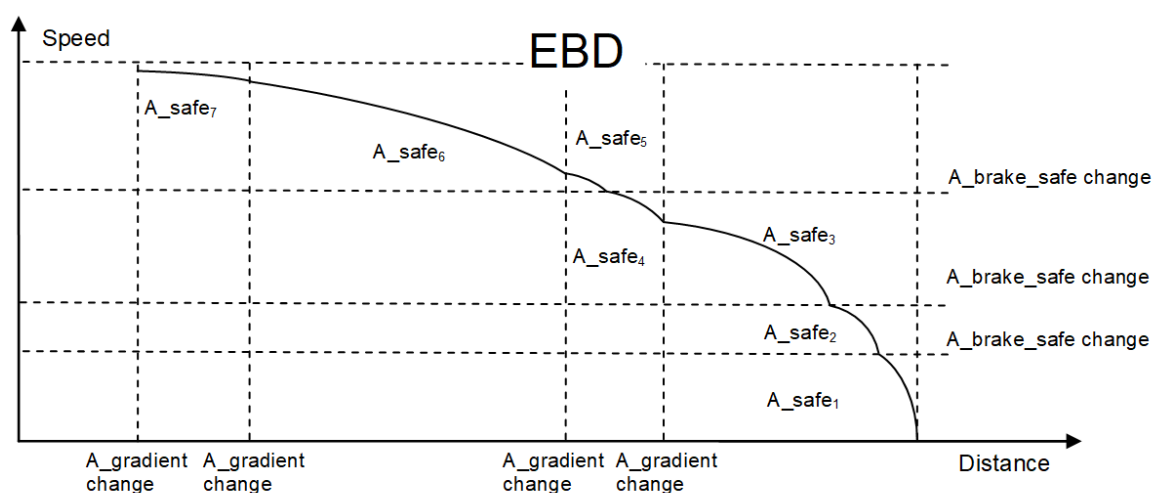


Figure 3.24: EBD evaluation through the a_{brake_safe} and $a_{gradient}$ contributions.

where a_{brake_safe} represents the deceleration which can be ensured by the emergency braking apparatus, while $a_{gradient}$ is the deceleration due to the track slope. The first one depends on the brake apparatus of the considered vehicle and is evaluated as a step function of deceleration with respect to the speed, while the gradient one is a step function of constant slope with respect to the distance. Figure 3.24 shows an example of an EBD calculation [41].

The a_{brake_safe} term is calculated through the application, at nominal emergency deceleration, of different corrective factors, which depend on the vehicle characteristics. The main characteristics, from which the mentioned factors are evaluated, are the following ones:

- Reliability of the brake components;
- Number of the independent elements, which compose the braking system architecture;
- Dispersion of braking system performance due to degraded conditions.

Moreover, the ETCS settles the reference conditions concerning the calculation of the nominal emergency deceleration, due to the safety margin, which is usually implemented in the nominal braking performance evaluation by the vehicle supplier. Figure 3.25 shows the dispersion of the emergency braking performance due to dry conditions of the track.

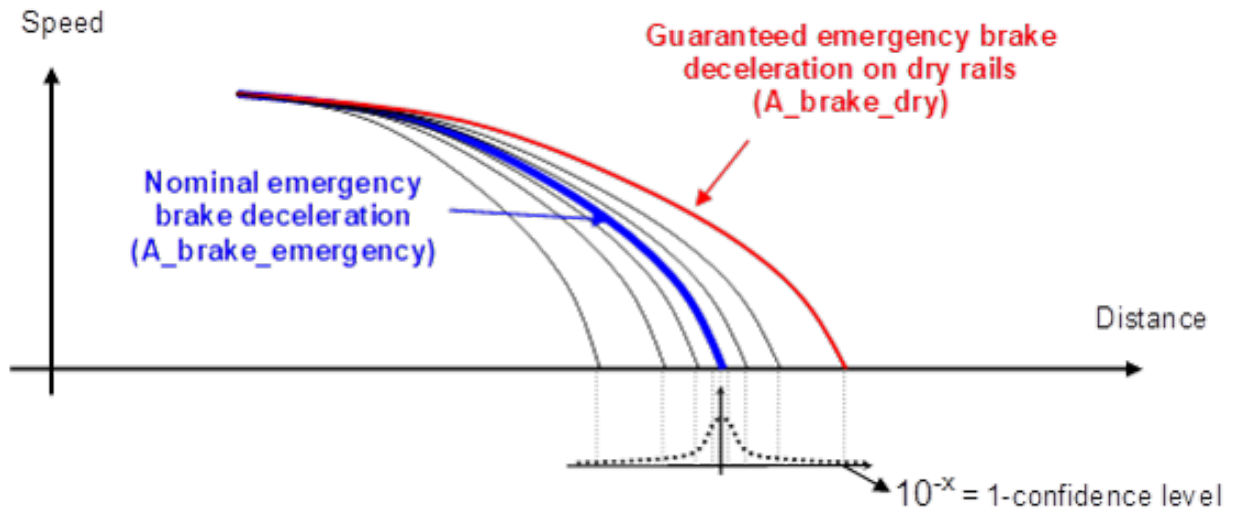


Figure 3.25: Emergency braking performance dispersion due to dry conditions.

3.3.2 Braking space calculation

In the developed signalling model, the calculation of EBI supervision point is based on two different RFI approaches [42]: in the following paragraphs, they have been denoted as *A1* for the approach based on the mathematical model developed from the *SCMT* system and *A2* for the one based on the European technical specifications. The braking space, denoted as S_{EBI} , is evaluated as follows:

$$S_{EBI} = (h + t_f) \cdot V_\beta + \frac{V_\beta^2 - V_0^2}{2 \cdot (d_p + d_i)}, \quad (3.29)$$

where h is the delay time, related to the SSB, i.e. the on board subsystem, and defined in Table 3.1, t_f represents the time needed for the braking deceleration to be equal to zero, V_β is the train speed when the SSB commands the braking action (evaluated from the initial velocity), V_0 is the target velocity, d_p is the guaranteed deceleration due to braking, while d_i represents the deceleration due to the track slope (positive in rises).

To determine the t_f parameter, through the *A1* approach, RFI uses the following Equation 3.30:

$$t_f = D_f \cdot t'_f, \quad (3.30)$$

where D_t is a safety coefficient (whose value ranges from 1 to 2), while t'_f is the delay time due to the depression propagation in the braking system, which is calculated, for a passengers vehicle, as follows:

$$t'_f = a_v + b_v \cdot \frac{L \cdot (1 - EP)}{100} + c_v \cdot \left[\frac{L \cdot (1 - EP)}{100} \right]^2, \quad (3.31)$$

where a_v , b_v and c_v are coefficients defined in Table 3.1, L represents the train length associable to the braking phase and it can be equal to the real train length or to a default value connected to the brake system type, depending on the rolling stock configuration, and EP value depends on the electro-pneumatic brake condition (1 if the electro-pneumatic system is inserted and efficient or 0 if it is not present, disabled or inefficient). The RFI indication also suggests the S_{EBI} calculation, as above, through Equation 3.29, but the delay time t_f has to be provided by the railway company, as for the d_p deceleration value (A2 approach).

To calculate d_i , the A1 approach is based on the following Equation:

$$d_i = \begin{cases} K_{i1} \cdot g \cdot i & \text{if } i > i_1 \\ K_{i2} \cdot g \cdot i & \text{if } i_2 < i \leq i_1, \\ K_{i3} \cdot g \cdot i & \text{if } i \leq i_2 \end{cases} \quad (3.32)$$

where K_{i1} , K_{i2} , K_{i3} , i_1 , i_2 are defined in Table 3.1, g is the gravity acceleration (equal to 9.81 m/s^2) and i represents the *secure* track slope, calculated as a pure number (positive in rises).

d_i can be also calculated, considering A2 approach, as showed in the following expression:

$$d_i = g \cdot \frac{100 \cdot i}{(100 + R)}, \quad (3.33)$$

where R is the rotating mass contribution (in %), provided by the railway company.

The deceleration d_p , due to the brake system, can be calculated through the following Equation 3.34 (A1 approach):

$$d_p = K_0 \cdot K_C \cdot K_r \cdot d_r. \quad (3.34)$$

K_0 represents a protection coefficient with respect to target speed, not equal to 0, and it is calculated as follows:

$$K_0 = 1 - c_r \cdot \frac{V_0}{V}, \quad (3.35)$$

Table 3.1: Braking space parameters values range.

Parameter	First attempt value	Definition range	Step
h	1.0	[0 ; 5]	0.1
a_v	3.5	[0 ; 20]	0.01
b_v	0	[-2 ; 2]	0.01
c_v	0.15	[1 ; -1]	0.01
K_{i1}	0.9	[0.8 ; 1]	0.01
K_{i2}	1	[0.8 ; 1.2]	0.01
K_{i3}	1.1	[0.8 ; 1.2]	0.01
i_1	0	[0; 0.035]	0.001
i_2	-0.021	[-0.035 ; 0]	0.001
c_r	0.05	[0 ; 0.1]	0.01
n_C	0.008	[-0.01 ; 0.01]	0.001
V_C	170 [km/h]	[0 ; 400]	5
A	0.00685	Real	-
B	0.094	Real	-
C	0.00756	Real	-
x	4.492	Real	-
y	0.443	Real	-
t_W	1.5	[-10 ; 10]	0.1
t_P	1.5	[-10 ; 10]	0.1

where c_r is defined in Table 3.1 and V and V_0 are respectively the initial and target speed.

K_C is a correction factor, used in the case of high speed, and it can be defined as:

$$K_C = \begin{cases} 1 & \text{if } V \leq V_C \\ 1 + n_c \cdot (V - V_C) & \text{if } V > V_C \end{cases}, \quad (3.36)$$

where n_C and V_C are defined in Table 3.1. Finally K_r represents a protection coefficient, defined in Table 3.1, which considers the brake performance dispersion, associable to the guaranteed characteristics of the vehicle.

d_r is the deceleration due to the braked mass percentage. It is evaluated through the following Equation:

$$d_r = \begin{cases} A \cdot \lambda + B & \text{if } V \leq V_L \\ (A \cdot \lambda + B) \cdot [1 - C \cdot (V - V_L)] & \text{if } V > V_L \end{cases}, \quad (3.37)$$

where A , B , C , x and y are defined in Table 3.1, λ is the braked mass percentage and V_L is calculated as follows:

$$V_L = x \cdot \lambda^y. \quad (3.38)$$

Finally, the speed V_β characterises the vehicle behaviour during the transient phase, where no application of braking forces on wheels has been assumed. This variable can be defined, basing on the A1 approach, as follows:

$$V_\beta = \begin{cases} V - d_i \cdot (t_f + h) & \text{if } V - d_i \cdot (t_f + h) > V_0 \\ V_0 & \text{if } V - d_i \cdot (t_f + h) \leq V_0 \end{cases}. \quad (3.39)$$

The V_β speed can be also evaluated, considering the A2 approach, as shown in Equation 3.40:

$$V_\beta = \begin{cases} V - d_i \cdot (t_f + h) + a_t \cdot t_{TT} & \text{if } V - d_i \cdot (t_f + h) + a_t \cdot t_{TT} > V_0 \\ V_0 & \text{if } V - d_i \cdot (t_f + h) + a_t \cdot t_{TT} \leq V_0 \end{cases}, \quad (3.40)$$

where a_T and t_{TT} are respectively the maximum acceleration due to the traction system and the possible maximum time from the traction stop command and the zeroing of acceleration due to the traction. They are provided by the railway company.

Table 3.2: Braking time characteristics values range.

Parameter	First attempt value	Definition range	Step
t_r (case 1)	4	[-10 ; 10]	0.1
t_r (case 2)	1	[-10 ; 10]	0.1

The SBI, W and P braking points are calculated starting from the EBI curve braking space. Concerning the SBI curve, the braking space is evaluated through the following Equation:

$$S_{SBI} = t_{SBI} \cdot V_{\beta} + S_{EBI}, \quad (3.41)$$

where t_{SBI} can be provided by the railway company (A2 approach) or evaluated as follows (A1 approach):

$$t_{SBI} = t_r + t_f, \quad (3.42)$$

where t_r is defined in Table 3.2. Two different cases can occur: the case where the SBI control commands only the traction cut and the electric braking (case 1) or it commands the service braking through the use of Multifunction Vehicle Bus (case 2).

The Warning braking space S_W is evaluated using the following Equation:

$$S_W = t_W \cdot V + S_{EBI}, \quad (3.43)$$

where t_W is the characteristic anticipation time, defined in Table 3.1 (A1 approach) or provided by the railway company (A2 approach), used to alert the railway personnel about the next service braking action, and V is the instantaneous vehicle velocity.

The last braking curve space, which has to be calculated, is the one relative to the Permitted speed:

$$S_P = t_P \cdot V + S_W, \quad (3.44)$$

where t_P is the time, defined in Table 3.1 (A1 approach) or provided by the railway company (A2 approach), which elapses between the Warning and the Permitted speed curves.

Through the application of A1 approach, the speed limits for EBI, SBI and W are calculated, from

the permitted speed, as follows:

$$V_W = \Delta V_W + V_P, \quad (3.45)$$

$$V_{SBI} = \Delta V_{SBI} + V_P, \quad (3.46)$$

$$V_{EBI} = \Delta V_{EBI} + V_P, \quad (3.47)$$

where:

$$\Delta V_W = \begin{cases} \Delta V_{W,min} + \frac{\Delta V_{W,max} - \Delta V_{W,min}}{V_S} \cdot V_P & \text{if } V_P < V_S \\ \Delta V_{W,max} & \text{if } V_P \geq V_S \end{cases}, \quad (3.48)$$

$$\Delta V_{SBI} = \begin{cases} \Delta V_{SBI,min} + \frac{\Delta V_{SBI,max} - \Delta V_{SBI,min}}{V_S} \cdot V_P & \text{if } V_P < V_S \\ \Delta V_{SBI,max} & \text{if } V_P \geq V_S \end{cases}, \quad (3.49)$$

$$\Delta V_{EBI} = \begin{cases} \Delta V_{EBI,min} + \frac{\Delta V_{EBI,max} - \Delta V_{EBI,min}}{V_S} \cdot V_P & \text{if } V_P < V_S \\ \Delta V_{EBI,max} & \text{if } V_P \geq V_S \end{cases}. \quad (3.50)$$

The parameters values are reported in Table 3.3.

The following paragraphs report how the A2 approach evaluates the speed limits. For the EBI point, the following Equation is used:

$$V_{EBI} = \Delta V_{EBI} + V_P, \quad (3.51)$$

where:

$$\Delta V_{EBI} = \begin{cases} \Delta V_{EBI,min} + C_{EBI} \cdot V_P \\ \Delta V_{EBI,max} \end{cases}. \quad (3.52)$$

Table 3.4 reports the speed limit parameters values for the EBI indication point. The SBI speed limit is evaluated as follows:

$$V_{SBI} = \Delta V_{SBI} + V_P, \quad (3.53)$$

where:

$$\Delta V_{SBI} = \max \left\{ \begin{array}{l} \frac{\Delta V_{EBI}}{2} \\ \Delta V_{SBI} \end{array} \right. \quad (3.54)$$

Table 3.3: Speed limits parameters values range, *A1* approach.

Parameter	First attempt value	Definition range	Step
V_S	50 [km/h]	[0 ; 400]	1
$\Delta V_{W,min}$ (case 1)	2 [km/h]	[0 ; 20]	0.5
$\Delta V_{W,max}$ (case 1)	4 [km/h]	[0 ; 20]	0.5
$\Delta V_{SBI,min}$ (case 1)	3 [km/h]	[0 ; 20]	0.5
$\Delta V_{SBI,max}$ (case 1)	8 [km/h]	[0 ; 20]	0.5
$\Delta V_{W,min}$ (case 2)	1 [km/h]	[0 ; 20]	0.5
$\Delta V_{W,max}$ (case 2)	3 [km/h]	[0 ; 20]	0.5
$\Delta V_{SBI,min}$ (case 2)	2 [km/h]	[0 ; 20]	0.5
$\Delta V_{SBI,max}$ (case 2)	7 [km/h]	[0 ; 20]	0.5
$\Delta V_{EBI,min}$	5 [km/h]	[0 ; 20]	0.5
$\Delta V_{EBI,max}$	15 [km/h]	[0 ; 20]	0.5

Table 3.4: Speed limits parameters values range, *A2* approach.

Parameter	First attempt value	Definition range	Step
C_{EBI}	0,1	[0 ; 2]	0,1
$\Delta V_{EBI,min}$	5 [km/h]	[0 ; 20]	0.5
$\Delta V_{EBI,max}$	15 [km/h]	[0 ; 20]	0.5

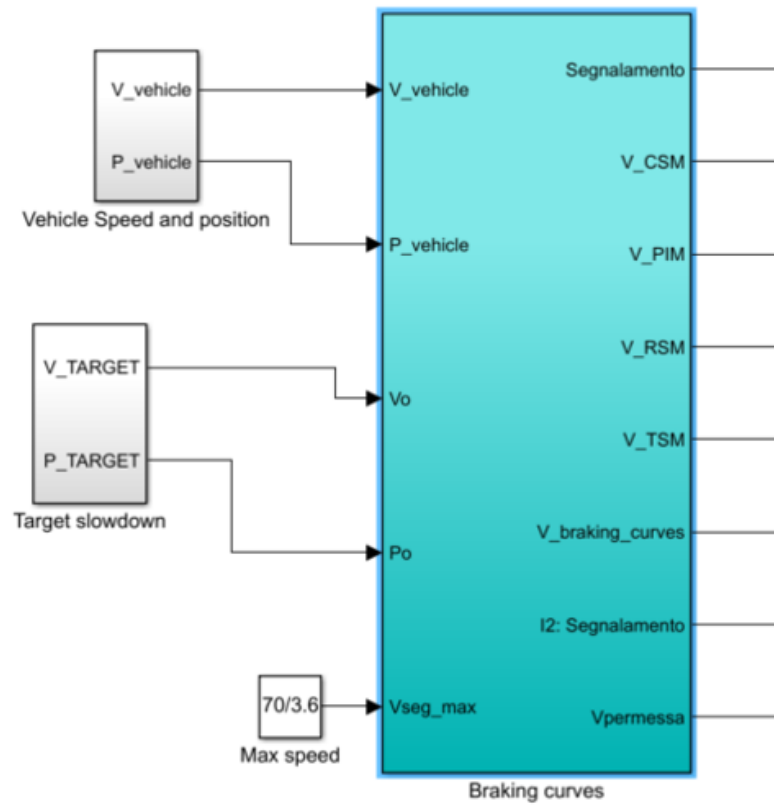


Figure 3.26: MATLAB[®] function for braking curves calculation.

$$\Delta V'_{SBI} = \begin{cases} \min \begin{cases} \Delta V_{EBI} - t_{TT} \cdot (a_T - g \cdot i) \\ \Delta V_{SBI} \end{cases} & \text{if } i > 0 \\ \Delta V_{EBI} - t_{TT} \cdot a_T + t_{SBI} \cdot g \cdot i & \text{if } i \leq 0 \end{cases}, \quad (3.55)$$

Finally, the W speed limit is calculated through the following Equation:

$$V_W = \Delta V_W + V_P, \quad (3.56)$$

where:

$$\Delta V_W = \frac{\Delta V_{SBI}}{2}. \quad (3.57)$$

Figure 3.26 shows the implementation of the MATLAB[®] function, where the braking curves are calculated: as inputs, it receives the current vehicle speed and position, maximum speeds allowed

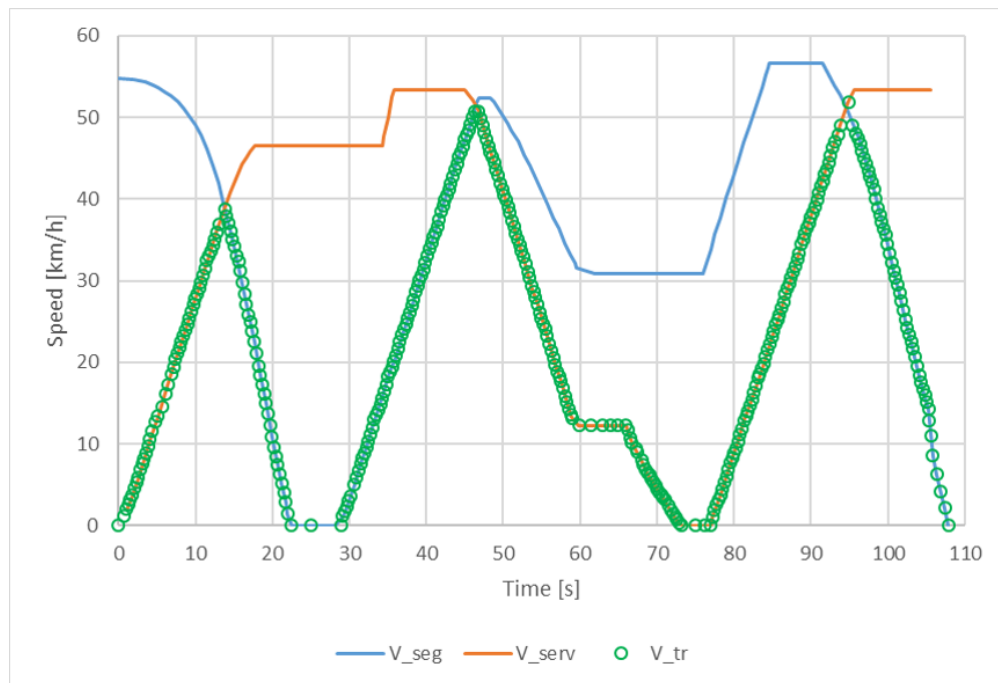


Figure 3.27: Vehicle speed as a result of the comparison between mission and signalling velocity profile.

along the considered line, and possible target slowdowns; as outputs, calculating the braking curves and the relative speed control zones for each time step, it provides a signalling speed profile. The instantaneous vehicle speed is the lower one between the mission profile and signalling one (see Figure 3.27).

3.4 Softwares and Mathematical Tools

The proposed model has been developed using Simulink and SIMSCAPE™ tools. Simulink is the classical software for the analysis of dynamical systems [43], [44]: it transposes the characteristics of the MATLAB® language in a dynamical environment, more suitable for the modelling of complex physical systems. SIMSCAPE™ is a physics-based modelling tool: it can be used stand-alone or integrated in Simulink itself. MATLAB® has also been used for the optimisation analyses, in which the Simulink-SIMSCAPE™ models have been directly handled through the MATLAB® language.

SIMSCAPE™ allows the creation of custom simulation blocks, in addition to the standard ones already implemented in SIMSCAPE™ libraries. Through the use of SIMSCAPE™, it is possible to write the element constitutive equations and avoid their explicit resolution, as in the Simulink approach. Those balance equations are usually implemented following a modular approach which suits well the representation and simulation of complex multi-physics dynamical systems [45]. Furthermore, SIMSCAPE™ language represents an extension of the MATLAB® language and it can be integrated in MATLAB® and Simulink models.

The equations which characterise the blocks of a model are handled by a symbolic solver during the simulation initialization: the symbolic solution of this equations system provides great numerical advantages for the simulation phase. Moreover, the developer has not to consider the numerical implementation of the equations during the model development.

Another important advantage is represented by the complete absence of algebraic loops (i.e. a set of blocks connected in a close loop, with inputs that depend on the outputs), which, in complex systems, represent a significant limit for a pure Simulink approach, where these problems can be only avoided through numerical delays or through the creation of additional auxiliary variables. Finally, the strong modularity of the approach allows to analyse complex scenarios with little effort.

Concerning the solver, two different differential equations solvers have been used to simulate the presented model, one for the dynamical-electrical simulation and another one for the signalling

model. The first solver is the ODE23t, *Ordinary Differential Equations* trapezoidal solver with variable order from 2 to 3: it fits stiff problems and it is suitable to solve differential algebraic equations systems. Classical solver can solve differential equations systems, expressed as follows:

$$\mathbf{M}(t) \mathbf{y}' = \mathbf{f}(t, \mathbf{y}), \quad (3.58)$$

where \mathbf{M} is the mass matrix. It can be singular and, in that particular case, the equations system is a Differential Algebraic Equations system (DAEs) [46]. Simulink and SIMSCAPE™ usually have to deal with DAEs systems, formulated as follows:

$$\begin{cases} \mathbf{u}' = \mathbf{f}_1(t, \mathbf{u}, \mathbf{v}) \\ 0 = \mathbf{f}_2(t, \mathbf{u}, \mathbf{v}) \end{cases}. \quad (3.59)$$

A DAEs system usually involves "algebraic loops". In this research work, the ODE23t solver has been used for the Dynamical and, in particular, for the Electrical model, where SIMSCAPE™ blocks involve physical variables, which can be properly solved through the use of a variable step solver: ODE23t shows the same convergence rate for differential and algebraic variables [47].

For the signalling model, the ODE3 solver, which is a fixed step solver, has been used. Through this solver type, the (n+1)-th simulation step is calculated as follows:

$$\mathbf{X}(\mathbf{n} + 1) = \mathbf{X}(\mathbf{n}) + \mathbf{h} \cdot \mathbf{dX}(\mathbf{n}), \quad (3.60)$$

where X represents the state vector, h is the step size of the time integration and dX represents the state derivative. To calculate $dX(n)$, different algorithms can be used, depending on the order of the method. The ODE3 computes the model state, at the following step of time, as an explicit function of the current value of the state and the state derivatives is computed through the Bogacki-Shampine integration formula. This solver is useful for the signalling model, which represents a control system: the task of the signalling system is to monitor the speed of the vehicle, regardless of the physical quantities dynamical evolution, which characterises the physical system. Due to this reason, it is necessary to use a fixed step solver to guarantee a regular integration.

The different models have to interchange information with each other: a transmission rate system has been implemented, to allow the interoperation of the different solvers.

4

Results

Chapter 4 reports the results obtained through the simulation of the developed model. The Chapter begins with the exposition of the two test cases: the E464 locomotive, to investigate the behaviour of a commuter train, along the Rimini-Bologna line, and the ETR 1000, a high-speed train, whose performances refer to the behaviour along the *Direttissima* line, from Firenze to Roma.

Then, the exposition focuses on the model validation, through a comparison with experimental data, provided by an industrial partner of the TESYS Rail project, concerning a manoeuvre performed by the ETR 1000 train.

The third part of the Chapter shows the results of a feasibility analysis, carried out for both trains in different traffic scenarios: the aim is to investigate the energy fluxes involved in regenerative braking and the batteries behaviour.

A section, which concerns the implementation of the signalling system, has been included: some comparisons, in presence or absence of the signalling system, have been carried out to understand how the constraints, connected with this system, affect the amount of the recovered energy. The last section focuses on a preliminary costs analysis, in particular concentrating on the installation of energy storage devices.

4.1 Test cases

To investigate the possible application of regenerative braking and to perform an optimisation analysis, two different test cases have been studied: E464 commuter train, along the Rimini-Bologna line, and ETR 1000, along the Firenze-Roma line, denoted as *Direttissima*. The two mentioned test cases have been chosen by an industrial partner of the TESYS Rail project: the partner has scheduled a future experimental campaign to perform the application of regenerative braking and evaluate the effective energy which can be stored in energy storage devices or reused by other vehicles along the line. The results will be compared with the numerical ones to validate the model developed within the TESYS Rail project.

The considered vehicles and lines are not equipped with energy storage devices, but both vehicles can perform regenerative braking: for this reason, they have been chosen to investigate the application of this technology and the energetic optimization which can be performed for high-speed and commuter trains.

4.1.1 E464 commuter train on Rimini-Bologna line

The considered E464 locomotive is connected with 5 ViValto coaches. Table 4.1 shows the main characteristics of the vehicle and of the electrical feeding line, which is a 3 kV DC line. Figure 4.1 shows the Rimini-Bologna line: in particular, the exposed results are referred to the section from Forlì Villanova to Rimini (about 50 km).

The considered locomotive has an electric traction and braking system, while the ViValto coaches are equipped with the traditional pneumatic braking system. Figure 4.2 illustrates the traction and electrical braking performances of the E 464 locomotive, technical data provided by RFI, industrial partner of the TESYS Rail project: the intervention of the pneumatic braking system proves to be necessary at low speeds, to compensate the limits of the electrical one at these velocities. Figure 4.3 shows the line curves calculated as equivalent slopes through Equation 3.4: in particular, as an example, the Figure represents the curves equivalent slope for the even rail of the line section from



Figure 4.1: Rimini-Bologna rail line, focus on the section from Forlì Villanova to Rimini.

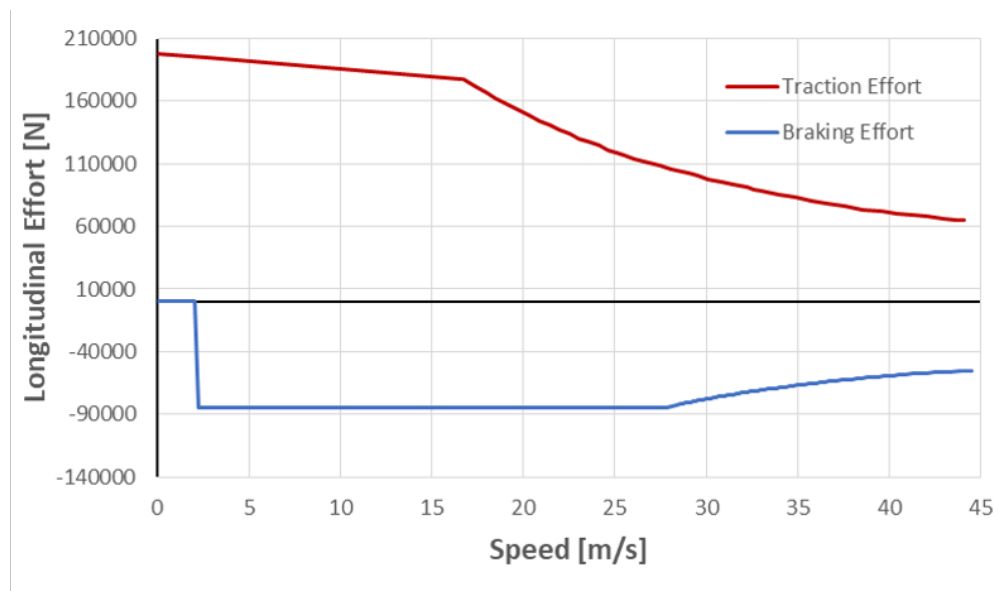


Figure 4.2: Traction and electrical braking performances of E464 locomotive.

Table 4.1: E464 commuter train and Rimini-Bologna line characteristics.

Train Mass	350 <i>t</i>
Train Length	150 <i>m</i>
Coaches number	5
Coaches type	ViValto
Gauge	Standard 1435 <i>mm</i>
Hourly power (wheels)	3.5 <i>MW</i>
Continuous power (wheels)	3.0 <i>MW</i>
Max Power in electric braking (up to 127 <i>km/h</i>)	3 <i>MW</i>
Max Traction Effort (standstill)	200 <i>kN</i>
Max Traction Effort (at 60 <i>km/h</i>)	180 <i>kN</i>
Max Traction Effort (at max speed)	67.5 <i>km/h</i>
Braking Effort (at 127 <i>km/h</i>)	85 <i>kN</i>
Max Speed	160 <i>km/h</i>
Supported Electrification Standards	3 <i>kV</i> DC, 1.5 <i>kV</i> DC
Braked mass percentage	125 %
Line Impedance (ρ)	About 0.04 Ω/km
ESS No Load Voltage	3660 <i>V</i>
ESS EQ. Impedance	About 0.1 Ω
Mean Power ESSs	5.4 <i>MW</i>

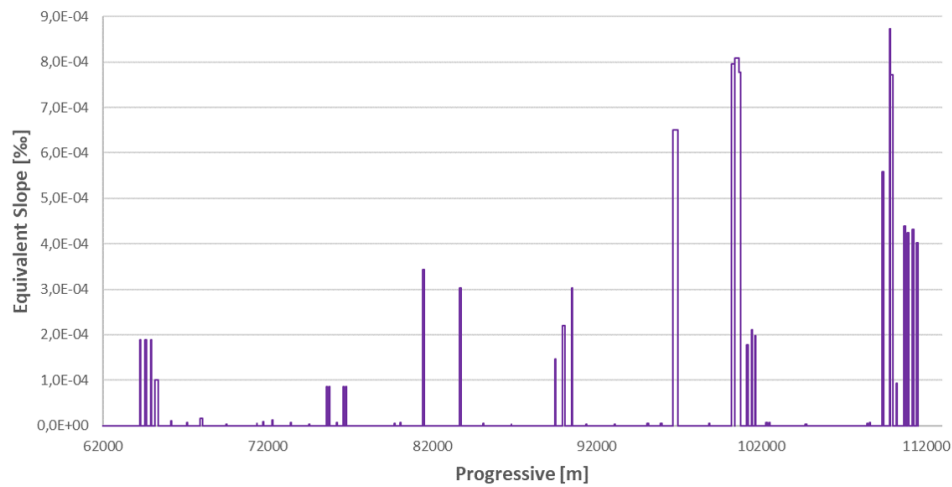


Figure 4.3: Equivalent slope for the even rail from Forlì Villanova to Rimini.

Forlì Villanova to Rimini.

4.1.2 ETR 1000 high-speed train on the *Direttissima* line

The second test case, analysed in the presented research work, is the ETR 1000 high-speed train on the Firenze-Roma line, denoted as *Direttissima*: it has been used to validate the proposed model.

ETR 1000 is a high-speed train developed by Bombardier and Hitachi Rail SpA. The characteristics of this vehicle are reported in Table 4.2, [48], [49], [50]. The considered line is a 3kV DC line, whose characteristics are reported in Table 4.2, but the mentioned vehicle can also operate under different electrification standards. Figure 4.4 shows the traction and braking performances of ETR 1000. As an example, Figure 4.5 reports the curves equivalents slope values of about 50 km of the track, calculated through Equation 3.4.

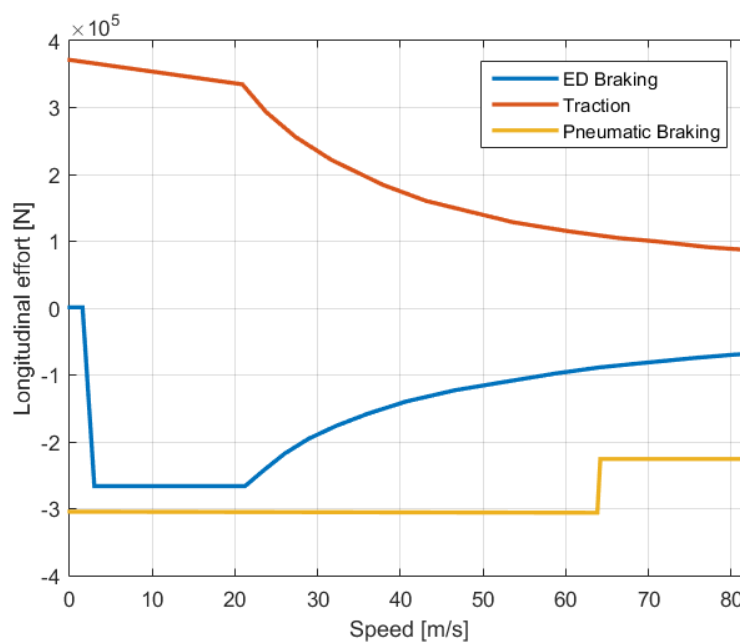


Figure 4.4: Traction and electrical braking performances of ETR 1000 high-speed train.

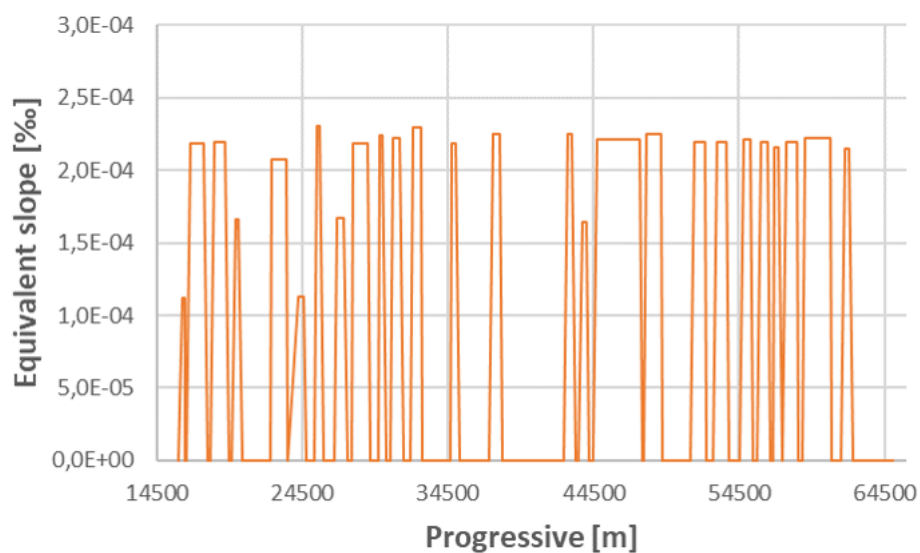


Figure 4.5: Equivalent slope of about 50 km of the *Direttissima* line.

Table 4.2: ETR 1000 High-Speed train and *Direttissima* line characteristics.

Total Seats	470
Car Body Construction	Aluminum Alloy
Train Mass	500 <i>t</i>
Train Length	202 <i>m</i>
Axle Load	17 <i>t</i>
Gauge	Standard 1435 <i>mm</i>
Rotating Inertia Respect to Train Mass	4 %
Wheel Diameter	920 <i>mm</i>
UIC Classification	Bo'Bo'+2'2'+Bo'Bo'+2'2'+2'2'+Bo'Bo'+2'2'+Bo'Bo'
Motorized Weight Fraction	0.5 [-]
Traction System	Water-cooled IGBT Converters and Asynchronous AC Traction Motors
Supported Electrification Standards	25 <i>kV</i> 50 <i>Hz</i> , 15 <i>kV</i> 16.7 <i>Hz</i> , 3 <i>kV</i> DC, 1.5 <i>kV</i> DC
Nominal Power	9.8 <i>MW</i>
Max Tractive Effort (standstill)	370 <i>kN</i>
Max Speed (design)	400 <i>km/h</i>
Max Speed (commercial)	360 <i>km/h</i>
Acceleration / Dec. Performances	0.7 <i>ms</i> ⁻² (acceleration phase) / 1.2 <i>ms</i> ⁻² (deceleration phase)
Braking System	Electro-Pneumatic, Electric Braking (both regenerative or dissipative), Magnetic Track Brake
Brake Pad Consumption	0.1-0.2 <i>cm</i> ³ / <i>MJ</i> (depending on installed brake pad and demanded brake power)
Line Impedance (ρ)	About 0.05 Ω / <i>km</i>
ESS No Load Voltage	3700 <i>V</i>
ESS EQ. Impedance	About 0.09 Ω
Mean Distance between ESSs	14.7 <i>km</i>
Min Distance between ESSs	12 <i>km</i>
Max Distance between ESSs	16.8 <i>km</i>

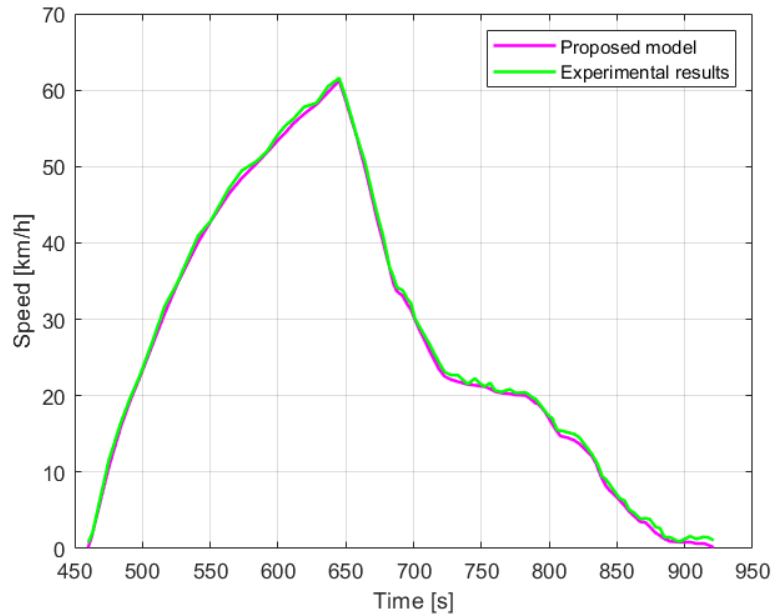


Figure 4.6: Comparison between numerical results and experimental data for the ETR 1000: speed profiles.

4.2 Experimental validation

To validate the developed model, experimental data, concerning a mixed manoeuvre performed by the ETR 1000 high speed train, along the *Direttissima* line, have been used.

The considered manoeuvre is composed of an acceleration from standstill to 60 m/s, followed by a full braking. Figures 4.6, 4.7, 4.8 and 4.9 show the comparisons between numerical results and the experimental ones concerning respectively speed profile, current at the pantograph, voltage at the pantograph and power consumption.

It is possible to see how the numerical results prove to be in good agreement with the experimental data, highlighting a good characterisation of the proposed model.

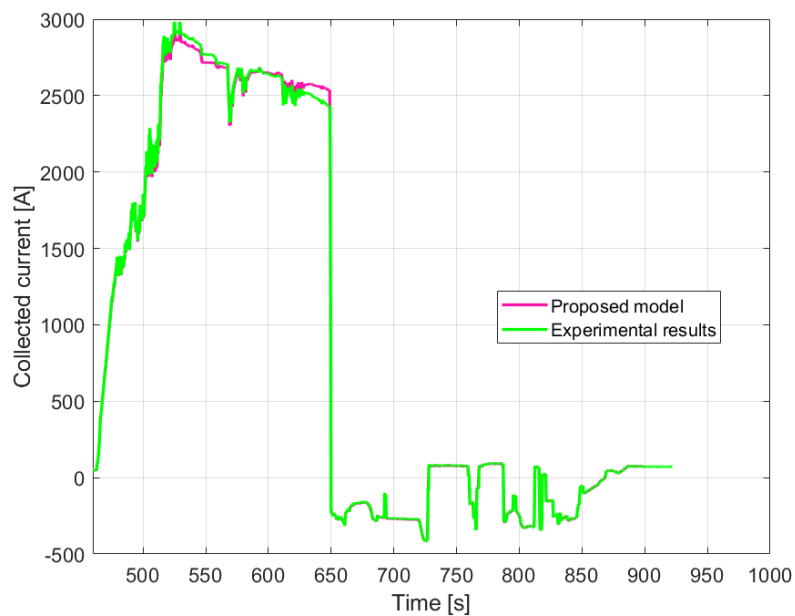


Figure 4.7: Comparison between numerical results and experimental data for the ETR 1000: current at the pantograph.

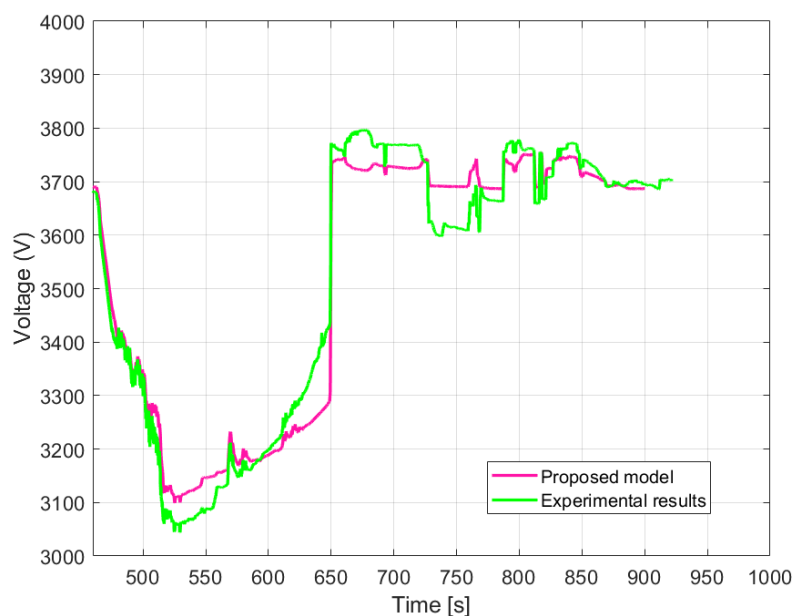


Figure 4.8: Comparison between numerical results and experimental data for the ETR 1000: voltage at the pantograph.

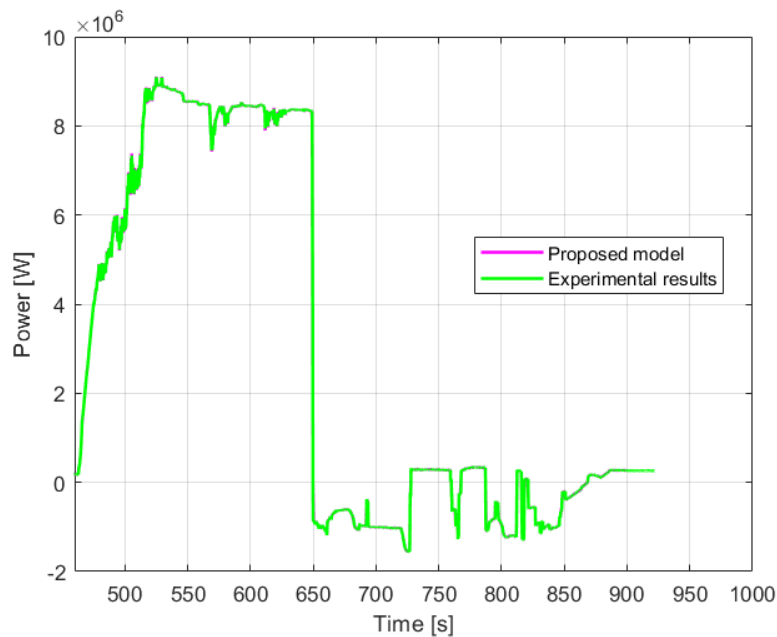


Figure 4.9: Comparison between numerical results and experimental data for the ETR 1000: power consumption.

4.3 High-speed and commuter train systems: feasibility analysis

To evaluate the perspectives of regenerative braking application, two feasibility analyses have been carried out, one for the E464 on the Rimini-Bologna line and one for the ETR 1000 on the *Direttissima* line. The simulations have been performed considering energy storage devices connected in parallel with the ESSs, to represent a reversible system, with an equivalent resistance R_{eq} .

All the analyses, including the ones explained in the following sections, consider as energy storage devices, Li-ion batteries, due to their high specific energy and power, negligible auto-discharge phenomena, high efficiency, long life-cycle and low environmental impact. In particular, basing on a reference nominal voltage of 3700 V and nominal capacity of 53 Ah for typical Li-ion batteries, to obtain the line voltage, which is 3 kV for both test cases, the battery pack is composed by 4

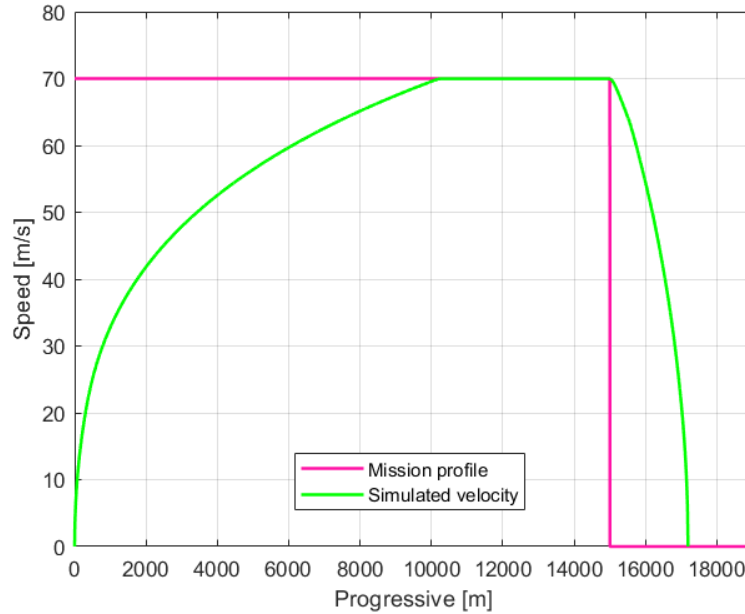


Figure 4.10: Feasibility analysis: ETR 1000 mission profile and simulated velocity.

stacks of 1010 cells in series, connected with each other in parallel to reach the needed capacity. Moreover, the batteries have been sized to operate at around 50% of S.O.C., where the battery voltage and efficiency can be considered constant.

The mentioned capacity is determined considering the maximum regenerative braking energy, which can be recovered (or the maximum provided one) for the considered test cases, aiming to store enough braking energy and to avoid the problems due to the charge/discharge cycles.

Concerning the ETR 1000 high-speed vehicle, Figure 4.10 shows the chosen mission profile and the simulated velocity: the vehicle accelerates up to 70 m/s, then, after a constant speed phase, applies a full braking. The two parameters, at the base of the feasibility analysis, are the *braking request* and the *braking position*.

The braking request is calculated as the ratio between the applied braking effort T_{appl} and the available one T_{avail} , as shown in the following Equation:

$$Brakingrequest = \frac{T_{b,appl}}{T_{b,avail}}. \quad (4.1)$$

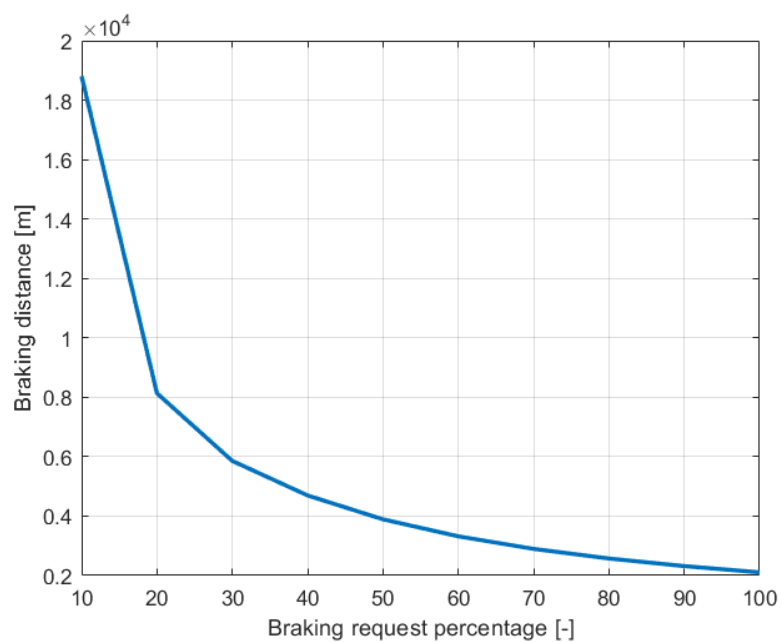


Figure 4.11: Feasibility analysis: ETR 1000 braking distance with respect to the braking request.

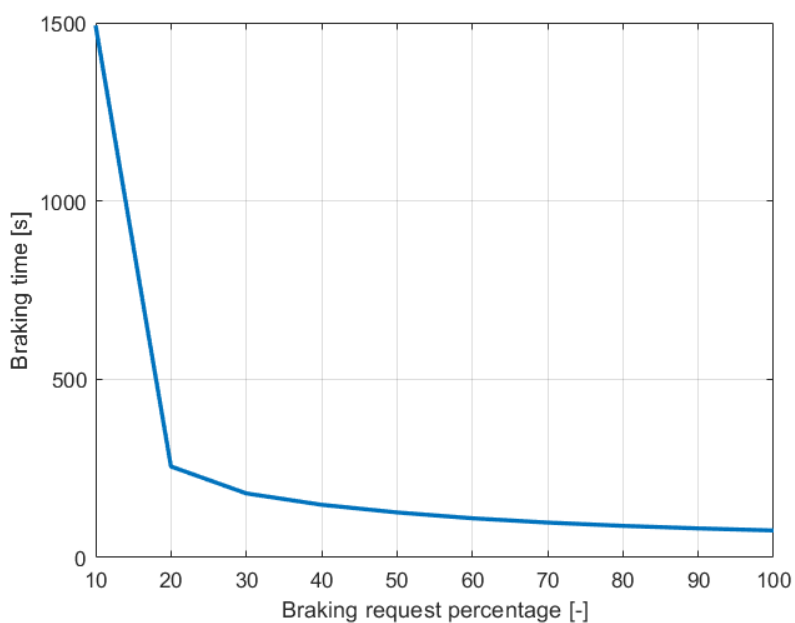


Figure 4.12: Feasibility analysis: ETR 1000 braking time with respect to the braking request.

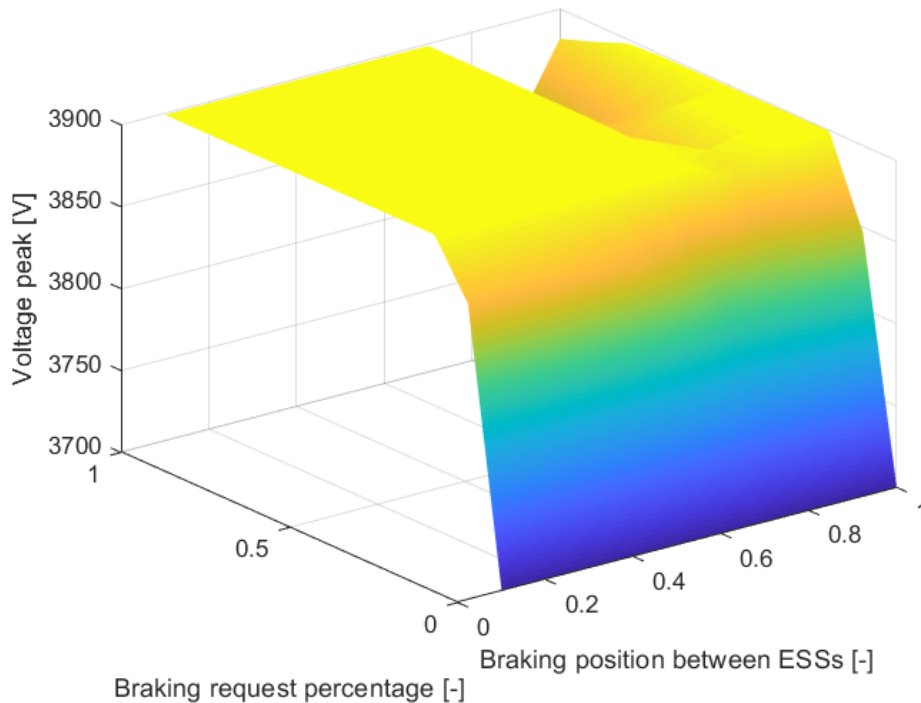


Figure 4.13: Feasibility analysis: ETR 1000 voltage peaks as a function of braking request and braking position.

The braking position is evaluated as the ratio between the vehicle position at the beginning of the braking phase and the span length:

$$\text{Braking position} = \frac{x}{l}. \quad (4.2)$$

The braking distance and time are inversely proportional to the braking request, see Figure 4.11 and 4.12; those quantities also depend on the altimetric profile and on the curvature radius of the track. Figure 4.13 shows the voltage peaks during the regenerative braking phase, as a function of braking request and braking position, including the voltage limiter: during the braking phase, the braking request affects the voltage peak value, which tends to increase at the increasing of the brake intensity, up to reaching the voltage limiter value (set equal to 3900 V). Furthermore, it can be highlighted that the maximum reached voltage value depends on the braking position, i.e. the position from which the vehicle begins the braking phase: in fact, the voltage limit value is reached

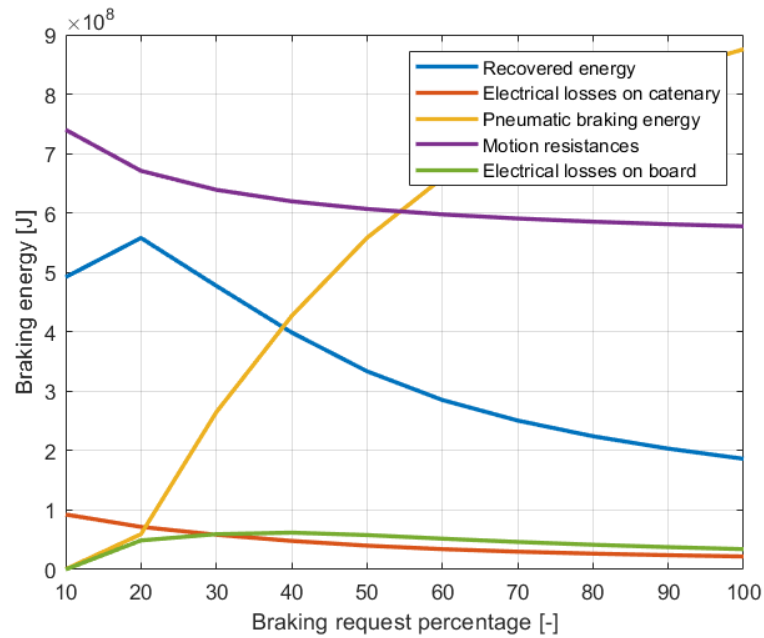


Figure 4.14: Feasibility analysis: ETR 1000 energy fluxes at 50% of braking position.

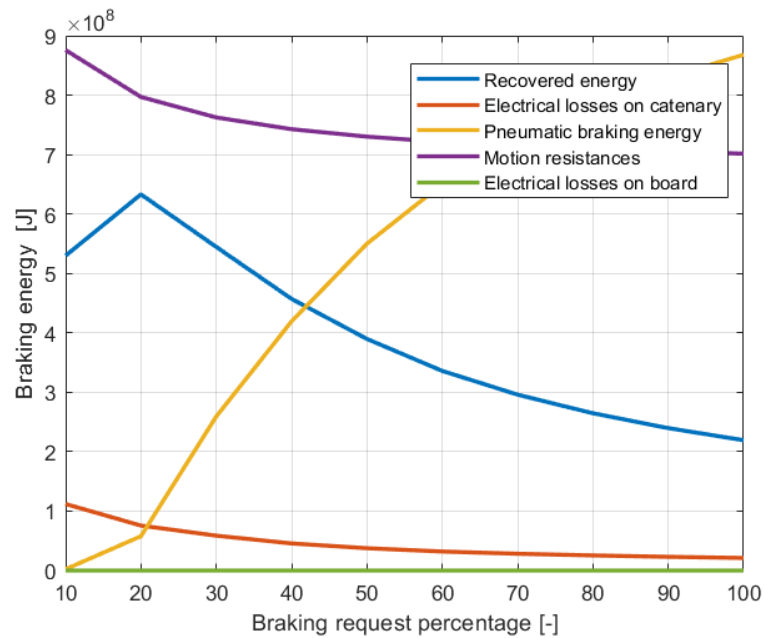


Figure 4.15: Feasibility analysis: ETR 1000 energy fluxes at 80% of braking position.

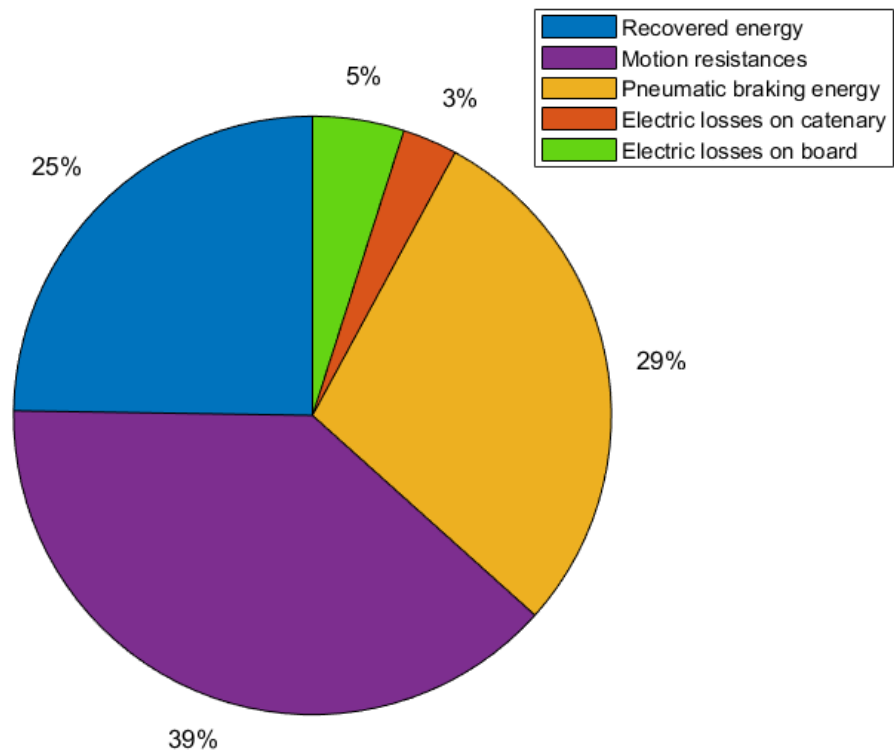


Figure 4.16: Feasibility analysis: ETR 1000 energy contributions at 50% of braking position with a 45% of braking request.

up to about 80% of braking position. From this value on, the voltage limiter is not activated thanks to the energy storage device connected in parallel with the ESS, which can handle the voltage peak.

Figure 4.14 and 4.15 illustrate the energy fluxes involved in the regenerative braking phase of the ETR 1000, respectively at 50% and 80% of the braking position: the Figures show that, getting closer to the substation, the electrical losses decrease, while the recovered energy increases. Both cases show a recovered energy peak located at about 20% of braking request, but, analysing Figure 4.11 and 4.12, with that value of braking request, braking distance and time are too high, over the limits for rail application. An acceptable operating condition is represented by the 40-50% braking request zone: the braking occurs with acceptable time and distance and the recovered

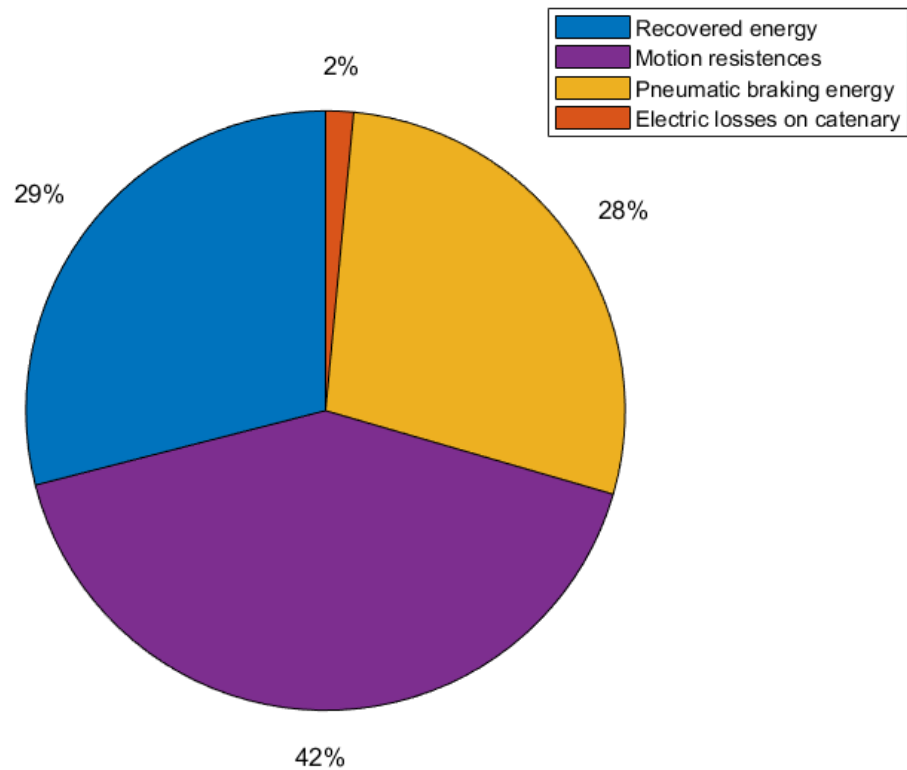


Figure 4.17: Feasibility analysis: ETR 1000 energy contributions at 80% of braking position with a 45% of braking request.

energy is still significant. Moreover, it can be highlighted, in Figure 4.15, how the electrical losses on board value is equal to 0: in fact, the voltage limit value is not reached and, consequently, no energy is dissipated on on-board braking resistors. Figure 4.16 and 4.17 show respectively the energy contributions at 50% and 80% of braking position with a braking request zone equal to 45%.

The above reported results are referred to the ETR 1000 investigation: to understand a commuter train behaviour, the E464 locomotive with 5 ViValto coaches, within the Rimini-Bologna line, have been studied, implementing the same mission profile.

Figure 4.18 shows the voltage peaks reached by the commuter train. The trend is similar to the one obtained for the ETR 1000: in fact, the voltage peak, close to the substation, is lower than the

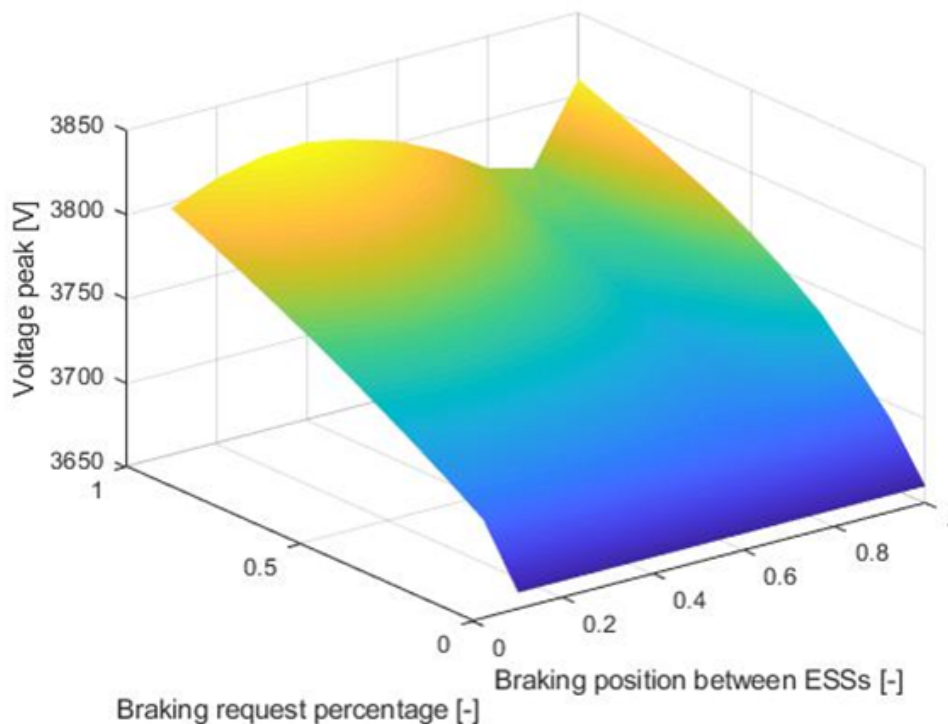


Figure 4.18: Feasibility analysis: E464 locomotive and 5 ViValto coaches voltage peaks as a function of braking request and braking position.

one reached in the middle of the span and this is due to the presence of the battery, which is able to manage the energy flux. However, the voltage values do not reach the voltage limiter value of 3900 V, even in the middle of the span, as, instead, occurs for the ETR 1000 (Figure 4.13). Figure 4.19 shows the energy fluxes during the braking phase: the dissipated energy is equal to 0 because the voltage limiter is not activated and, indeed, the recovered energy increases with the increment of the braking request percentage. The braking distance and time have trends similar to the ones of the ETR 1000: however, in this case, the highest recovered energy values occur with the higher braking request percentage, which corresponds to acceptable braking distance and time, see Figure 4.20, which is referred to a braking position equal to 80%.

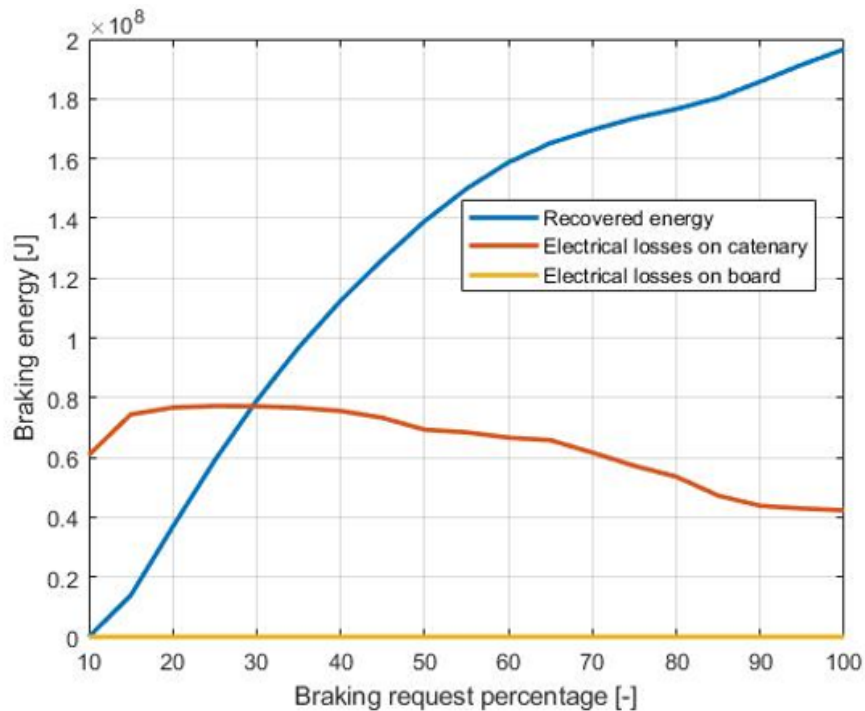


Figure 4.19: Feasibility analysis: E464 locomotive and 5 ViValto coaches energy fluxes.

4.4 Optimisation investigation on different operating scenarios

The feasibility analysis has been carried out considering one vehicle crossing the line: this scenario cannot be considered representative of a complete rail system, since a single vehicle which crosses alone an entire line is not a typical traffic condition. To perform a more complete overview, different traffic scenarios have been investigated: Figure 4.21 shows the considered operating scenarios.

The first scenario, i.e. the one way scenario, involves two vehicles which move along the same line (the first train is the one which departs earlier), with the same travelling direction, and two different simulations have been carried out:

- First simulation: the trains depart with a temporal offset and, once reached a velocity equal to 70 m/s, after a constant speed phase, simultaneously apply a full braking.
- Second simulation: the trains depart with a temporal offset, reach a velocity equal to 70

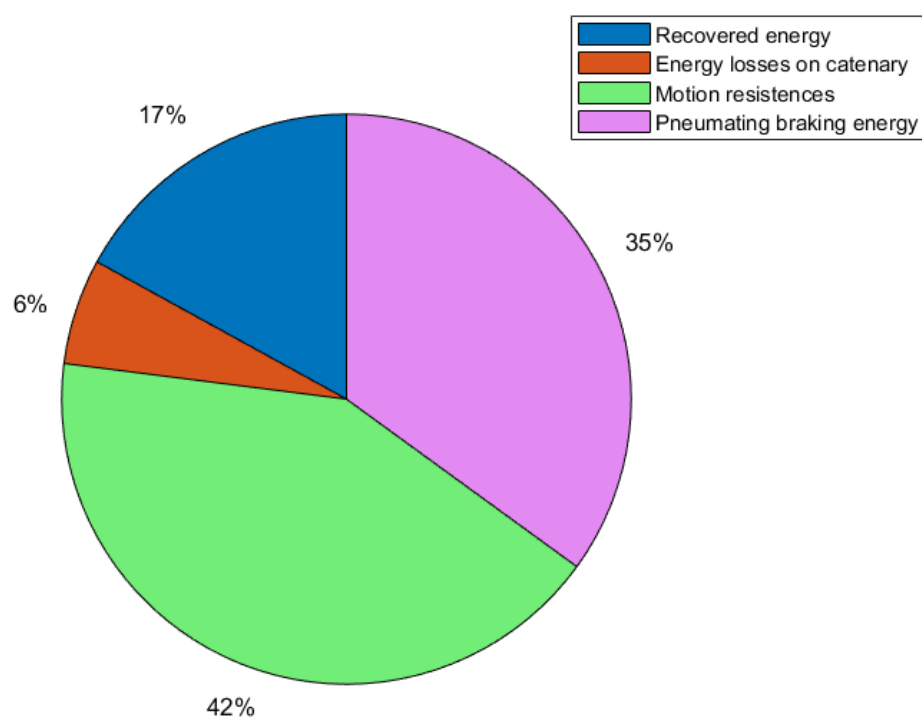


Figure 4.20: Feasibility analysis: E464 locomotive and 5 ViValto coaches energy contributions at 80% of braking position with the maximum braking request.

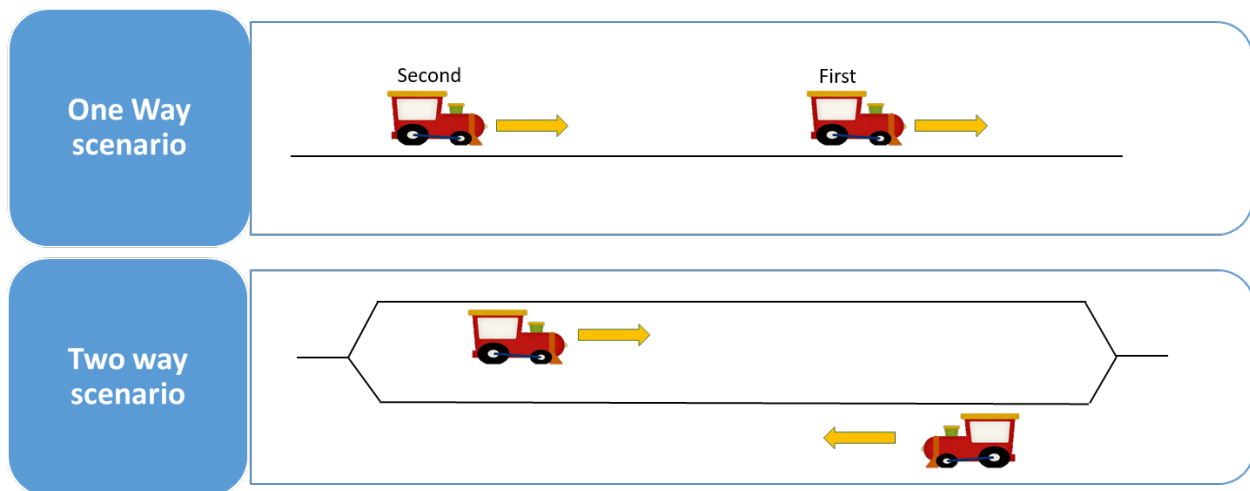


Figure 4.21: Considered operating scenarios: two vehicles, moving in the same direction and two vehicles moving in opposite directions.

m/s and then the vehicle which follows starts a full braking application, while the other one continues its itinerary, starting its braking phase, only after the complete stop of the following one.

The second traffic scenario, i.e. the two way scenario, involves two vehicles which move in opposite directions, in parallel rails, connected and fed by the same substations:

- First simulation: the vehicles depart at the same time, starting from opposite position in the line. Once reached a velocity equal to $70 m/s$, after a constant speed phase, the vehicles simultaneously brakes in different spans (no meeting).
- Second simulation: the vehicles depart at the same time, starting from opposite position in the line. Once reached a velocity equal to $70 m/s$, the trains proceed until they arrive in the same span: then, one vehicle applies a full braking while the other goes on, starting its braking phase in the following span.
- Third simulation: the vehicles depart at the same time, starting from opposite position in the line. Once reached a velocity equal to $70 m/s$, the trains proceed until they arrive in the same span and then brake simultaneously.

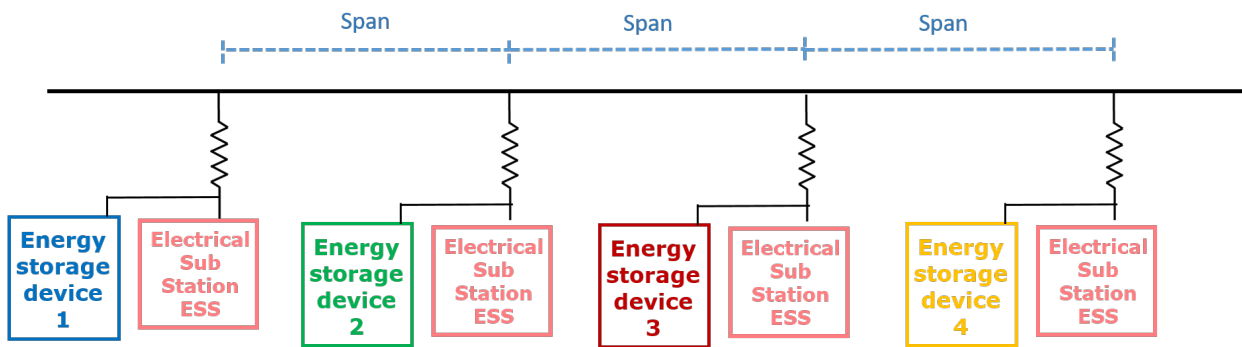


Figure 4.22: Scheme of line architecture for the optimisation analysis.

To better understand the following results, Figure 4.22 shows a scheme of the line architecture used to perform the optimisation analysis. The first part of this section reports the results obtained through the simulation of the ETR 1000 within the *Direttissima* line, in terms of behaviour of the batteries located in parallel to the substations.

Figure 4.23 represents the different time departure of the vehicles for the first simulation of the *one way* scenario. Figure 4.24 shows the batteries behaviour during the braking phase: it can be highlighted that the higher S.O.C. increase occurs in the battery located between the two spans involved in the braking phase. In particular, the increase of the central battery S.O.C. is about 5%, with a full brake application, while the S.O.C. variation of the batteries located at the limits of the two spans, involved in the braking phase, are lower, about 2-3%. Figure 4.25 shows the energy fluxes involved in the first simulation, for two vehicles which move in the same direction: the recovered energy can be considered relevant even if the electrical losses, due to the energy dissipation, are high; this is due to the simultaneous braking phases, which imply the activation of the voltage limiter.

The second simulation includes two trains: the first one goes on while the other one stops. Despite the not negligible distance imposed to the vehicles, in Figure 4.26, it can be noticed how the recovered energy is lower than the one showed in Figure 4.25, as well as the on-board losses: the lower values can be attributed to the lower current peaks, generated only by the braking train, and to the first vehicle which, moving at constant speed, directly uses the regenerated energy to feed its traction phase. These results prove to be interesting from an optimisation point of view: in

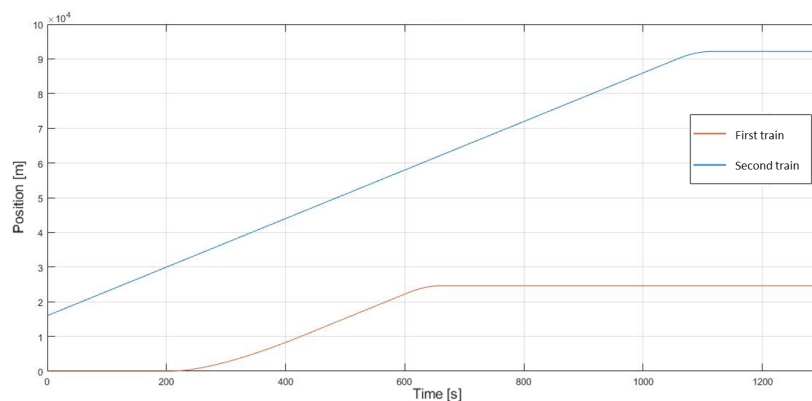


Figure 4.23: ETR 1000 optimisation analysis, first scenario: delayed departures of the two trains.

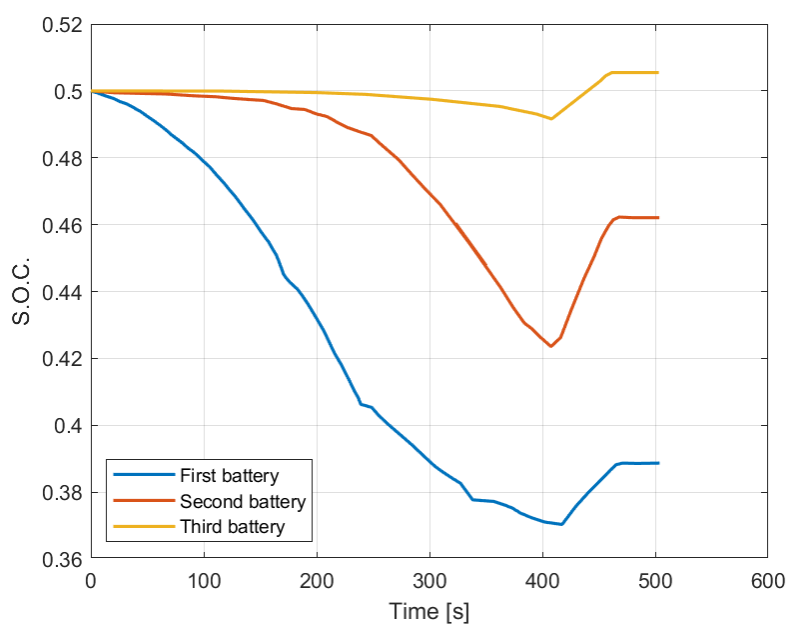


Figure 4.24: ETR 1000 optimisation analysis, first scenario, first simulation: batteries behaviour.

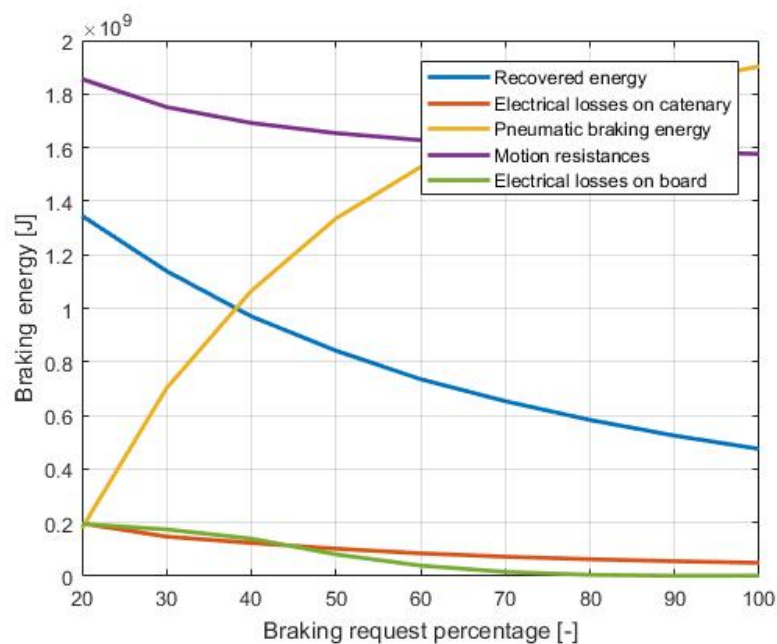


Figure 4.25: ETR 1000 optimisation analysis, first scenario, first simulation: energy fluxes.

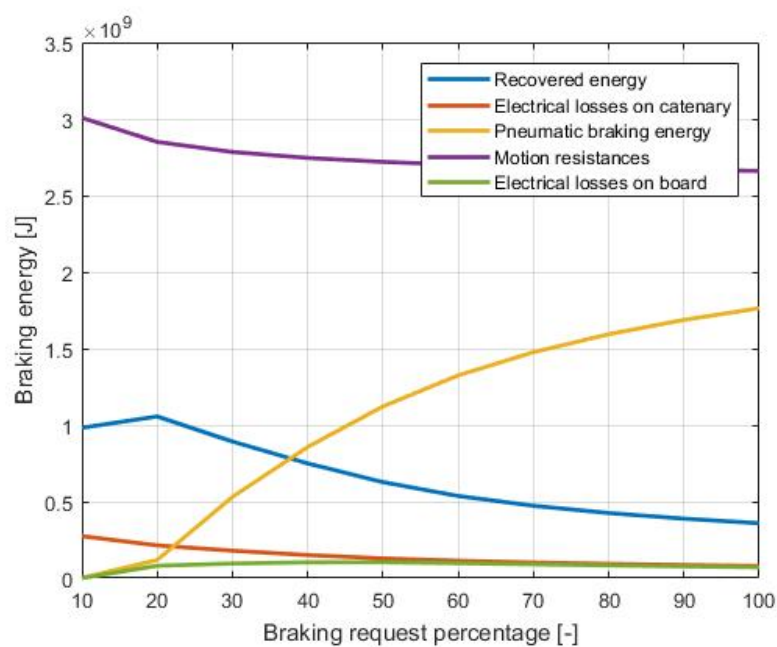


Figure 4.26: ETR 1000 optimisation analysis, first scenario, second simulation: energy fluxes.

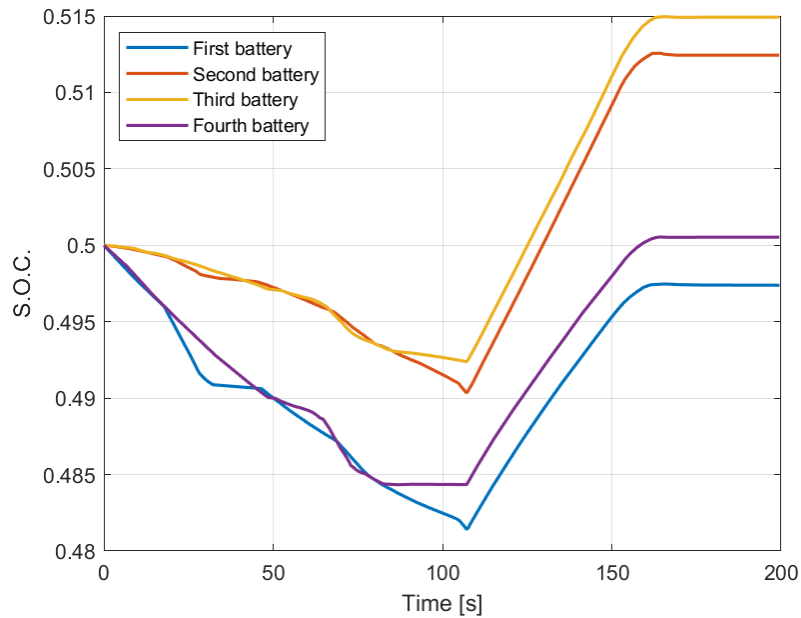


Figure 4.27: ETR 1000 optimisation analysis, second scenario, first simulation: batteries behaviour.

fact, the direct use of the regenerative braking energy, avoiding the implementation along the line (or on board) of energy storage devices, represents a significant advantage in terms of investment costs, in addition to the advantages concerning maintenance, dismantling and replacement.

To better investigate complex railway traffic scenarios, the optimisation analysis has been carried out studying also the scenario in which two vehicles move in opposite directions in parallel rails. As mentioned, the first simulation concerns the trains braking within two different spans, avoiding the vehicles meeting: in particular, the braking phase occurs in two not adjacent spans. Figure 4.27 shows the behaviour of the batteries which delimit the braking spans: the results report the S.O.C. of the four mentioned batteries, highlighting an increment of about 2%, due to the presence of many energy storage devices: the total recovered energy is about 800 MJ, equal to about 222 kWh, see Figure 4.28. The recovered energy, even if it cannot be considered negligible, do not justify the cost of the storage system: in fact the S.O.C. increase should reach about 5%, as explained in Subsection 3.2.2.

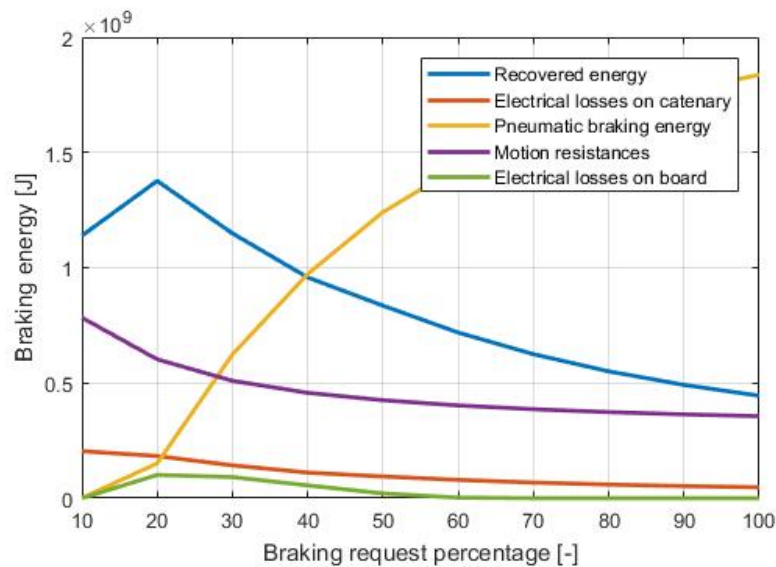


Figure 4.28: ETR 1000 optimisation analysis, second scenario, first simulation: energy fluxes.

The second simulation concerns two vehicles travelling in opposite directions and the results are shown in Figure 4.29 and 4.30: as in the previous scenario, the vehicle which continues its trip, directly uses the recovered energy of the braking one. This scenario proves to be the more favourable operating condition: here, the installation of energy storage devices is almost unnecessary. To apply this optimised operating scenario, a proper scheduling of the stops (or significant slowdowns) or, in an overall context, the planning of the vehicles time-tables is essential and also extremely difficult to be completely achieved.

The last simulation, carried out for the ETR 1000 within the *Direttissima* line, concerns two vehicles which simultaneously brake in the same span: the batteries involved in the braking phase are mainly the two which delimit the considered span. The S.O.C. incrementation for the energy storage devices is about 4-5%, shown in Figure 4.31. Concerning the recovered energy, see Figure 4.32, it can be noticed how the value is lower with respect to the first simulation, where the trains brake in different spans: this is due to higher current peaks which, through the activation of the voltage limiter, cause the dissipation of the excess energy.

The second part of Section 4.4 focuses on the results achieved for the E464 locomotive with 5 ViValto coaches within the Rimini-Bologna line. The analysed operating scenarios are the same

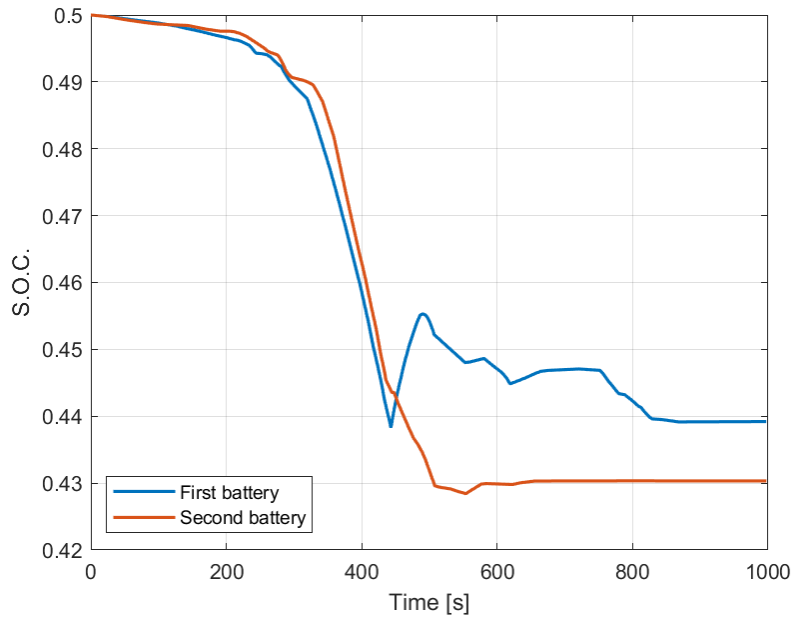


Figure 4.29: ETR 1000 optimisation analysis, second scenario, second simulation: batteries behaviour.

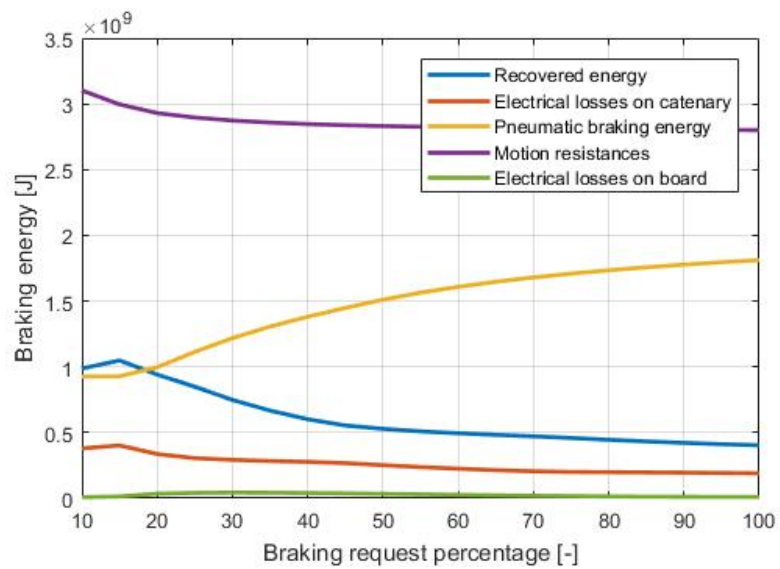


Figure 4.30: ETR 1000 optimisation analysis, second scenario, second simulation: energy fluxes.

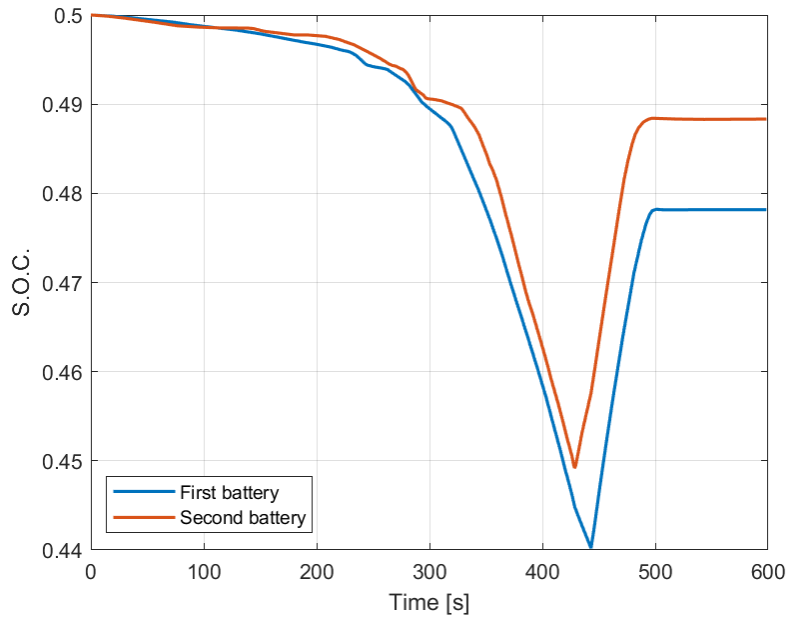


Figure 4.31: ETR 1000 optimisation analysis, second scenario, third simulation: batteries behaviour.

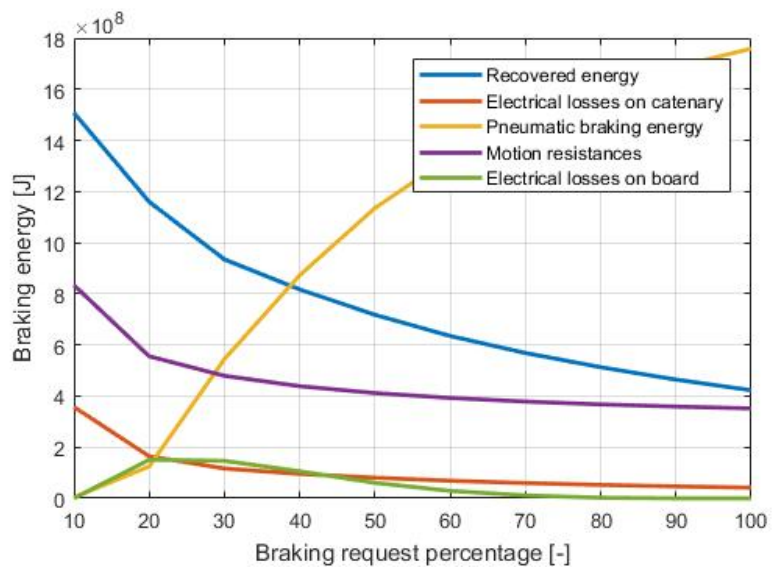


Figure 4.32: ETR 1000 optimisation analysis, second scenario, third simulation: energy fluxes.

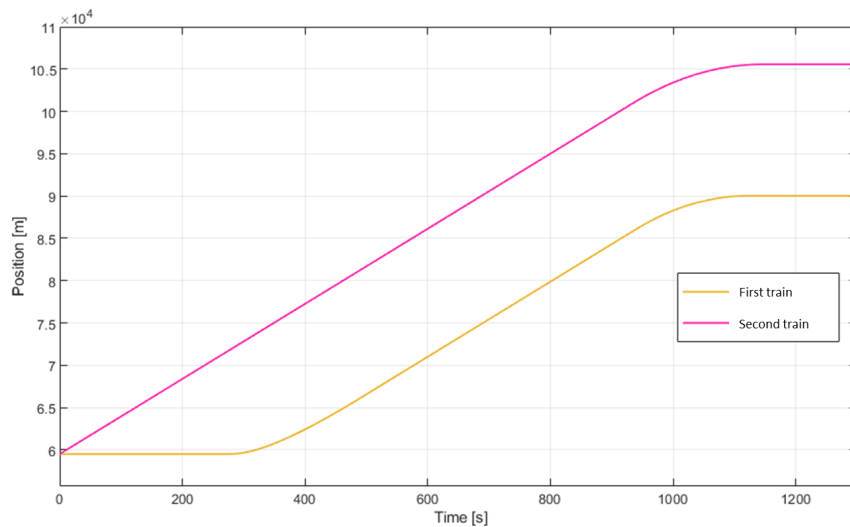


Figure 4.33: E464 optimisation analysis, first scenario, first simulation: delayed departures of the two trains.

described in the previous paragraphs: the only difference is represented by the speed which can be reached by the two vehicles. The E464 locomotive cannot travel at 250 km/h , as the high-speed train, and its maximum velocity is 160 km/h .

The first scenario involves two vehicles which move in the same direction, one in a more advanced position with respect to the other, and which brake simultaneously. As shown for the ETR 1000 simulations, Figure 4.33 represents the different time departure of the vehicles. Figure 4.34 shows the results concerning the batteries S.O.C., in particular the ones affected by the braking phase. As in the ETR 1000 corresponding simulation, the higher S.O.C. increment concerns the battery at the beginning of the first span and the one located between the two considered spans, while the S.O.C. of the battery located at the end of the second span experiences a negligible increment: the E464 does not reach the same velocity of the high-speed vehicle and, due to this characteristic, the braking effort is lower.

The batteries interested by the braking phase are, indeed, the ones closer to the position of the braking application. Figure 4.35 shows the energy fluxes involved in the braking phase: the voltage limiter is not activated and thus there is not peak of recovered energy, since it assumes an increasing trend.

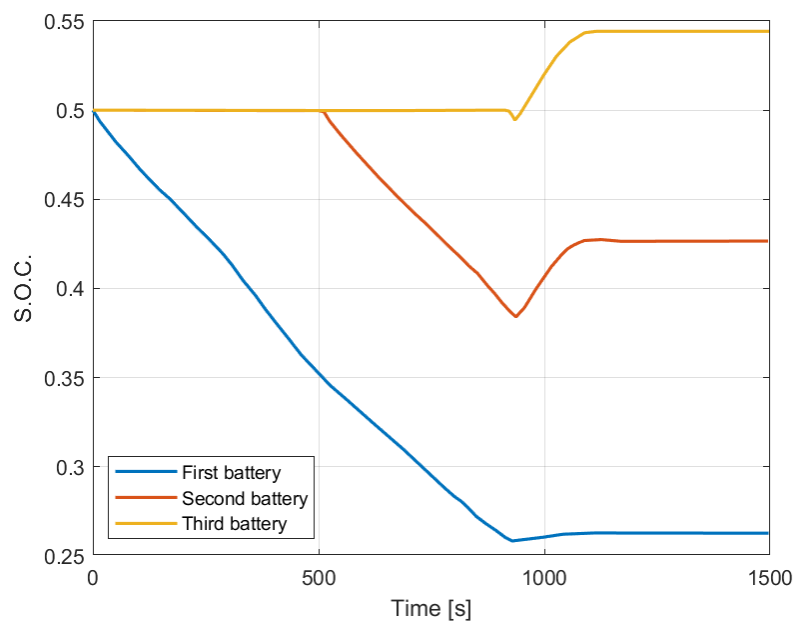


Figure 4.34: E464 optimisation analysis, first scenario, first simulation: batteries behaviour.

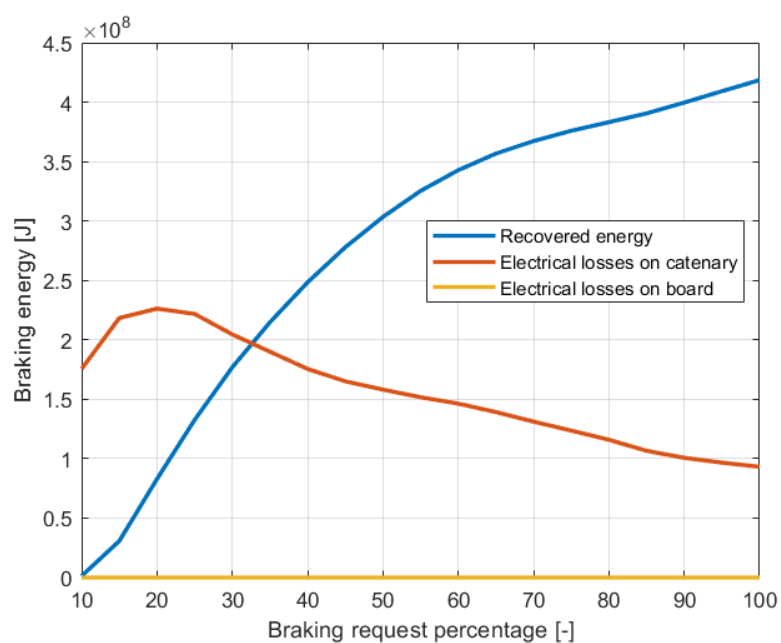


Figure 4.35: E464 optimisation analysis, first scenario, first simulation: energy fluxes.

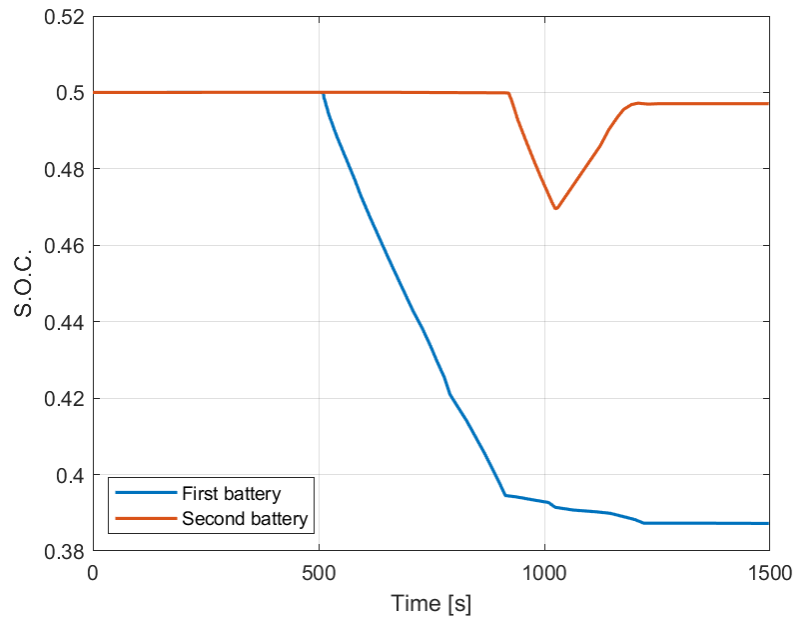


Figure 4.36: E464 optimisation analysis, first scenario, second simulation simulation: batteries behaviour.

The second simulation results, concerning the batteries S.O.C. behaviour are shown in Figure 4.36: as occurred in the corresponding ETR 1000 operating scenario, the regenerated energy of the braking vehicle is directly used by the one which goes on and the battery S.O.C. increment for the central battery is not enough to justify the energy storage device installation and maintenance costs; this solution proves to be the ideal one with a proper traffic time-tables scheduling.

The simulation of the second operating scenario provides analogous results with respect to the ETR 1000 ones. For the sake of synthesis the results of the first simulation are not shown: the S.O.C. of the 4 batteries which delimit the two spans involved in the braking phase have the same trends of the ones related to the high-speed results.

The main result of the second simulation is shown in Figure 4.37: the S.O.C. is related to the battery between the two spans, which is the most significant. The slope of the S.O.C. trend changes when the train in the backward position applies the braking effort: in fact, as for the ETR 1000 simulation, the vehicle in the advanced position directly uses the recovered energy produced by

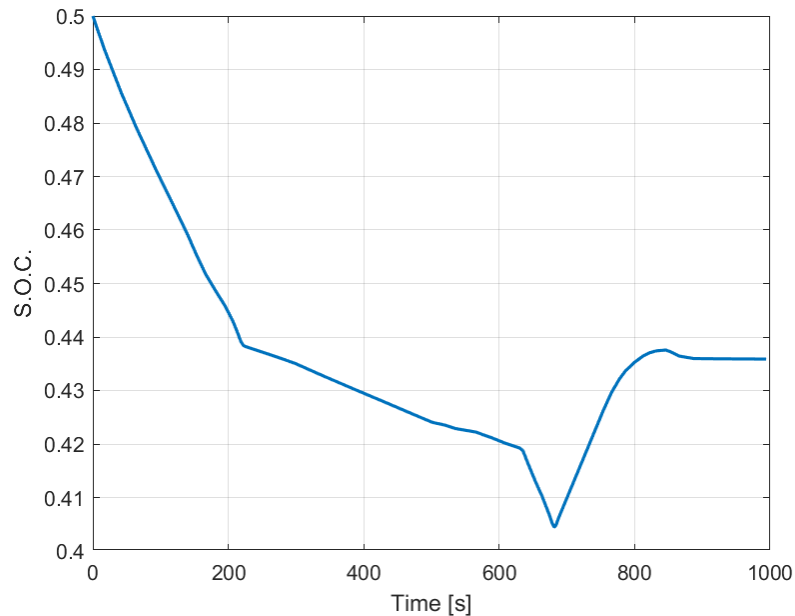


Figure 4.37: E464 optimisation analysis, second scenario, second simulation: battery behaviour.

the backward vehicle; then, the S.O.C. increases due to the braking of the first vehicle itself.

The last simulation concerns the simultaneous braking phase of the two vehicles in the same span: Figure 4.38 shows the S.O.C. increment for one of the batteries which delimit the span (for a better clarity, only one trend has been reported in the Figure, since the other one is almost superimposed). The increment is about 7%, a significant value: the braking phase is longer than the one performed by the ETR 1000 and the voltage limit is not been reached by the voltage peaks, thus avoiding energy dissipation.

Basing on the shown results, the optimised solution proves to be the one where, while a vehicle is braking, another one can directly use the regenerated energy: this approach avoids the implementation of energy storage devices where the traffic scenario does not include a large number of braking phases. A proper time-table scheduling of the vehicle traffic can make the most of the regenerated energy utilisation, decreasing, at the same time, the battery costs installation and maintenance. Moreover, the installation of energy storage devices represents an ideal solution where more vehicles apply their braking phase, as in stations or zones where the vehicle shall

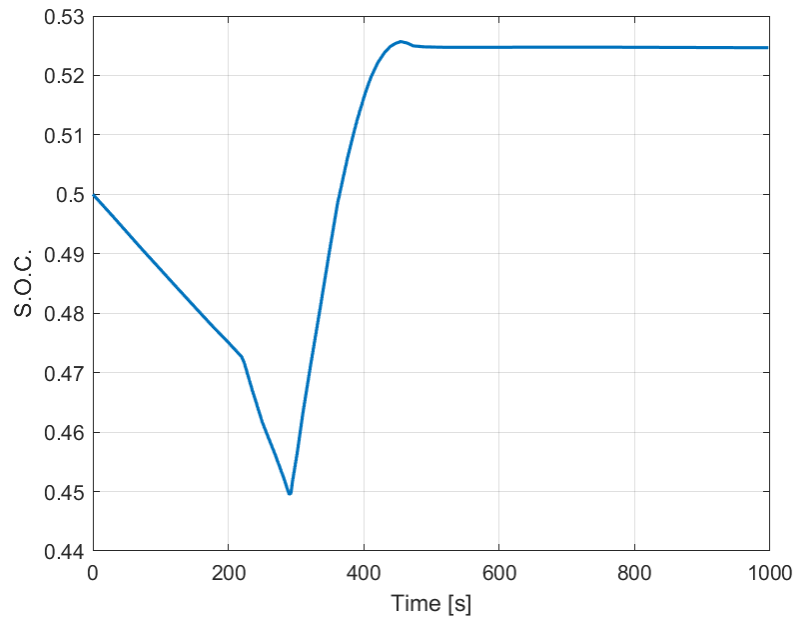


Figure 4.38: E464 optimisation analysis, second scenario, third simulation: battery behaviour.

slowdown or stop.

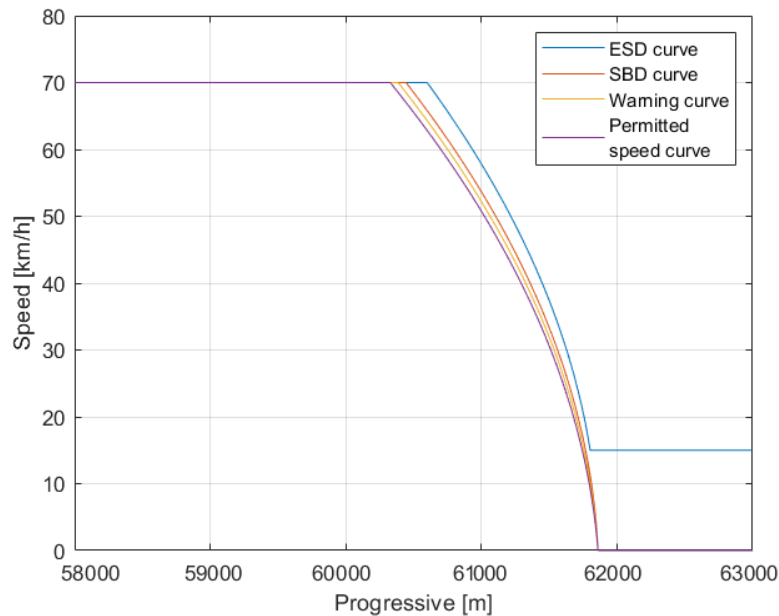


Figure 4.39: Example of braking curves calculated by the developed model.

4.5 Signalling results

This section of Chapter 4 focuses on the results achieved through the implementation of a signalling system: the purpose is to analyse an operating scenario which includes dynamical constraints represented by the signalling profile. In a real traffic scenario, in fact, the vehicle cannot follow a free mission profile, even if it is an energetic optimised one: the implementation of a signalling profile permits to analyse the energetic optimisation of a railway system in presence of unexpected events which impede the maximum energy recovery.

In Section 3.3, the braking curves due to signalling have been described. In particular, to calculate the braking spaces, the formulas need some parameters values provided by the railway company or calculated through RFI standards which furnish first attempt values and their definition range. Due to the absence of information from the railway company and since the determination of the exact values is beyond the scope of this research work, to calculate the braking curves and spaces, the first attempt values have been used; as a further development, the parameters can be evaluated through a sensitivity analysis. Figure 4.39 shows an example of the braking curves calculation in

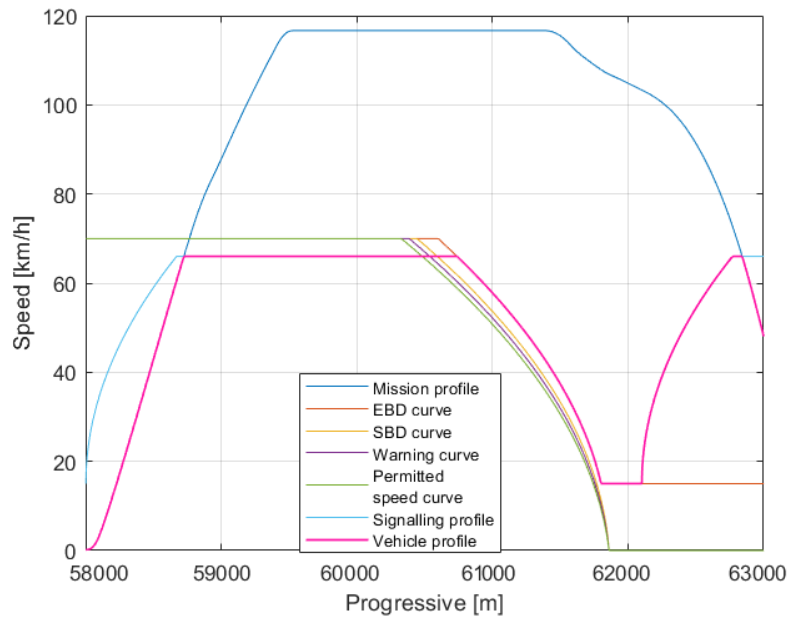


Figure 4.40: Example of comparison between signalling, mission and vehicle speed profiles.

the developed model. The simulation has been performed considering the ETR 1000 high speed train: due to a stop *constraint* at about 62000 m of the line progressive, the four braking curves have been calculated and, comparing them with the vehicle speed, the proper braking curve is applied.

Figure 4.40 illustrates the velocity profiles simulated by the complete model, including the signalling one. The vehicle speed is the lower one between the mission and signalling ones: it can be noticed that, if the vehicle exceeding the *Permitted*, *Warning* and *ServiceBrake* deceleration curves, the vehicle brakes follows the EBD curve, as suggested by the European normative. Figure 4.41 shows the signalling profile splitting as explained in Section 3.3: the splitting in different phases allows the system to control the vehicle position and velocity, to respect the safety limits and to apply the proper braking effort.

To investigate a real traffic scenario, in this research work, a set of simulations has been carried out: the model, including the vehicle dynamics, the feeding line, the energy storage devices and the signalling system is able to represent a complex railway system and it allows to properly investigate

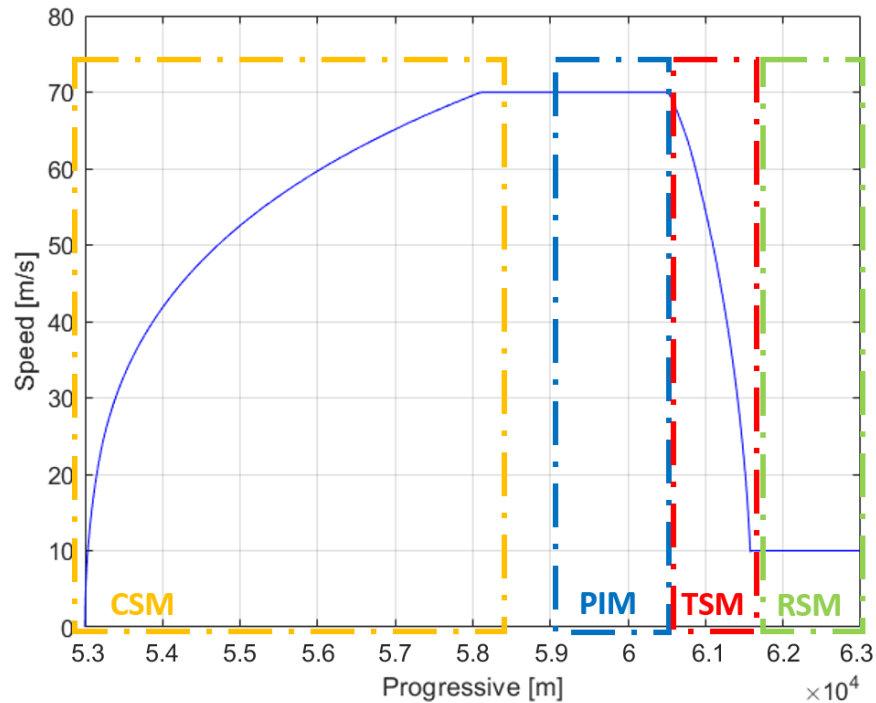


Figure 4.41: Signalling profile division to supervise vehicle velocity and position.

the feasibility of regenerative braking and to provide accurate hints on how to optimise from an energetic point of view the whole system. The simulations have been carried out for both railway applications, i.e. commuter and high-speed trains.

The first analyses focus on the total recovered energy, in presence or absence of the signalling system. In particular, the analyses have been performed implementing a different numbers of batteries, to compare the correlation between recovered energy and energy storage devices and to understand where their implementation and costs are justified: in fact, even a perfectly cost optimised scenario could transform itself in a disaster when taking into account signalling. Figure 4.42 shows the recovered energy achieved through regenerative braking application for the E464 commuter train. The Figure shows how, as could be expected, the recovered energy percentage is lower when the signalling system has been implemented: in fact, the signalling profile takes into account the dynamical constraints which can occur in a real traffic condition and which must not neglected in an optimised speed profile, where the braking phase is scheduled to maximise the

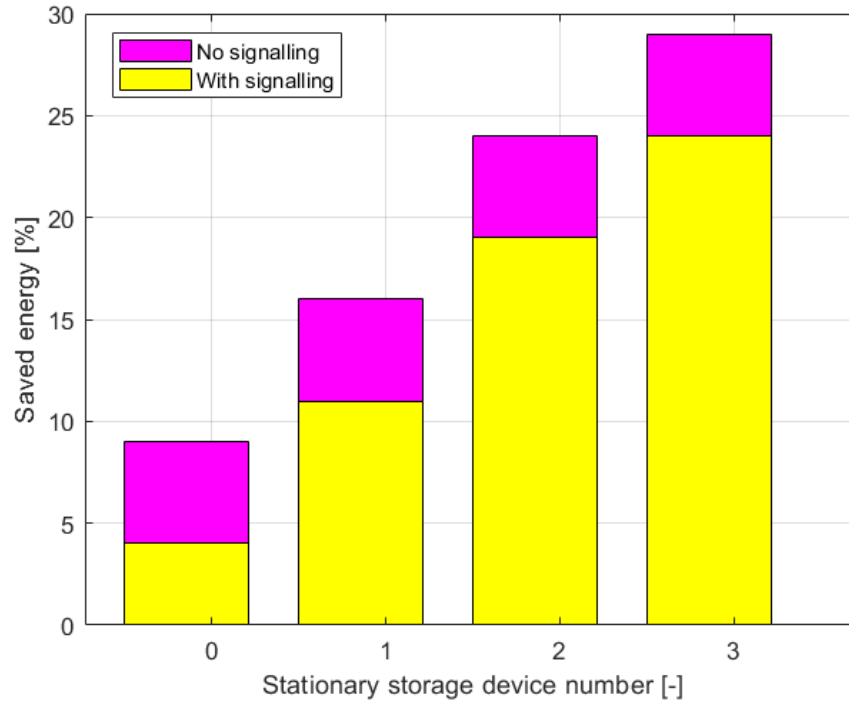


Figure 4.42: Recovered energy, for the E464 commuter train, in presence or absence of the signalling system.

recovered energy. Furthermore, the amount of saved energy when no battery has been implemented confirms that the regenerated energy can be also directly used by other vehicles, avoiding the presence of energy storage devices along the electrical line. Moreover, a lower incrementation of saved energy, from two to three implemented batteries, can be noticed: this suggests that the amount of saved energy does not increase with the same trend of batteries installation and maintenance costs. An accurate investigation of the whole line can establish the proper number of energy storage devices which can guarantee a significant energy advantage.

As for the commuter train, a set of simulations has also been carried out for the ETR 100 high-speed train. Figure 4.43 shows the obtained numerical results. The results are similar to those obtained for the commuter train; the amount of the saved energy is usually higher for the same number of installed batteries, due to the higher velocity and braking efforts. With a low number of energy storage devices (0 or 1), the saved energy is not as high as with more batteries, with respect

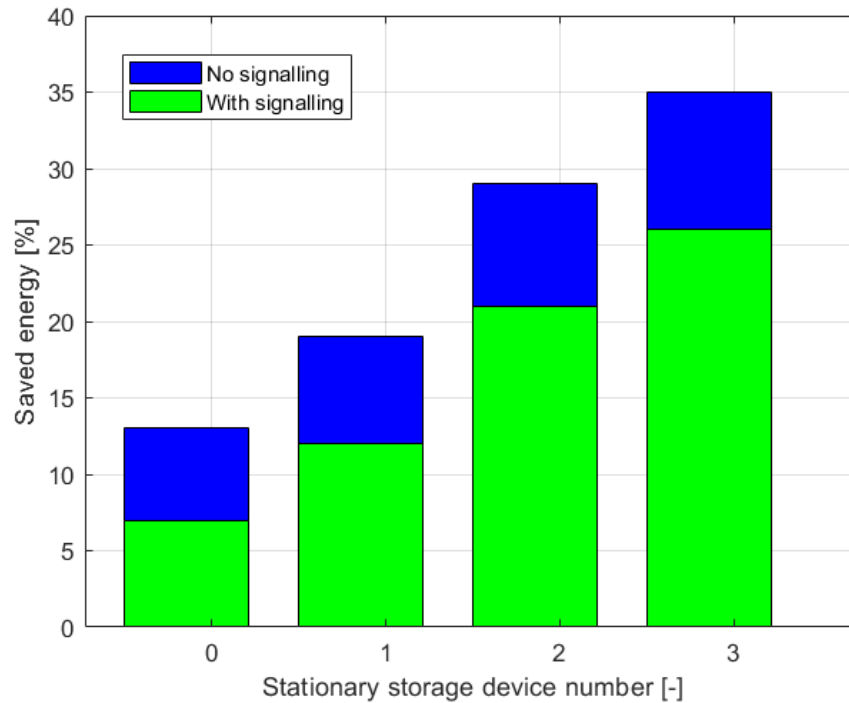


Figure 4.43: Recovered energy, for the ETR 1000 high-speed train, in presence or absence of the signalling system.

to the commuter train: this can be attributed to the voltage limiter which dissipate a significant amount of energy on on-board resistor because of the absence of batteries to store the regenerated braking energy.

To deepen the analysis of the signalling system from an energetic optimisation point of view, a set of simulation concerning the intervention of the emergency braking deceleration, applied through the use of emergency braking system, has been carried out, both for commuter train and high-speed one. The simulations include different number of EBD interventions, which represent, from a regenerative or saved energy point of view, the worst operative condition: the regenerative energy is connected to the use of the motor as a generator and the emergency brake system excludes the mentioned braking approach.

Some preliminary considerations on the energy contributions should be highlighted: Figure 4.44 shows the energy contributions of the ETR 1000 vehicle when a sudden slowdown occurs

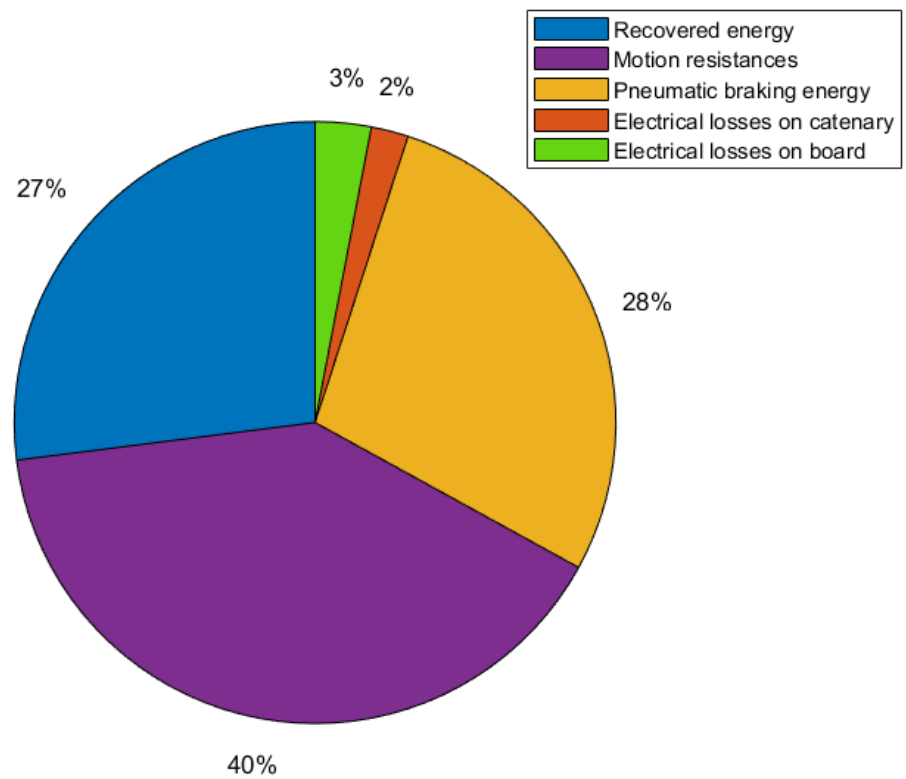


Figure 4.44: Energy contributions with a slowdown during the vehicle route.

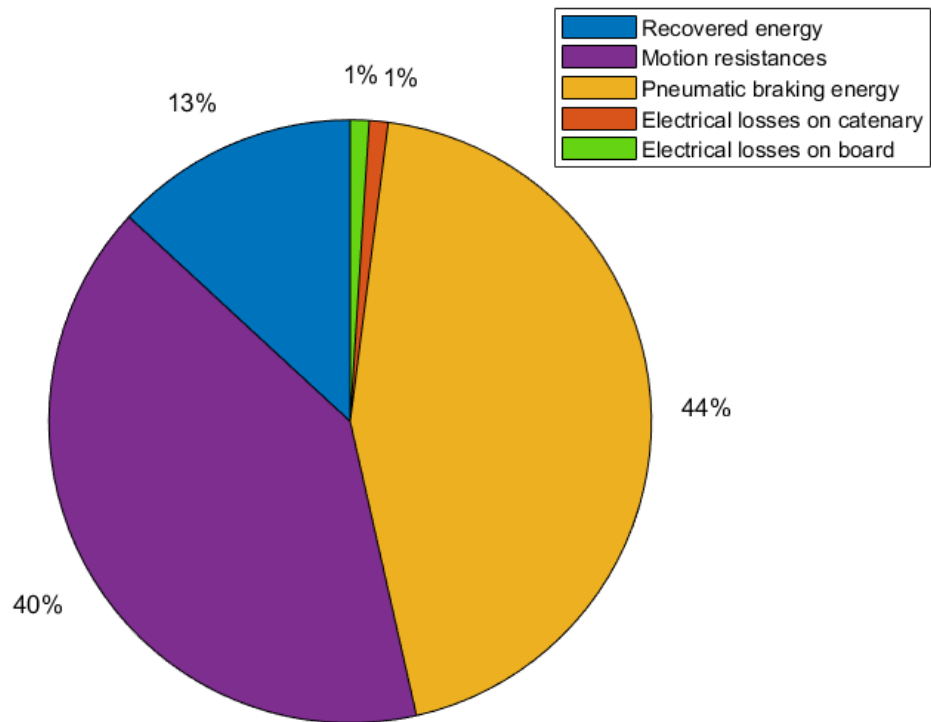


Figure 4.45: Energy contributions with a service brake deceleration due the ETCS intervention, during the vehicle route.

during its route. The recovered energy is lower than the one which can be recovered by the same vehicle braking close to the substations, but it is still significant. Figure 4.45 shows the results for the same vehicle with the same route when a service brake deceleration due to the intervention of the ETCS system occurs for the same sudden slowdown: the recovered energy is drastically reduced, corresponding to a rapid increase of the pneumatic braking energy. The emergency brake intervention totally cancels the possibility to recover energy and the braking phase is totally handled by the pneumatic systems, see Figure 4.46.

The application of emergency brake deceleration has hence to be avoided, both for the passengers safety and comfort and for the consequent increase of wheel/rail wear, and it has to occur only in

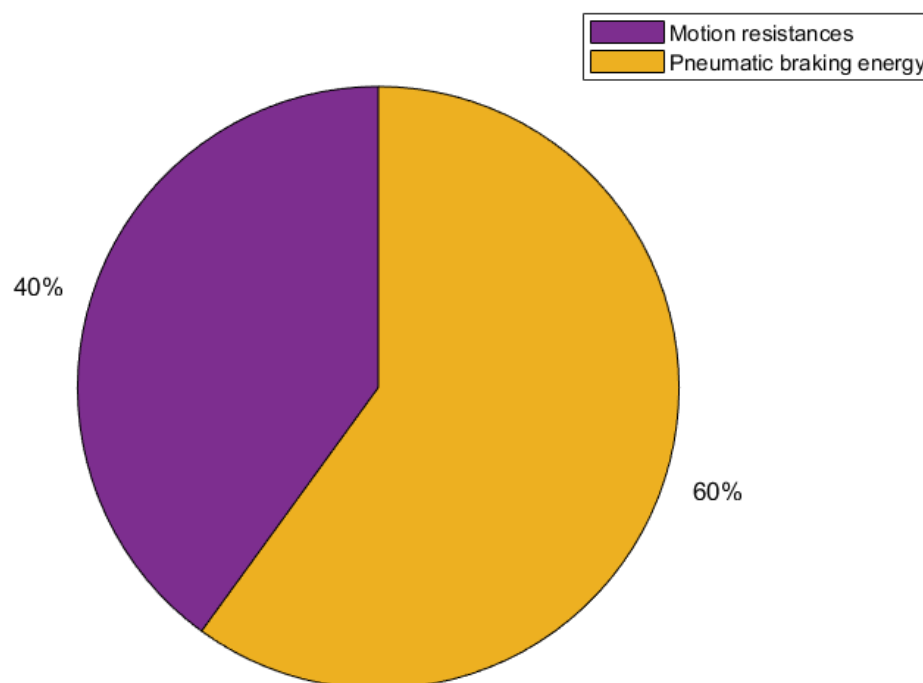


Figure 4.46: Energy contributions with an emergency brake deceleration due to the ETCS intervention, during the vehicle route.

dangerous situation. Due to the mentioned considerations, no more than three EBD applications have been considered for the simulation of the commuter train within the Rimini-Bologna line (about 50 km). Figure 4.47 shows the saved energy with respect to different number of Emergency Brake Deceleration intervention and the analysed line length: it can be noticed that, in a brief line route, where the applications of regenerative braking are already reduced, even a single emergency braking application strongly reduces the saved energy, while three interventions almost cancel the saved energy within the considered route. However, three emergency brake interventions represent an unrealistic operating scenario and, in a line of 50 km, the saved energy can still be considered significant.

Similar considerations apply for the ETR 1000: the considered line is longer, about 200 km, and,

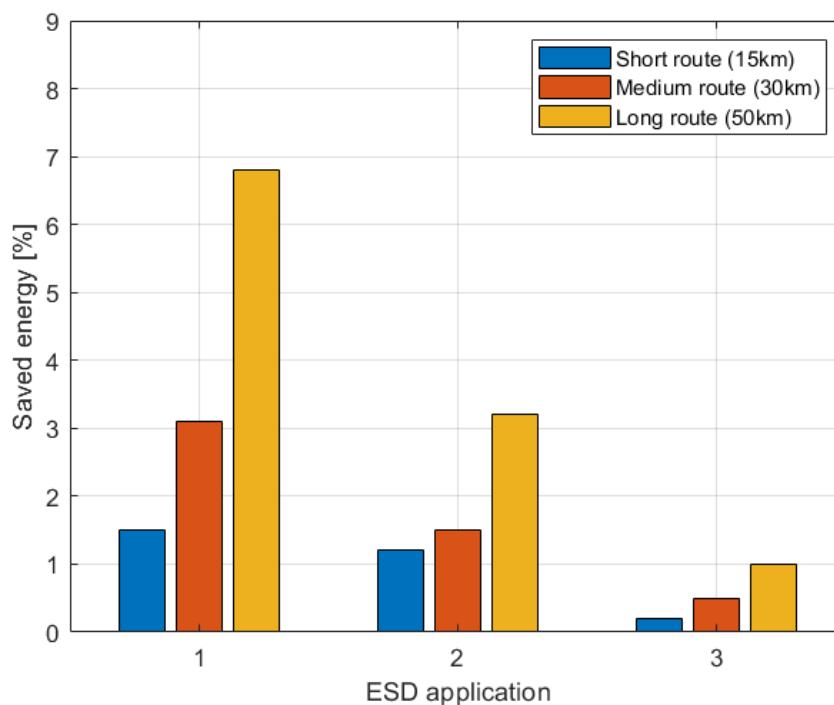


Figure 4.47: Results on saved energy with respect to different EBD application number, for the commuter train, for short, medium and long routes.

due the same reason explained for the E464, three EBD applications have been considered. Figure 4.48 highlight the lower impact of three emergency braking interventions in this scenario: this can be associated to the longer line and to the higher amount of saved energy.

The implementation of the signalling system highlights how the amount of energy, saved through regenerative braking and storage devices implementation, is sensitive to every change which can affect the optimised condition: to save energy in a railway scenario proves to be the result of a complex balance between energetic optimisation considerations and the constraints which characterise the whole system.

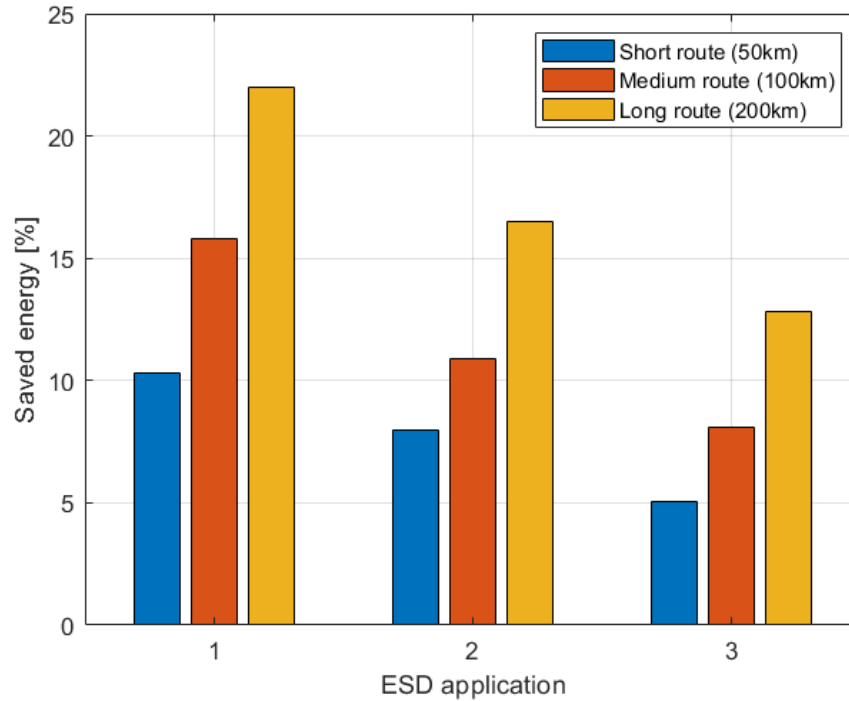


Figure 4.48: Results on saved energy with respect to different EBD application number, for the high-speed vehicle, for short, medium and long routes.

4.6 Preliminary cost analysis

A preliminary cost analysis, performed to find a first possible optimised scenario, has been carried out. To reach this goal, first of all, the energy storage device has to be defined: in section 3.2.2, the considered energy storage devices are Li-ion batteries, composed by 4 stacks in parallel to reach the capacity, each one composed by 1010 cells in series. In particular, the chosen battery has a nominal voltage equal to 3700 V and a nominal capacity equal to 53 Ah. To calculate the whole battery energy, the following Equation has been used:

$$E_{batt} = V_0 \cdot C_0, \quad (4.3)$$

where V_0 and C_0 represent the nominal voltage and capacity. The Equation 4.3 result is expressed in kWh: concerning the chosen Li-ion battery, the battery energy is about 784 kWh.

For the Li-ion battery, a cost of about 600 €/kWh has been assumed: the installation cost of the

Table 4.3: Analysis cost of battery implementation within the considered lines.

	High-speed train line	Commuter train line
Recovered energy	400 [MJ]	200 [MJ]
Battery cycles (day)	15	18
Saving energy (life battery)	8200 [MWh]	4900 [MJh]
Electrical energy cost saving	820 [k€]	492 [k€]
Payback time	8,5 [y]	14,3 [y]

considered energy storage device is about 470000 €.

The battery efficiency η_{batt} has been considered equal to 90% and the electrical energy supply, provided by the stakeholder, costs about 100 €/MWh: it is possible to calculate how much money is possible to invest to obtain certain energy savings.

As shown in the previous Section, the recovered energy (E_{rec}) can be considered to be about 400 MJ for the high-speed train and 200 MJ for the commuter one. The considered battery should perform about 15 cycles each day within the line travelled by the high speed train, while 18 cycles for the one travelled by the commuter train (considering that it is possible to assume 25 cycles or more in a railway station). The savings can be calculated as follows:

$$E_{sav} = \frac{E_{rec}}{3600s} \cdot \eta_{batt} \cdot O_{batt}, \quad (4.4)$$

where O_{batt} represents the total number of cycles for the entire battery life, calculated as the product between the cycles performed each year and the assumed battery life (15 year for both the considered cases, being the daily number of cycles similar). The cost of electrical energy, supplied by the energy provider, is 100 M€/h. Table 4.3 shows the results of the cost analysis.

The results highlight how the installation of the considered battery proves to be convenient only for high-speed vehicles, while the economic gain for commuter trains is negligible with respect to the cost installation, where the direct use of recovered energy, generated by the regenerative braking of other vehicles which are travelling the line, proves to be a better solution. The analysis of other energy storage devices is not the focus of this research work, but, even for the high speed

vehicle, other types should be considered, to increase the economic gain. The reported cost analysis has been performed considering known the number of cycles performed by a battery, located in a certain line position, and considering only a type of vehicle (high-speed or commuter) crossing the line: to carry out a more accurate cost analysis, a real traffic condition within a line should be provided by the industrial partner. Moreover, innovative battery systems should be considered.

5

Conclusions and Future Developments

Due to environmental issues, which have a great impact on the current worldwide politics, the transport sector is pushing toward the research on energetic optimisation solutions. Within the TESYS Rail project, the use of regenerative braking has been investigated for railway applications. In particular, in this research work, commuter and high-speed vehicles have been considered, since they are usually neglected for this kind of applications due to their low number of braking phases during a route with respect to light railway systems, where regenerative braking has been deeply investigated.

The proposed model, developed in MATLAB[®] and Simulink-SIMSCAPE[™] environments, includes three main sub-systems, which can simulate a complex railway system. The first one is the vehicle dynamics model, which simulates the behaviour of the train, taking into account braking and traction effort, motion resistances and adherence limits. Furthermore, the electrical main systems have been modelled, in particular the feeding line, the electrical substations and the energy storage devices. The line has been modelled to analyse different topologies: the simplified approach needs a lower amount of information, because of the entire line is represented through the characterisation of only one span, which is crossed periodically, while the complex one requires the implementation of a larger number of details, since every span is included in the model. Finally, the above-mentioned models interchange information with a signalling model, which supervises the vehicle behaviour and acts through the use of proper braking curves: the model calculates the

Permitted Speed, Warning Service Brake Deceleration and Emergency Brake Deceleration curves, which, in a real operating scenario, guarantee the respect of safety limits, independently from the behaviour of the vehicle driver.

After a validation through experimental data provided by an industrial partner, a feasibility analysis, concerning regenerative braking application, has been carried out for the ETR 1000, an Italian high-speed train, along the Firenze-Roma line, and the E464 locomotive with 5 ViValto coaches, a commuter train, within the Rimini-Bologna line. Furthermore, different operating scenarios have been investigated: the presence of two vehicles within the same line, travelling in the same direction or opposite ones, has been studied to analyse its impact on the energy savings. The first outcome is represented by the energy storage devices capability to handle the voltage peaks due to the braking phase, especially significant for the high-speed vehicles: in fact, the voltage peaks of these vehicles are higher than the ones produced by commuter trains. The installation of energy storage devices along the line, in parallel with the substations, improves the management of regenerated energy, avoiding the use of on board resistors to dissipate the exceeding energy. Another important results is the possible usage by another vehicle of the regenerative braking energy, which represents the best solution in terms of energetic optimisation: the results, in fact, show that an accelerating vehicle can directly use the energy sent back to the line by a braking vehicle. This represents an ideal solution, due to the avoidance of batteries installation, which involves not negligible costs. The implementation of energy storage devices along the line proves to be necessary where more vehicles simultaneously produce braking energy (e.g. stations).

The signalling system has been considered to analyse the effects, on an already optimised mission profile, of dynamical constraints, introduced through the signalling mission profile, e.g. red light signals or slowdowns. In particular, the braking curves of the ETCS system have been implemented, to act in case of risk for the vehicle safety. The results show how the signalling system significantly impacts on energy savings considerations: unexpected events reduce the amount of energy savings with respect to a mission profile, designed to maximise them. In particular, the emergency braking intervention has a great impact on recovered energy: the

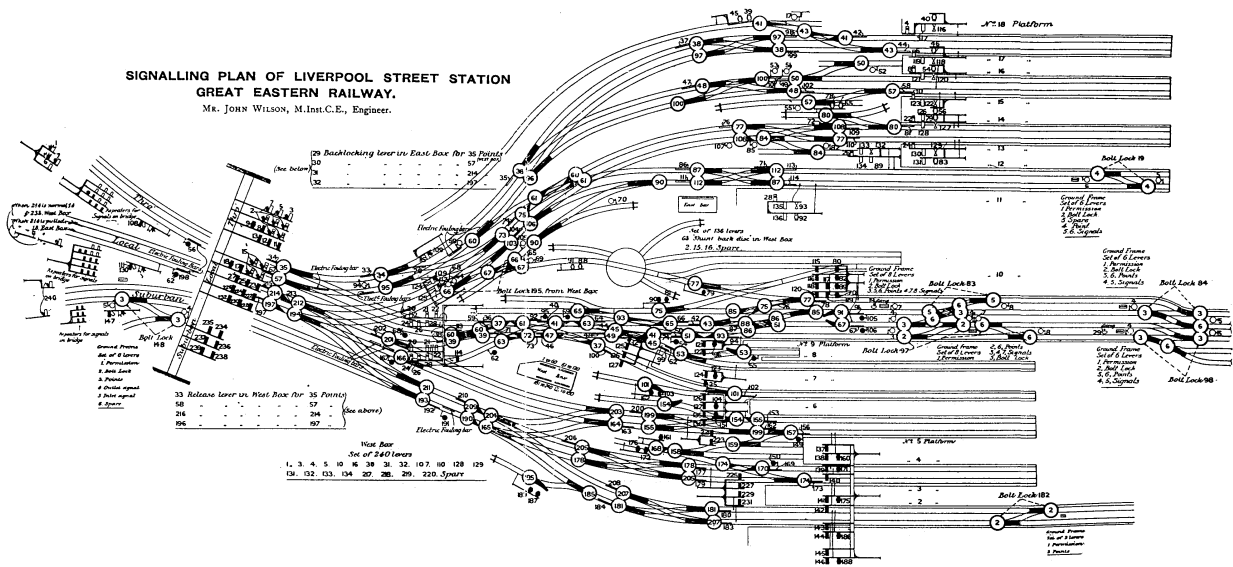


Figure 5.1: Example of station with its signalling plan.

intervention of the Emergency Braking Deceleration curve leads to a great difference between the optimised mission profile and the effective one, reducing the possible regenerated energy. Despite these considerations, considering the EBD application an uncommon event, which has to be avoided, the regenerative braking application represents an important solution to improve the energetic efficiency of a railway system and the energy savings potential is significant in both applications, i.e. high-speed and commuter systems.

The analyses, within this research work, have been carried out implementing free mission and signalling profiles. As future developments of further research works, a validation of the described considerations through the use of real signalling profiles and vehicles time-tables has to be performed. Consequently, more complex scenarios, involving a certain number of different vehicles along the same line or a station, can be analysed, see Figure 5.1.

Another step of future developments is represented by the improving of the current models themselves. The implementation of wheel slide protection and anti-skid systems should be foreseen to simulate more accurately the vehicle behaviour, considering more in detail the degraded adhesion between rolling surfaces, through, e.g., a real time model [51]. Moreover, the electrical substations have to be modelled in detail, since, in the current model, they have been modelled in a

Bibliography

- [1] European Environment Office. [III](#), [3](#), [4](#)
- [2] European Environment Agency. Progress of eu transport sector towards its environment and climate objectives. [III](#), [3](#), [4](#)
- [3] A. González-Gil, R. Palacin, P. Batty, and J.P. Powell. A systems approach to reduce urban rail energy consumption. *Energy Conversion and Management*, 80:509–524, 2014. [III](#), [14](#), [16](#)
- [4] J. Matheys, J.M. Timmermans, W. Van Autenboer, J. Van Mierlo, G. Maggetto, S. Meyer, A. De Groof, W. Hecq, and P. Van den Bossche. Comparison of the Environmental impact of 5 Electric Vehicle Battery technologies using LCA. *Proceedings of LCE 2006*, pages 97–102, 2006. [IV](#), [18](#), [20](#)
- [5] RFI. Piano di sviluppo di ertms (etcs e gsm-r) sulla rete rfi. [IV](#), [26](#), [27](#)
- [6] RFI. Sistema controllo marcia treno. [VIII](#), [24](#), [120](#)
- [7] M. Granovskii, I. Dincer, and M.A. Rosen. Economic and environmental comparison of conventional, hybrid, electric and hydrogen fuel cell vehicles. *Journal of Power Sources*, pages 1186–1193, 2006. [3](#)
- [8] TSI. Technical specifications for interoperability. [4](#)

- [9] D.K. Ware and R.N.H. Jones. Recent developments in light rail systems. *Proceedings of the Institution of Mechanical Engineers, Part F: Journal of Rail and Rapid Transit*, 206(1):47–65, 1992. [5](#)
- [10] A. Frilli, E. Meli, D. Nocciolini, L. Pugi, M. Ceraolo, and G. Lutzemberger. Improved Sustainability of Railway Systems: The Tesys Rail Project. *Proceedings of the Third International Conference on Railway Technology: Development and Maintenance*, (Paper 289):–, 2016. [7](#)
- [11] R. Conti, E. Galardi, E. Meli, D. Nocciolini, L. Pugi, and A. Rindi. Energy and wear optimisation of train longitudinal dynamics and of traction and braking systems. *Vehicle System Dynamics*, pages 1–2, 2015. [7](#)
- [12] M. Malvezzi, L. Pugi, R. Conti, P. Toni, S. Tesi, E. Meli, and A. Rindi. A tool for prediction and optimization of railway traction systems with respect to an expected mission profile. *CHEMICAL ENGINEERING*, 33:–, 2013. [7](#)
- [13] X. Zhang, D. Göhlich, and J. Li. Energy-Efficient Torque Allocation Design of Traction and Regenerative Braking for Distributed Drive Electric Vehicles. *IEEE Transactions on Vehicular Technology*, 67:–, 2017. [12](#)
- [14] R. Gehrig, M. Hill, P. Lienemann, C.N. Zwicky, N. Bukowiecki, E. Weingartner, U. Baltensperger, and B. Buchmann. Contribution of railway traffic to local PM10 concentrations in Switzerland. *Atmospheric Environment*, 41(5):923–933, 2007. [12](#)
- [15] S. Abbasi, A. Jansson, L. Olander, U. Olofsson, and U. Sellgren. A pin-on-disc study of the rate of airborne wear particle emissions from railway braking materials. *Wear*, 284:18–29, 2012. [12](#)
- [16] I. Salma, T. Weidinger, and W. Maenhaut. Time-resolved mass concentration, composition and sources of aerosol particles in a metropolitan underground railway station. *Atmospheric Environment*, 41(37):8391–8405, 2007. [12](#)

- [17] M. Bartłomiejczyk and M. Połom. Multiaspect measurement analysis of braking energy recovery. *Energy Conversion and Management*, 127:35–42, 2016. [12](#)
- [18] W.W. Marr, W.J. Walsh, and P.C. Symons. Modeling battery performance in electric vehicle applications. *Energy Conversion and Management*, 33(9):843–847, 1992. [12](#)
- [19] M. Shimada, R. Oishi, D. Araki, and Y. Nakamura. Energy storage system for effective use of regenerative energy in electrified railways. *Hitachi Review*, 59:33–38, 2010. [12](#)
- [20] M. C. Falvo, D.A. Sbordone, A. Fernández, A.P. Cucala, R.R. Pacharromán, and A.J. Lopez. Energy savings in metro-transit systems: A comparison between operational Italian and Spanish lines. *Proceedings of the Institution of Mechanical Engineers, Part F: Journal of Rail and Rapid Transit*, 230(2):345–359, 2016. [14](#)
- [21] A. González-Gil, R. Palacin, and P. Batty. Sustainable urban rail systems: Strategies and technologies for optimal management of regenerative braking energy. *Energy Conversion and Management*, 75:374–388, 2013. [14](#)
- [22] A. González-Gil, R. Palacin, and P. Batty. Energy-efficient urban rail systems: strategies for an optimal management of regenerative braking energy. *Proceedings of the Fifth Transport Research Arena, Paris*, pages –, 2014. [14](#)
- [23] M. Ceraolo and G. Lutzemberger. Stationary and on-board storage systems to enhance energy and cost efficiency of tramways. *Journal of Power Sources*, 264:128–139, 2014. [14](#)
- [24] R. Barrero, J. Van Mierlo, and X. Tackoen. Energy savings in public transport. *IEEE Vehicular Technology Magazine*, 3(3):26–36, 2008. [14](#)
- [25] M. Steiner, M. Klohr, and S. Pagiela. Energy Storage System with UltraCaps on Board of Railway Vehicles. *Power Electronics and Applications European Conference*, pages 1–10, 2001. [14](#)

- [26] R. Barrero, J. Van Mierlo, and X. Tackoen. Enhanced Energy Storage Systems for Improved On-Board Light Rail Vehicle Efficiency. *IEEE Vehicular Technology Magazine*, pages 26–36, 2008. [14](#)
- [27] F. Ciccarelli and A. Del Pizzo. Improvement of Energy Efficiency in Light Railway Vehicles Based on Power Management Control of Wayside Lithium-Ion Capacitor Storage. pages –. [14](#)
- [28] I. Grigorchenkov, D. Jhonson, and K. Pullen. Evaluation of mobile and stationary applications of energy storage for DC railways and rapid transit. *Proceedings of the RRUKA Annual Conference, London*, pages –, 2012. [14](#)
- [29] L. Pugi, A. Rindi, A.G. Ercole, A. Palazzolo, J. Auciello, D. Fioravanti, and M. Ignesti. Preliminary studies concerning the application of different braking arrangements on Italian freight trains. *Vehicle System Dynamics*, 49(8):1339–1365, 2011. [16](#)
- [30] L. Pugi, M. Malvezzi, S. Papini, and G. Vettori. Design and preliminary validation of a tool for the simulation of train braking performance. *Journal of Modern Transportation*, 21:247–257, 2013. [16](#)
- [31] L. Pugi, A. Palazzolo, and D. Fioravanti. Simulation of railway brake plants: An application to SAADKMS freight wagons. *Proceedings of the Institution of Mechanical Engineers, Part F: Journal of Rail and Rapid Transit*, 222(4):321–329, 2008. [16](#)
- [32] A. Frilli, E. Meli, D. Nocciolini, L. Pugi, A. Rindi, B. Romani, M. Ceraolo, and G. Lutzemberger. The Tesys Rail Project: Innovative Models to Enhance the Energetic Sustainability of Railway Systems. *International Journal of Railway Technology*, pages –, In publication. [17](#)
- [33] J. Kondoh, I. Ishii, H. Yamaguchi, A. Murata, K. Otani, K. Sakuta, N. Higuchi, S. Sekine, and M. Kamimoto. Electrical energy storage systems for energy networks. *Energy Conversion and Management*, 41(17):1863–1874, 2000. [17](#)

- [34] S. Hillmansen and C. Roberts. Energy storage devices in hybrid railway vehicles: A kinematic analysis. *Proceedings of the Institution of Mechanical Engineers, Part F: Journal of Rail and Rapid Transit*, 221:135–143, 2007. [18](#)
- [35] K.M. Tsang, L. Sun, and W.L. Chan. Identification and modelling of Lithium ion battery. *Energy Conversion and Management*, 51(12):2857–2862, 2010. [19](#)
- [36] S. Baccari, G. Cammeo, C. Dufour, L. Iannelli, V. Mungiguerra, M. Porzio, G. Reale, and F. Vasca. Real-Time Hardware-in-the-Loop in Railway: Simulations for Testing Control Software of Electromechanical Train Components, Railway Safety, Reliability, and Security. *Technologies and Systems Engineering*, pages 221–248, 2012. [19](#)
- [37] E. Anders, G. Theeg, and S.V. Vlasenko. *Railway signalling & interlocking : international compendium*. Hamburg : Eurailpress, 2009. [19](#)
- [38] D. Zaninelli. *Sistemi elettrici per l'alta velocità ferroviaria*. Hoepli, Milano, 2011. [47](#)
- [39] F. Perticaroli. *Sistemi Elettrici per i Trasporti*. CEA Editore. [47](#)
- [40] D. Cornic. Efficient recovery of braking energy through a reversible dc substation. *Electrical Systems for Aircraft, Railway and Ship Propulsion*, pages –, 2010. [47](#)
- [41] ERA-European Railway Agency. Introduction to etcs curves. [60](#), [61](#)
- [42] RFI. Modello di frenatura per ssb av. [62](#)
- [43] L. Pugi, R. Conti, D. Nocciolini, E. Galardi, A. Rindi, and S. Rossin. A Tool for the Simulation of Turbo-Machine Auxiliary Lubrication Plants. *International Journal of Fluid Power*, 15(2):87–100, 2014. [71](#)
- [44] L. Pugi, E. Galardi, C. Carcasci, A. Rindi, and N. Lucchesi. A thermo-hydraulic tool for automatic virtual hazop evaluation. *Metrology and Measurement Systems*, 21(4):631–648, 2014. [71](#)

-
- [45] S. Miller and J. Wendlandt. Real-Time Simulation of Physical Systems Using Simscape. *MATLAB News and Notes*, pages –, 2010. [71](#)
- [46] L.F. Shampine, M.W. Reichelt, and J.A. Kierzenka. Solving Index-1 DAEs in MATLAB and Simulink. *SIAM Review*, 41:538–552, 1999. [72](#)
- [47] M.E. Hosea and L.F. Shampine. Analysis and implementation of tr-bdf2. *Applied Numerical Mathematics*, 20(1):21 – 37, 1996. Method of Lines for Time-Dependent Problems. [72](#)
- [48] ETR1000 – Technical specifications. [77](#)
- [49] F. Gherardi and L. Vannelli. The European interoperability and the related engineering and certification challenges. *ZEV rail Glasers Annalen*, 137:188–195, 2013. [77](#)
- [50] CIFI Symposium 2015. L’evoluzione del sistema av e il frecciarossa 1000. [77](#)
- [51] L. Pugi, M. Malvezzi, A. Tarasconi, A. Palazzolo, G. Cocci, and M. Violani. HIL simulation of WSP systems on MI-6 test rig. *Vehicle System Dynamics*, 44:843–852, 2006. [119](#)